

AD-A144 448

ATMOSPHERIC ICING ON SEA STRUCTURES(U) COLD REGIONS
RESEARCH AND ENGINEERING LAB HANOVER NH L MAKKONEN
APR 84 CRREL-MONO-84-2

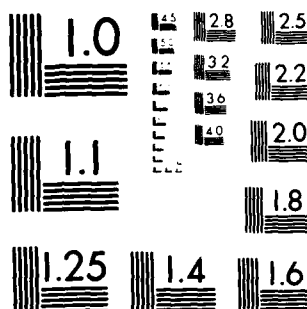
1/2

UNCLASSIFIED

F/G 8/12

NL





MICROCOPY RESOLUTION TEST CHART
NATIONAL BUREAU OF STANDARDS-1010-A

CRREL

MONOGRAPH 84-2



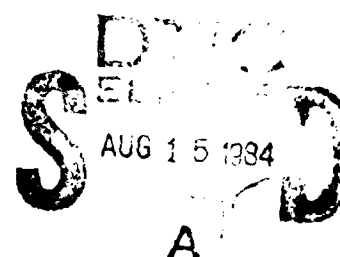
US Army Corps
of Engineers

Cold Regions Research &
Engineering Laboratory

Atmospheric icing on sea structures

AD-A144 448

DTIC FILE COPY



This document has been approved
for public release and sale; its
distribution is unlimited.

84 08 14 156

For conversion of SI metric units to U.S./British customary units of measurements consult ASTM Standard E380, Metric Practice Guide, published by the American Society for Testing and Materials, 1916 Race St., Philadelphia, Pa. 19103.

Cover: Atmospheric ice on a chain on ice-breaker Urho on the Baltic Sea (photo by L. Makkonen).

Monograph 84-2

April 1984



Atmospheric icing on sea structures

Lasse Makkonen

Unclassified

SECURITY CLASSIFICATION OF THIS PAGE (When Data Entered)

| REPORT DOCUMENTATION PAGE | | READ INSTRUCTIONS BEFORE COMPLETING FORM |
|---|--|---|
| 1. REPORT NUMBER Monograph 84-2 | 2. GOVT ACCESSION NO. A144448 | 3. RECIPIENT'S CATALOG NUMBER |
| 4. TITLE (and Subtitle) ATMOSPHERIC ICING ON SEA STRUCTURES | 5. TYPE OF REPORT & PERIOD COVERED | |
| | 6. PERFORMING ORG. REPORT NUMBER | |
| 7. AUTHOR(s) Lasse Makkonen | 8. CONTRACT OR GRANT NUMBER(s) Order No. 2LA6000-1067 | |
| 9. PERFORMING ORGANIZATION NAME AND ADDRESS U.S. Army Cold Regions Research and Engineering Laboratory Hanover, New Hampshire 03755 | 10. PROGRAM ELEMENT, PROJECT, TASK AREA & WORK UNIT NUMBERS | |
| 11. CONTROLLING OFFICE NAME AND ADDRESS U.S. Minerals Management Service Reston, Virginia 22091 | 12. REPORT DATE April 1984 | |
| | 13. NUMBER OF PAGES 102 | |
| 14. MONITORING AGENCY NAME & ADDRESS (if different from Controlling Office) | 15. SECURITY CLASS. (of this report) Unclassified | |
| | 15a. DECLASSIFICATION/DOWNGRADING SCHEDULE | |
| 16. DISTRIBUTION STATEMENT (of this Report) Approved for public release; distribution unlimited. | | |
| 17. DISTRIBUTION STATEMENT (of the abstract entered in Block 20, if different from Report) | | |
| 18. SUPPLEMENTARY NOTES | | |
| 19. KEY WORDS (Continue on reverse side if necessary and identify by block number) Atmospheric icing Offshore environment Ice Sea structures Ice accretion Ice prevention | | |
| 20. ABSTRACT (Continue on reverse side if necessary and identify by block number) Atmospheric icing (icing due to fog, precipitation and water vapor in air) as a physical process and the problems it causes for ships and stationary offshore structures are reviewed. Estimation of the probability and severity of atmospheric icing based on climatological and geographical factors is discussed, and theoretical methods for calculating the intensity of atmospheric icing at sea are suggested. Existing data on the dependence of the atmospheric icing rate and the properties of the accreted ice on the meteorological conditions are analyzed. The methods of measuring the icing rate and ice prevention methods are discussed. | | |

DD FORM 1 JAN 73 1473

EDITION OF 1 NOV 65 IS OBSOLETE

Unclassified

SECURITY CLASSIFICATION OF THIS PAGE (When Data Entered)

PREFACE

This report was prepared by Lasse Makkonen while on leave from the Institute of Marine Research in Helsinki, Finland. The author is grateful to the U.S. Minerals Management Service for funding this research under Department of the Interior Order No. 2LA6000-1067. He also thanks the Institute of Marine Research for granting him sabbatical to prepare this report.

This report was technically reviewed by L. David Minsk of the U.S. Army Cold Regions Research and Engineering Laboratory and Jon Nauman of the U.S. Minerals Management Service. In particular, the author thanks Mr. Minsk for his role in the review and editing process.

The contents of this report are not to be used for advertising or promotional purposes. Citation of brand names does not constitute an official endorsement or approval of the use of such commercial products.

0010
COPY
INSTRUCTIONS

| | |
|---------------|---------|
| Accession For | |
| NTIS GRAM | |
| DTIC TAB | |
| Unannounced | |
| Justification | |
| By | |
| Distribution/ | |
| Availability | |
| Dist | Special |
| A-1 | |

CONTENTS

| | <u>Page</u> |
|--|-------------|
| Abstract----- | 1 |
| Preface----- | ii |
| Nomenclature----- | vi |
| Introduction----- | 1 |
| Icing processes and their relative importance----- | 2 |
| Ship icing----- | 2 |
| Icing on stationary sea structures----- | 4 |
| Estimation of icing intensity----- | 6 |
| Freezing process----- | 6 |
| Theoretical estimates----- | 9 |
| Empirical verification----- | 27 |
| Meteorological conditions during icing events----- | 31 |
| Boundary layer conditions----- | 32 |
| Synoptic weather conditions----- | 41 |
| Effect of meteorological conditions on properties of the ice----- | 42 |
| Density----- | 42 |
| Ice type----- | 46 |
| Crystal structure----- | 47 |
| Strength of adhesion----- | 48 |
| Shape----- | 50 |
| Geographical and seasonal distribution of icing probabilities----- | 52 |
| Methods for measuring icing severity----- | 62 |
| Anti-icing methods----- | 64 |
| Structural design----- | 64 |
| Heating----- | 65 |
| Chemical methods----- | 67 |
| Other methods----- | 67 |
| Deicing methods----- | 69 |
| Mechanical methods----- | 69 |
| Thermal methods----- | 71 |
| Surface materials and coatings----- | 71 |
| Summary and conclusions----- | 75 |
| Literature cited----- | 77 |

ILLUSTRATIONS

Figure

1. Vertical distribution of spray water content over the sea surface at moderate and strong winds----- 4
2. Variation of average diameter and weight of ice accumulation with height on meteorological tower at Obninsk, U.S.S.R.----- 6
3. Droplet trajectories in front of a cylinder in an airstream----- 9
4. Local impingement efficiency at the stagnation point as a function of the inertia parameter K and parameter ϕ ----- 11

| Figure | Page |
|---|------|
| 5. Critical radius $D/2$ of a cylinder above which icing theoretically does not occur----- | 12 |
| 6. Median-volume droplet diameter vs liquid water content in stratiform clouds----- | 13 |
| 7. Variation in liquid water content in air with air temperature and wind speed----- | 14 |
| 8. Liquid water content of evaporation fogs at various temperatures----- | 15 |
| 9. Liquid water content as a function of visibility in Barrow fogs----- | 15 |
| 10. The lines separating the dry-growth and wet-growth processes on a 5-cm-diameter cylinder----- | 20 |
| 11. Ice accretion intensity in the stagnation region of a 5-cm-diameter cylinder as a function of air temperature----- | 20 |
| 12. Icing efficiency E_1 , freezing fraction n and collection efficiency E on the stagnation line of a 15-mm-diameter cylinder as a function of the wind speed--- | 20 |
| 13. Theoretical icing intensity as a function of wind speed and air temperature----- | 23 |
| 14. Numerical simulation of ice accretion on a 1-cm-diameter wire----- | 24 |
| 15. Effect of air temperature and relative wind speed on reported icing severity for fishing vessels steaming at low speeds----- | 29 |
| 16. Dependence of the overall icing efficiency on the wind speed for various liquid water contents w according to Glukhov (1971)----- | 29 |
| 17. Dependence of cylinder icing intensity on wind speed according to observations in the natural outdoor environment and according to the theory with arbitrary constant parameters----- | 29 |
| 18. Icing intensity vs wind speed----- | 30 |
| 19. Icing intensity divided by wind speed vs air temperature----- | 31 |
| 20. Ice load vs wind speed multiplied by the estimated time of in-cloud conditions----- | 31 |
| 21. Frequency of atmospheric ice accretion related to the air temperature----- | 33 |
| 22. Frequency of atmospheric ice accretion related to the wind speed----- | 33 |
| 23. Frequency of atmospheric ice accretion related to the wind shear----- | 34 |
| 24. Typical temperature profiles during supercooled precipitation at the ground----- | 35 |
| 25. Icing events related to air temperature and dewpoint spread----- | 36 |
| 26. Glaze events related to air temperature and dewpoint spread----- | 36 |
| 27. Regime of supercooled advection fog over the ocean--- | 38 |
| 28. Conditions necessary for evaporation fog----- | 39 |
| 29. Vertical extent of evaporation fog vs the difference between the air temperature at 2 m and the critical temperature given by the theory of Saunders (1964)--- | 39 |

| Figure | Page |
|--|------|
| 30. Accreted 100- μ m-diameter droplets at different air temperatures and deposit temperatures----- | 43 |
| 31. Atmospheric icing events in relation to air temperature and wind speed----- | 46 |
| 32. Variation of mean width of ice crystal with the ambient temperature and the radial distance above the conductor surface----- | 47 |
| 33. Adhesive strength of ice accretion vs density at various air temperatures----- | 48 |
| 34. Adhesive strength of ice accretion grown at different ambient temperatures and air velocities----- | 49 |
| 35. Typical ice profiles on cylinders----- | 51 |
| 36. Horizontal and vertical cross sections of an ice deposit formed by droplet accretion----- | 51 |
| 37. Observed ice profiles----- | 51 |
| 38. Regions where ship icing was observed by Soviet observers----- | 53 |
| 39. Probability of supercooled fog by month----- | 54 |
| 40. Average number of days with fog at coastal stations in northern Norway----- | 59 |
| 41. Distribution of fog events in relation to air-sea temperature difference at two arctic marine weather stations----- | 59 |
| 42. Ten-year summaries (1948-1958) of the number of precipitation events occurring during freezing air temperatures at two arctic marine weather stations--- | 61 |
| 43. Mean annual percentage of hourly weather observations with freezing rain, North America----- | 61 |
| 44. Icing gauge----- | 62 |
| 45. Icing rod----- | 63 |
| 46. Rosemount model 872DC ice detector----- | 64 |
| 47. Working principle of a thermosyphon----- | 66 |
| 48. Heat pipe deicing system installed on a ship----- | 66 |
| 49. Adhesive strength of ice vs electric field strength-- | 69 |
| 50. Pneumatic deicer----- | 70 |
| 51. Dependence of adhesion of ice on the height of irregularities----- | 74 |

TABLES

Table

| | |
|--|----|
| 1. Cause of icing on Soviet trawlers in 1965-66----- | 3 |
| 2. Characteristics of icing sources in the atmospheric surface layer----- | 5 |
| 3. Synoptic conditions at the time of ship icing----- | 41 |
| 4. Glaze and rime adhesion on different substances----- | 49 |
| 5. Period of ship icing----- | 52 |
| 6. Example of the properties of the adiabatic mixed layer as functions of the downwind distance from the shore, with a lifted inversion----- | 58 |
| 7. Ice adhesion on different coatings----- | 73 |

NOMENCLATURE

| | |
|-----------------|---|
| A | surface area |
| a | constant (eq 14) |
| C _e | transfer coefficient for water vapor |
| c _d | droplet drag coefficient |
| c _i | specific heat of ice |
| c _p | specific heat of air |
| c _w | specific heat of water |
| D | cylinder diameter |
| d | droplet diameter |
| d _m | median volume diameter of the droplets |
| E | collection efficiency |
| E _i | icing efficiency |
| e _a | water vapor pressure in air at t _a |
| e _{as} | saturation water vapor pressure in air at t _a |
| e _i | water vapor pressure over ice at t _s |
| e _s | water vapor pressure over water at t _s |
| F | adhesive strength |
| h | convective heat transfer coefficient |
| h _o | height of temperature inversion in the atmospheric boundary layer |
| I | icing intensity (mass per time and surface area) |
| I _m | maximum icing intensity |
| I _s | rate of snow accumulation (mass per time and surface area) |
| i | index for the formation of evaporation fog |
| K | inertial parameter |
| k | ratio of molecular weight of water vapor to dry air |
| k _a | thermal conductivity of air |
| L | Monin-Obukhov length |
| L _c | latent heat of condensation |
| L _e | latent heat of evaporation |
| L _f | latent heat of fusion |
| M | Macklin's ice density parameter (eq 32) |
| M _i | ice load |
| Nu | Nusselt number |
| n | freezing fraction |
| P | precipitation rate |
| P _f | critical rate of mixing in the atmospheric boundary layer |
| p _a | air pressure |
| q | heat flux |
| R | relative humidity |
| r | recovery factor for viscous heating of air |
| Re | Reynolds number |
| Re _d | droplet Reynolds number |
| t _a | air temperature |
| t _s | temperature on the ice deposit surface |
| t _w | sea surface temperature |
| U _a | x component of the velocity vector \bar{V}_a |
| V | volume |
| V _a | y component of the velocity vector \bar{V}_a |
| \bar{V}_a | two-dimensional air velocity vector |
| \bar{V}'_a | dimensionless air velocity vector |
| \bar{V}_d | two-dimensional droplet velocity vector |
| \bar{V}'_d | dimensionless droplet velocity vector |
| v | wind speed |

| | |
|---------------|--|
| v_o | impact speed of the droplets |
| W_m | energy required by mechanical ice removal |
| W_t | energy required by thermal ice removal |
| w | liquid water content in air (mass per volume) |
| w_c | critical liquid water content |
| w_s | snow particle content in air (mass per volume) |
| z_f | vertical extent of evaporation fog |
| β | local collection efficiency |
| Δt | difference in droplet temperature after bouncing or shedding and before impact |
| $\Delta \tau$ | time interval between droplets |
| δ | displacement distance of ice removal |
| θ | angle around cylinder surface (measured from the stagnation line) |
| θ_a | potential temperature in air |
| θ_s | potential temperature on water surface |
| θ_w | potential temperature of water |
| λ | visibility |
| μ | absolute viscosity of air |
| π | wetness index of the ice surface |
| ρ | ice density |
| ρ_a | air density |
| ρ_w | water density |
| σ | Stefan-Boltzmann constant |
| τ | time |
| τ_f | time of droplet freezing |
| ϕ | dimensionless parameter |
| ψ | stream function |

ATMOSPHERIC ICING ON SEA STRUCTURES

Lasse Makkonen

INTRODUCTION

Icing on structures in the marine environment is a hazard to navigation and other offshore activities in regions where freezing temperatures exist over the sea. Several ships are lost due to ship icing each year, and icing on towers, buoys, automatic meteorological instruments, helicopter platforms and other structures causes many safety risks and inconveniences.

Ship icing has been recognized as a serious problem for a long time and has been discussed in the scientific literature for more than one hundred years (Nature 1881). Ship icing is caused primarily by sea spray, so little attention has been paid to atmospheric ice accretion at sea, i.e. icing due to water vapor, fog and precipitation particles. However, during the past decade the need for deeper understanding of atmospheric icing in the marine environment has increased considerably as human activities such as offshore oil drilling have intensified in arctic and subarctic waters. The assessment of factors such as safety criteria and structural design requires knowledge of the hazards caused by the arctic environment; atmospheric icing is one of the dangers, especially to stationary structures at sea.

The purpose of this report is to give an up-to-date presentation on atmospheric icing on stationary structures in the marine environment. The probabilities of encountering atmospheric icing, the expected hazards caused by it, and the means of combating it are analyzed using theoretical calculations, relations between icing and other atmospheric conditions, climatological considerations, and available icing data. The report is also a review of the literature on atmospheric icing on sea structures. Both spray icing and atmospheric icing in continental regions are dealt with, but only when they are connected with the main topic; no complete review is attempted here of either ship icing or atmospheric icing in gen-

eral. However, the theoretical aspects are discussed in enough detail so that the report may be used as a review of atmospheric icing physics. Also, parts of the report review anti-icing and deicing methods of ships and stationary structures. Readers interested in atmospheric icing in continental regions should consult Dranevic (1971), Minsk (1980) and the following collections: Symposium Nebelfrost und Glatteisablagerungen, Abhandl. Meteor. Dienst, DDR, 107 (1973) and Proceedings of First International Workshop on Atmospheric Icing of Structures published by CRREL in 1983. The most general references on spray icing on ships are Panov (1976) and Aksiutin (1979); the most complete reviews on ship icing published in English are by Shellard (1974), Minsk (1977), Stallabrass (1980), Horjen (1981), and the translation of the 1974 Russian collection Investigation of the Physical Nature of Ship Icing (CRREL Draft Translation 411).

ICING PROCESSES AND THEIR RELATIVE IMPORTANCE

Ship icing

Ice on sea structures originates either from seawater (spray icing) or from atmospheric freshwater (atmospheric icing). Atmospheric ice accretions can be further classified according to the source of the ice: glaze and rime are formed from water droplets, hoarfrost from water vapor, and wet snow from snowflakes. Dry snow does not accrete in substantial amounts on vertical surfaces, which are of primary concern regarding icing of structures.

The outer appearance and internal structure of ice accreted from supercooled water droplets vary considerably. Therefore, this type of ice is generally divided into three groups, the main criterion being the density. These are

- 1) glaze, which is hard, almost bubble-free, clear, homogeneous ice with a density close to that of pure ice (0.92 g cm^{-3}),
- 2) hard rime, which is rather hard, granular, white or translucent ice with a density of $0.6\text{--}0.9 \text{ g cm}^{-3}$, and
- 3) soft rime, which is white or opaque ice with a loosely bonded structure and a density of less than 0.6 g cm^{-3} .

For the purpose of theoretical treatment it is convenient to divide glaze and rime according to the thermal conditions prevailing during ice formation: glaze forms in wet-growth conditions with a surface temperature

Table 1. Cause of icing on Soviet trawlers in 1965-66 (After Shektman 1968).

| Icing intensity | Cause of icing (%) | | | | | Number of cases |
|-----------------|--------------------|---------------|-----|-------------------------|---------------|-----------------|
| | Spray | Spray and Fog | Fog | Spray and Precipitation | Precipitation | |
| Fast growth | 82 | 12 | 2 | 4 | 0 | 52 |
| Slow growth | 90 | 5 | 2 | 1 | 2 | 303 |
| No growth | 94 | 0 | 2 | 2 | 2 | 54 |
| All cases | 89 | 5 | 2 | 2 | 2 | 409 |

of 0°C, and rime forms in dry-growth conditions with a surface temperature below 0°C. The division into the three ice types is subjective, and slightly different criteria for ice density have been used by different authors (e.g. Dranevic 1971, Glukhov 1971, Minsk 1977). Moreover, a mixture of the different types is not uncommon, because the atmospheric conditions change during an icing storm. Also, as will be shown in the theory section, ice density and type may even vary in constant environmental conditions, so that the type of ice differs in different layers in the ice deposit.

Sea spray is a major source of ship icing (Table 1). According to the data from more than 2000 ship reports from around the world, ocean spray alone causes ship icing in 89.8% of all cases, spray combined with rain or fog in 6.4%, spray combined with snow in 1.1%, and atmospheric icing alone in 2.7% (Borisenkov and Panov 1974). In arctic seas, ship icing is caused by spray alone in 50% of all cases, spray combined with atmospheric icing in 41%, fog in 3%, and precipitation in 6%. Hoarfrost has not been reported as a cause of ship icing.

Spray icing and atmospheric icing are often observed simultaneously on ships, and their relative importance should change with height above the sea surface; this has not been documented. It is only known that spray icing is restricted to lower levels and to structures such as decks, derricks and handrails, and that superstructure icing on ships due to sea spray does not usually reach higher than about 16 m above the sea surface (World Meteorological Organization 1962). The relative importance of atmospheric icing, then, is generally at its maximum on the upper parts of the ship (masts, antennas etc.). It therefore seems that rapid atmospheric ice accretion may be more dangerous to the ship's stability than spray icing of

the same intensity. However, the relative intensity of spray icing and atmospheric icing on a ship depends on the speed of the vessel, the wave heading and the roughness of the sea. (Spray icing has been observed on structures at a height of more than 30 m on the Finnish high-speed turbine ship Finnjet.)

Icing of stationary sea structures

In the icing of stationary sea structures, there is not the mechanical impact caused by the movement of the structure itself, as in ship icing. Therefore, spray icing is limited to lower levels on stationary structures. On the lighthouses in the Baltic Sea, for example, the upper limit where traces of spray icing are observed is 5-10 m. Spray generated directly from the wave tops without the effect of the impact with the structure is a cause of icing only in the first few meters above the sea surface, since only very small droplets are forced upwards by wave action and air turbulence. Droplets more than 30 μm in diameter rise above 7 m only when the wind speed v is more than 12 m s^{-1} , and 100- μm droplets only when v is more than 25 m s^{-1} (Preobrazhenskii 1973). Preobrazhenskii's data on the vertical distribution of liquid water content in air due to sea spray are given in Figure 1. These field observations show that only very slight icing can be caused by spray directly from waves on stationary structures above 4 m in wind speeds less than 25 m s^{-1} . The liquid water content w at 4 m in Figure 1 is one to two orders of magnitude smaller than the typical maximum values of w during atmospheric icing (Table 2).

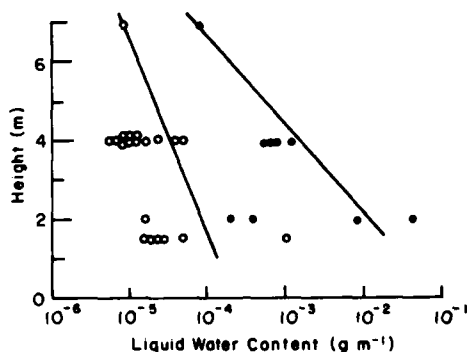


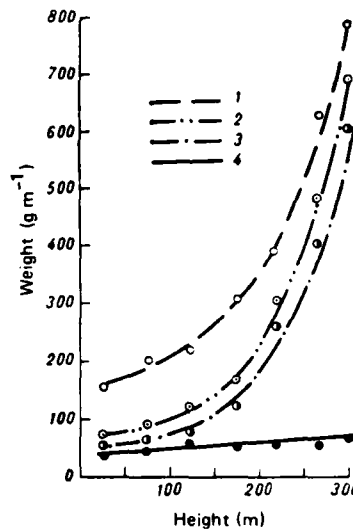
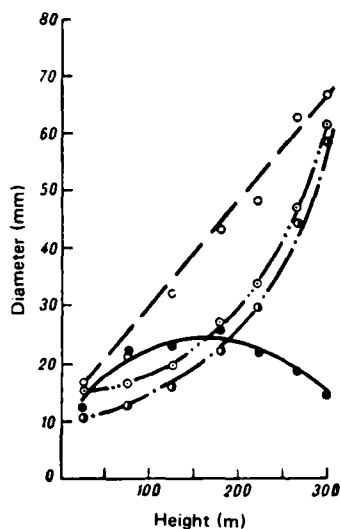
Figure 1. Vertical distribution of spray water content over the sea surface at moderate ($6\text{--}10 \text{ m s}^{-1}$) and strong ($15\text{--}25 \text{ m s}^{-1}$) winds. (From Preobrazhenskii 1973.)

Since wave impact on stationary structures seldom causes large amounts of sea spray at high levels and since this amount can be restricted by structural design, atmospheric icing is the major potential source of ice accretion, especially on tall sea structures. The relative importance of the different sources of atmospheric icing is not well known except for what can be seen in Table 1, that is, that considerable icing from both supercooled fog and precipitation has been ob-

Table 2. Characteristics of icing sources in the atmospheric surface layer.

| Source | Droplet diameter (μm) | | Liquid water content (g m^{-3}) | Reference |
|---|------------------------------------|----------|--|--------------------------------|
| | Range | Mean | | |
| Sea spray on a moving ship | 1000 - 3500 | 2400 | 0 - 219 | Borisenkov and Panov (1974) |
| Sea spray in first 10 cm | 10 - 1000 | 200 | -- | Wu (1979) |
| Sea spray on a stationary ship | | | | |
| $v > 15 \text{ m s}^{-1}$, $h = 2 \text{ m}$ | 3 - 2000 | 5 - 30 | 0.03 | Preobrazhenskii (1973) |
| $v > 15 \text{ m s}^{-1}$, $h = 7 \text{ m}$ | 3 - 90 | 5 - 30 | 0.00 | Preobrazhenskii (1973) |
| Marine advection fog | -- | 8 - 16 | 0.03 - 0.17 | Fitzgerald (1978) |
| Coastal fog | 4 - 20 | -- | 0.01 - 0.16 | Goodman (1977) |
| Evaporation fog | 6 - 120 | 13 - 38* | 0.01 - 0.30 | Houghton and Radford (1938) |
| Evaporation fog | -- | -- | 0.04 - 0.14 | Bashkirova and Krasikov (1958) |
| Evaporation fog | -- | 8 - 10 | 0.20 | Currier et al. (1974) |
| Arctic fog | 7 - 130 | 16 | 0.00 - 0.15 | Kumai (1973) |
| Arctic fog | 2 - 75 | 18 | 0.02 | Kumai and Francis (1962) |
| Arctic fog | 6 - 60 | -- | 0.04 - 0.17 | Reiquam and Diamond (1959) |
| Continental winter fog | -- | 10 | 0.00 - 0.45 | Pinnick et al. (1978) |
| Mountain fog | -- | 7 - 23* | 0.05 - 0.30 | Bain and Gayet (1982) |
| Low stratus | 2 - 43 | 5 | 0.05 - 0.25 | Pillie and Kocmond (1967) |

*Median-volume diameter.



a. Average diameter vs height.

b. Average weight vs height.

Figure 2. Variation of average diameter and weight of ice accumulation (1-mixture, 2-hard rime, 3-glaze ice, 4-soft rime) with height on meteorological tower at Obninsk, U.S.S.R. (From Minsk 1977.)

served on ships and that the formation of hoarfrost is negligible. Wet snow also seems to be less important than fog and precipitation.

In continental regions the total amount of ice usually increases with height; the proportion of hard rime and glaze increases with height and the role of soft rime decreases (Fig. 2). It is not known whether the same relationship occurs in the marine environment, but there may be substantial differences due to different boundary layer structures over land and over sea. The measurements by McLeod (1981) indicate that the mean monthly and seasonal values of total ice deposition increase with height in the marine environment as well, but these measurements were made over land on small islands. More representative data from real offshore conditions are needed to confirm these results.

ESTIMATION OF ICING INTENSITY

Freezing process

When supercooled water drops fall or move with wind, hit a structure, and freeze, the complicated freezing phenomenon is affected by various properties of the air flow, the icing object, and the impinging water drops.

There are a large number of parameters that affect icing on structures, but only a few can be dealt with in a practical experiment. Therefore, a theoretical approach is needed to explain the basic characteristics of the icing process. An understanding of icing mechanics is essential for estimating icing intensity and developing successful means for reducing the hazards and inconveniences caused by atmospheric icing of structures.

Water drops in air may remain liquid at temperatures as low as about -40°C before spontaneous freezing occurs. Droplet freezing at higher air temperatures is caused by mechanical impact or the presence of a freezing nucleus. Impurities in air, such as ice crystals and dust particles, act as freezing nuclei. The mechanical impact may be a collision with another droplet, with the ground, or with a structure.

When a supercooled droplet hits a solid obstacle, it spreads and turns to ice. The freezing process can be divided into two stages: first, part of the supercooled water in the droplet freezes rapidly, releasing the latent heat of fusion and thereby raising the temperature of the remaining water to 0°C . In the second stage this remaining part turns to ice, since the droplet gives up heat to its surroundings by convection, evaporation and conduction; the speeds of these processes determine the time required for this second stage. The initial stage is one or two orders of magnitude shorter than the subsequent stage (Macklin and Payne 1968, Murray and List 1972). The time required for the droplet to spread completely under different conditions is not well known, but it obviously depends on the impact speed and the droplet size. The spreading probably occurs while most of the droplet is in the liquid state (Brownscombe and Hallett 1967).

The time τ_f of the droplet freezing can be estimated as a first approximation from the heat balance of an individual droplet, since τ_f is determined by the rate at which the latent heat released in the freezing is transferred to the environment. Using this idea, Macklin and Payne (1968) have calculated τ_f for unventilated drops that remain hemispherical during freezing and that are in contact with the underlying ice surface. These calculations resulted in τ_f values of about 10^{-2} s for $10\text{-}\mu\text{m}$ droplets at temperatures t_a typical of atmospheric icing. Wind action in the natural environment may, however, increase the heat transfer from the droplet considerably, resulting in smaller values of τ_f . The freezing time τ_f is approximately proportional to $-t_a$ (in $^{\circ}\text{C}$) and to the square of the droplet diameter (Johnson and Hallett 1968).

The time required for the droplet to freeze is an important parameter, since it affects the properties of the ice formed and the way in which the problem of theoretical estimation of icing intensity must be treated. If $\Delta\tau$ denotes the time interval between droplets striking the same spot on the surface, then the type of ice formed may be determined as follows:

$\tau_f \ll \Delta\tau$: soft rime,

$\tau_f < \Delta\tau$: hard rime,

$\tau_f \geq \Delta\tau$: glaze.

The time interval $\Delta\tau$ for droplets of a fixed size depends on the droplet velocity (i.e., the wind speed) and the number of droplets in the air. The freezing time τ_f depends on the factors involved with the heat transfer from the droplet, such as droplet size, air temperature and wind speed. Qualitatively, high wind speed, high air temperature and large droplets favor the situation where $\tau_f > \Delta\tau$. The time of droplet spreading may be important, too, in influencing the type of ice, since even if $\tau_f < \Delta\tau$ the ice may be quite compact and glaze-like if the droplets spread efficiently and form spots of water film before they turn to ice. This may be the case during freezing rain, for example. The ratio Π of the time that the icing surface remains in the liquid phase to the time interval between droplet impacts is

$$\Pi = \frac{\tau_f}{\Delta\tau} . \quad (1)$$

In the growth condition where $\tau_f \ll \Delta\tau$ the ratio Π approaches zero, and the process is called dry growth. When $\tau_f \approx \Delta\tau$, then Π approaches one, and hard rime or sometimes glaze is formed, but the process is still called dry growth. Only when $\tau_f \geq \Delta\tau$ is the process called wet growth. It might be more logical to divide dry growth and wet growth at $\Pi = 0.5$, but the criterion $\Pi = 1$ is generally used when there is a uniform water film on the icing surface. One reason for using $\Pi = 1$ as the criterion is that the existence of the uniform water film is easier to define than any specific value of Π , because in nature there are droplets of different size and because the impinging of droplets is a stochastic process, so that the time interval $\Delta\tau$ is not constant. Another reason for using $\Pi = 1$ as the dividing condition is that only when $\Pi \geq 1$ is the mean temperature of the icing surface 0°C , and unfrozen water runs off from the surface. This runoff water is an important factor affecting the intensity of ice accretion.

Theoretical estimates

Rime. In dry growth all the impinging water droplets freeze completely and rime is formed. Hence, when calculating the rate of rime formation it is only necessary to determine the amount of impinging water per unit time and unit surface area. Consequently the icing intensity I (in $\text{g cm}^{-2} \text{h}^{-1}$, for example) of rime formation on a vertical surface can be formulated as

$$I = E v w \quad (2)$$

where v = wind speed (the terminal velocity of the small droplets causing rime formation is small enough to be neglected)

w = liquid water content in air

E = collection efficiency, that is, the ratio of the mass flow of water droplets striking the surface to the mass flow that would strike the surface if the droplets had not been deflected in the air stream (Fig. 3).

The droplets are deflected by viscous drag forces, making them follow streamlines around the icing object. However, the inertia of the droplets causes their trajectories to deviate from the streamlines, so that some of them strike the surface and give a non-zero value of E . It is possible to determine E by calculating the droplet trajectories, which are controlled by the balance between droplet inertia and drag forces.

In the conditions prevailing during atmospheric icing, the potential flow is a good approximation of the air flow upstream from the boundary layer separation point, where practically all the droplets that contribute to E are collected by a typical icing object. The potential flow satisfies the Laplace equation, whose solution yields the stream function ψ for the potential flow

$$\nabla \psi^2 = 0. \quad (3)$$

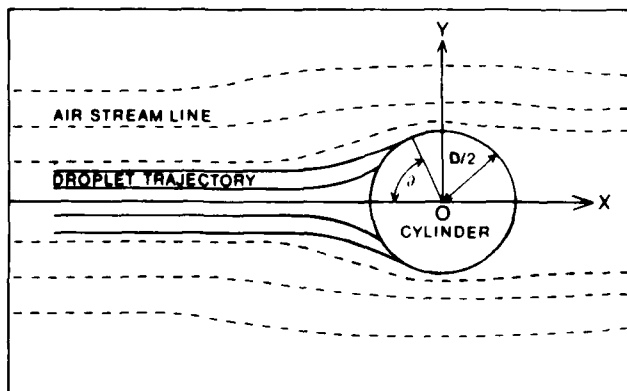


Figure 3. Droplet trajectories in front of a cylinder in an airstream.

The components U_a and V_a of the two-dimensional velocity vector \bar{V}_a are the partial derivatives of the stream function

$$U_a = \frac{\partial \psi}{\partial y}, \quad V_a = -\frac{\partial \psi}{\partial x}. \quad (4)$$

The stream function and the velocity components at each point around the object can be solved analytically for simple objects such as circles and ellipses if the free stream velocity v is known. For more complex objects numerical methods must be used.

A typical icing object is a cylinder. The dimensionless equation of motion for spherical droplets around a cylinder (the balance between inertial and viscous forces) is, according to Langmuir and Blodgett (1946),

$$K \frac{d\bar{V}'_d}{d\tau} = \frac{c_d Re_d}{24} (\bar{V}'_a - \bar{V}'_d) \quad (5)$$

where K = inertial parameter analogous to mass in dimensionless form
 $[K = (d^2 \rho_w v)/(9 \mu D)]$

τ = time

c_d = drag coefficient

Re_d = droplet Reynolds number based on the droplet's relative velocity ($Re_d = d \rho_a |\bar{V}_a - \bar{V}_d|/\mu$)

\bar{V}'_a = dimensionless air velocity vector ($\bar{V}'_a = \bar{V}_a/v$)

\bar{V}'_d = dimensionless droplet velocity vector ($\bar{V}'_d = \bar{V}_d/v$)

\bar{V}_a = air velocity vector

\bar{V}_d = droplet velocity vector

d = droplet diameter

ρ_w = water density

μ = absolute viscosity of air

D = cylinder diameter

ρ_a = air density.

The drag coefficient c_d is a function of Re_d . Empirical expressions based on laboratory measurements in steady motion have been given by Langmuir and Blodgett (1946) and Beard and Pruppacher (1969), among others. The deceleration of the droplets may have some influence on c_d (Temkin and Mehta 1982), but this is obviously of minor importance in solving for \bar{V}_d from eqs 3-5, since verification of theoretical values for E have been convincing even though this effect is neglected (Lozowski and Oleskiw 1983).

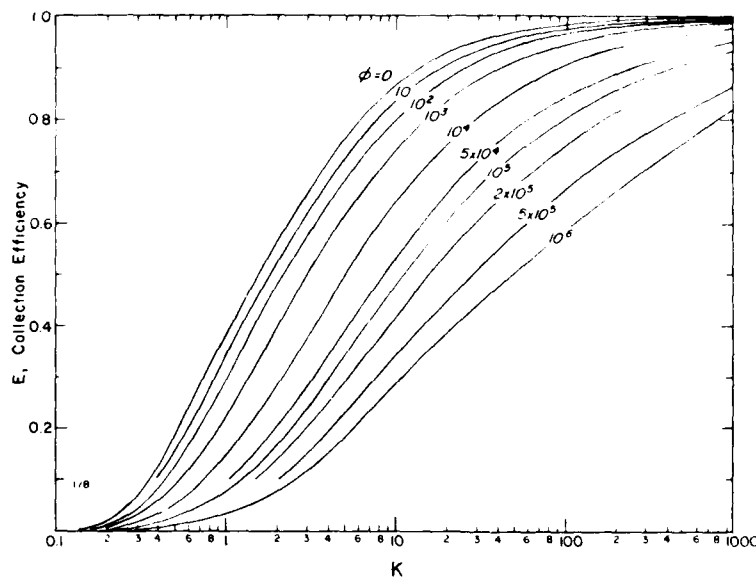


Figure 4. Local impingement efficiency at the stagnation point as a function of the inertia parameter K and parameter ϕ . (From Minsk 1980.)

Calculating droplet trajectories requires an iterative numerical method of solution, which involves considerable computation time. However, the solution of E for a circular cylinder can be presented conveniently as a function of two dimensionless parameters [K and ϕ , where $\phi = (9 \rho_a^2 D v) / (\mu \rho_w)$], either in the form of analytical expressions (Cansdale and McNaughtan 1977) or as curves (Fig. 4). Qualitatively the dependence of the collection efficiency E on the atmospheric parameters is such that E increases with increasing wind speed and droplet size and with decreasing cylinder dimensions. It is unfortunate that in typical atmospheric icing conditions E is very sensitive to the droplet diameter, which is difficult to measure or estimate. Air temperature t_a has an effect on E because ρ_a and μ depend on t_a , but this effect is negligible in practical applications.

The local collection efficiency β at angle θ from the stagnation line of a cylinder varies and has its maximum value at the stagnation line. When the conditions cause E to approach zero, icing will occur near the stagnation line only. Under some circumstances $E = 0$ and no icing will occur. Langmuir and Blodgett (1946) showed that this happens when $K = 1/8$. Hence, it is possible to calculate the combinations of wind speed, droplet size and cylinder diameter for which icing theoretically does not occur (Fig. 5). The curves

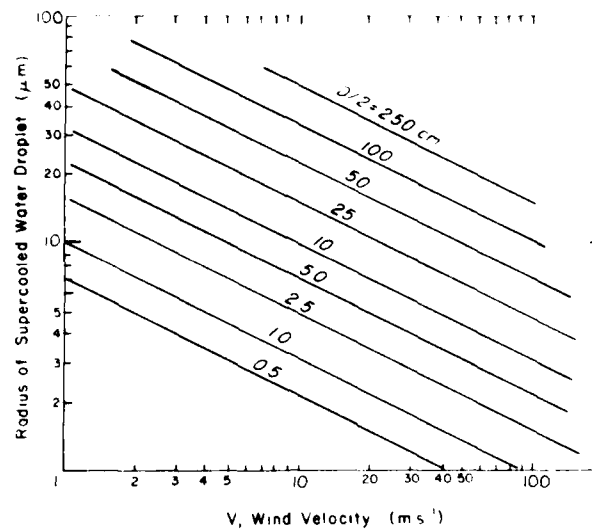


Figure 5. Critical radius $D/2$ of a cylinder above which icing theoretically does not occur. (From Kuroiwa 1965.)

in Figure 5, however, may not be fully applicable to the real world, where the air flow is turbulent and the droplets are not of uniform diameter. Also, since E is so dependent on the object dimensions, ice may sometimes accrete on small irregularities on the icing object and form rime feathers, although $E = 0$ for the object as a whole. These feathers usually grow from the side of the object.

For other object shapes, such as a ribbon (Langmuir and Blodgett 1946) and a rectangular half body (Lewis and Brun 1956), theoretical values of the collection efficiency are also available.

The problem in calculating E and β for the rather wide size distribution of droplets in natural clouds can be solved by determining these parameters differently for each size category. Then the effective E (or β) is the sum of the values for each size times the fraction of the total liquid water content represented by that size. Since this procedure is more laborious, E and β are often calculated for the droplets that have the median volume diameter of the droplet distribution. This method gives fairly accurate results on cylinders for the typical size distributions in icing fogs and clouds except at very low values of E (Makkonen, in press).

As an ice deposit grows during ice accretion, its dimensions change continuously, and therefore both the collection efficiency and the collecting surface area also change. This can be taken into account in the theoretical

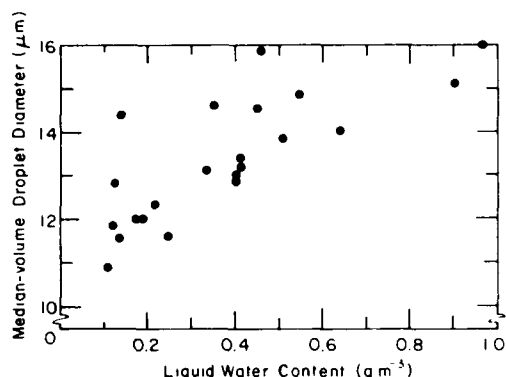


Figure 6. Median-volume droplet diameter vs liquid water content in stratiform clouds. (Data from Bain and Gayet 1982.)

considerations by time-dependent numerical modeling. Such models have been developed recently for simulating icing under dry-growth conditions, particularly on airfoils (Ackley and Templeton 1979, McComber and Touzot 1981, Oleskiw 1982, Lozowski and Oleskiw 1983).

These models are capable of determining E and β , and hence the theoretical icing intensity, for each time step on the ice profile obtained after the preceding time step, and are therefore not

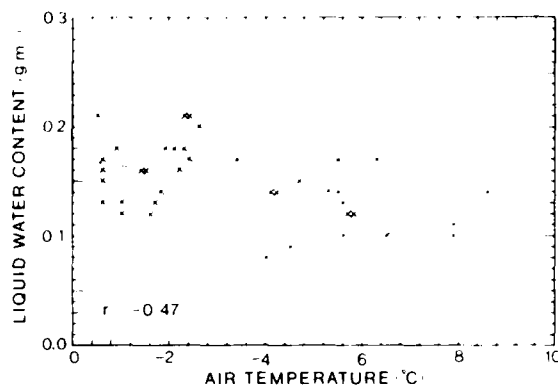
not limited to purely cylindrical surfaces. The models have given some promising results, but their use is restricted because of numerical instability problems. They also use constant ice density, which may degrade the results (Bain and Gayet 1983). MacArthur (1983) has developed a sophisticated, stable, time-dependent model for ice growth on airfoils. The wire-icing model by Makkonen (in press) also simulates ice density variation but is restricted to modeling accretions of near-cylindrical shapes. For overall estimates of the ice loads the non-time-dependent solution for E for a cylindrical surface applied in eq 2 should generally give useful results, since the width of the ice deposit usually does not increase very much in the dry-growth process and since E is not very sensitive to the relatively even form of the rime deposit (McComber and Touzot 1981).

In practical applications of eq 2 and the models based on it, determining E is not the only problem; estimating and predicting the liquid water content w are also difficult. These difficulties originally result from our inability to measure w and the droplet diameter d in clouds and fogs other than by expensive and laborious methods, so that there are few data on these variables and on their correlations with other more easily measurable parameters.

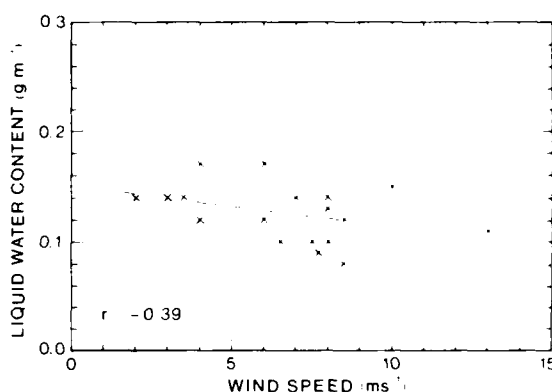
The relationship between d and w for different kinds of fogs is presently poorly known quantitatively, but for freezing rain the Marshall-Palmer distribution may be used (Pruppacher and Klett 1978). Qualitatively the observations made in mountain fogs (Diem 1956) and in stratiform clouds (Fig. 6) indicate that d increases with increasing w . In evaporation fogs (Saunders 1964) this relationship is probably reversed.

There may be a useful relationship between w and wind speed v or between w and air temperature t_a . By estimating w using these relationships it might also be possible to calculate E more accurately and relate median volume diameter d_m with w . An attempt to relate w in icing fogs with v and t_a using available continental data is shown in Figure 7. The correlation is weak, but a slight decrease in w seems to be related to a decrease in t_a and an increase in v . In the marine environment the situation may be somewhat different, especially for evaporation fogs, for which w increases with decreasing t_a (Fig. 8).

Visibility λ is a potential indicator of w , since a reduction in λ is often associated with fog or precipitation. Even on high structures, the upper parts of which sometimes reach the cloud base, the horizontal visibility λ may be used as an indicator of icing events since λ and the height of the lower cloud boundary are statistically correlated, at least in continental locations (Milyutin and Yaremenko 1981). Stanev (1976), for example, demonstrated that w and λ are correlated, and he has used this fact in ice load calculations. However, Mie theory and observations (Kumai 1973) suggest that the relationship between w and λ is not simple but is considerably affected by the droplet size distribution. This is demonstrated in Figure 9, where observations and theoretical relationships for two fogs with different durations (and therefore with different mean droplet diameters) are given. In Figure 9 it can be seen that w can vary by a factor of 3 for the same value of λ . Waibel (1956) has studied experimentally the correlation between the icing intensity and the liquid

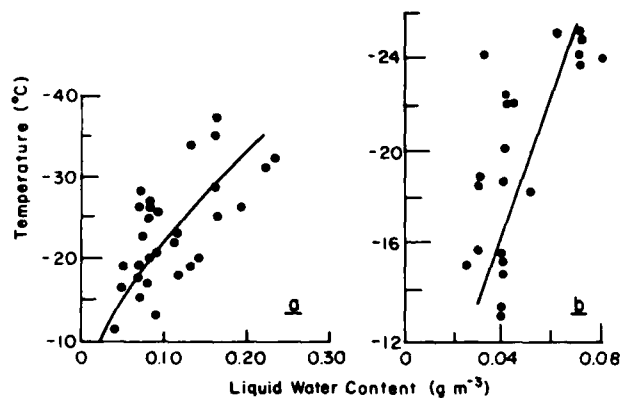


a. Liquid water content vs air temperature.



b. Liquid water content vs wind speed.

Figure 7. Variation in liquid water content in air with air temperature and wind speed. (Data from Glukhov 1971.)



a. Angara.

b. Kola Bay.

Figure 8. Liquid water content of evaporation fogs at various temperatures. (After Bashkirova and Krasikov 1958.)

water content w , and found "only an incidental relation," which is not encouraging either. Hence, visibility alone is not useful for estimating icing intensity, since reliable prediction of the droplet size spectrum of fogs is mostly beyond our abilities. If, however, the median droplet diameter d_m can be estimated, then a better indicator for w can be found: the results of Kumai (1973) indicate that $w = 1.3 d_m / \lambda$ for arctic fogs (Fig. 9). The scatter of the data in Figure 9 is quite large, and there are no data for the whole possible range of conditions. Therefore, more measurements should be made to establish a quantitative relationship between w and λ to be used in estimating icing intensity.

Glaze. In the wet-growth process, which involves the loss of unfrozen water, the intensity of ice accretion can be formulated as

$$I = n E v w \quad (6)$$

where n is the freezing fraction, that is, the ratio of the icing intensity

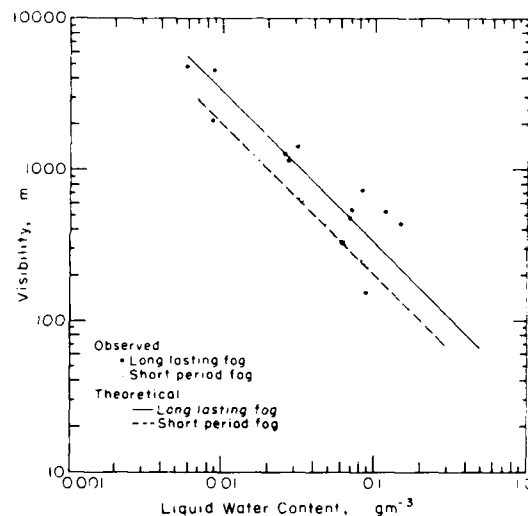


Figure 9. Liquid water content as a function of visibility in Barrow fogs. The lines are calculated by Mie theory for mean size distributions. (From Kumai 1973.)

to the mass flow of the impinging water. In eq 6, n is assumed to be determined by the heat balance of the water film on the icing surface only. Equation 6 can also be expressed in terms of the icing efficiency $E_i = nE$. Accordingly E_i is the ratio of the icing intensity to the mass flow of droplets that would have struck the surface if they had not been deflected in the airstream, and must also be a function of the factors controlling the heat balance of the icing surface.

The heat balance equations for the water film on the stagnation line of the icing surface in the wet-growth process is

$$q_f + q_v + q_k = q_c + q_e + q_w + q_r + q_s + q_i \quad (7)$$

where q_f = latent heat released during freezing

q_v = frictional heating of air

q_k = kinetic energy of the impinging water

q_c = loss of sensible heat to air

q_e = evaporative heat loss

q_w = heat loss in warming to 0°C the mass of water that does freeze

q_r = heat loss in warming the runoff water to the temperature it has when leaving the area of the surface under consideration

q_s = heat loss due to radiation

q_i = heat loss to the substrate due to conduction.

The terms in eq 7 can be parameterized as follows:

$$q_f = I L_f \quad (8)$$

where I is the intensity of ice accretion (mass per unit time and unit area) and L_f is the latent heat of fusion. For the frictional heating of air

$$q_v = (h r v^2) / (2 c_p) \quad (9)$$

where h = heat transfer coefficient

r = recovery factor for viscous heating ($r = 0.9$ at the stagnation line of a cylinder)

v = wind velocity

c_p = specific heat of air at constant pressure.

The kinetic energy of the droplets q_k can safely be neglected on stationary objects under natural atmospheric conditions. For the loss of sensible heat to air

$$q_c = h (t_s - t_a) \quad (10)$$

where t_s is the surface temperature (assumed to be 0°C) and t_a is the air temperature ($^\circ\text{C}$). For the evaporative heat loss

$$q_e = h k L_e (e_s - e_{as}) / (c_p p_a) \quad (11)$$

where $k = 0.62$

L_e = latent heat of evaporation

e_s and e_{as} = saturation vapor pressures over water at t_s and in air at t_a , respectively

p_a = free atmospheric pressure.

In eq 11 it is assumed that the air in a fog is saturated.

The temperature of the droplets in the free stream is very nearly the same as that of air; hence

$$q_w = I c_w (t_s - t_a) \quad (12)$$

where c_w is the specific heat of water.

The temperature of the runoff water leaving the deposit has a considerable effect on the ice accretion, and its determination has been seen as a difficulty in estimating the accretion intensity in the wet-growth process (e.g. List 1977). The problem is much simplified, however, if we consider the stagnation area only, because the water is lost within the water film and its temperature is therefore that of the surface (0°C) unless the impinging droplets bounce. No evidence of noticeable bouncing has been reported near the stagnation line in the conditions corresponding to atmospheric icing on stationary objects. Hence

$$q_r = c_w (E v w - I) (t_s - t_a). \quad (13)$$

The radiation budget at the surface can be estimated, as a first approximation, by neglecting the short-wave radiation in fog conditions and assuming that the emissivity of the fog in the horizontal direction approaches one (Herman 1980). Linearizing the equation for the difference in the emitted radiation of the icing surface and fog, we obtain

$$q_s = \sigma a (t_s - t_a) \quad (14)$$

where σ is the Stefan-Boltzmann constant and $a = 4(273)^3 \text{ K}^3$, assuming that the surface emissivity equals 1.

The Nusselt number $Nu (=hD/k_a)$ and the Reynolds number $Re (=vD \rho_a/\mu)$ in a flow around a smooth cylinder are related at the stagnation point by (Schlichting 1979)

$$Nu = Re^{1/2} \quad (15)$$

where k_a = molecular thermal conductivity

ρ_a = air density

μ = absolute viscosity of air

D = diameter of the cylinder.

Using this result the local heat exchange coefficient h in eqs 9-11 can be expressed as

$$h = k_a (v \rho_a / D \mu)^{1/2} . \quad (16)$$

It has been shown both experimentally (Seban 1960) and theoretically (Sunden 1979) that the Nusselt number depends on turbulent intensity and scale. This effect is not very pronounced during icing in the free atmosphere since it is caused by turbulent eddies much smaller than the icing object and the intensity of turbulence in a free stream on this scale is not very high. The situation may be different near the ground or sea surface and close to other structures that produce small-scale turbulence, as shown by Kowalski and Mitchell (1976), who studied heat transfer from a sphere in the natural environment. They found that the ratio of Nu of the natural environment to Nu in a low-intensity wind tunnel varied from 1.1 at a height of 2 m from the ground to 1.8 at a height of 10 cm.

Another factor that considerably influences the heat transfer coefficient h is the surface roughness. Increasing surface roughness moves the transition point from laminar to turbulent flow upstream, leading to increased heat transfer. Experiments have been made to examine the heat transfer from rough surfaces (Achenbach 1977, Smith et al. 1983), but it is not easy to say which kind of roughness would represent the true accretion surfaces well in different conditions. Lozowski et al. (1979) attempted to account for the effect of roughness on h in their icing model by applying the data of Achenbach for the roughest cylinder tested. This resulted in $Nu = 1.2 Re^{1/2}$ for the stagnation point and a maximum $Nu = 3.6 Re^{1/2}$ at $\theta = 50^\circ$, where θ is the angle measured from the stagnation point. This is valid for $Re = 3.8 \times 10^5$ only; for more precise estimates of Nu on ice accretions, heat transfer measurements should be made for the whole range of Re relevant to atmospheric icing.

The conductive term q_1 is difficult to parameterize, since it depends on the thermodynamic properties of the object undergoing icing. The treat-

ment here is limited to the case where the conductivity of the structure is low, and the case where icing has been going on for a sufficient time for an ice deposit several centimeters thick to develop.

The relative magnitudes of the heat balance terms largely depend on the environmental conditions. In general q_f is the major heat gain term, and q_c and q_e are the dominating heat loss terms; however, q_w becomes more important with increasing liquid water content, and q_s with decreasing wind speed. The term q_v can be neglected except when the wind speed is very high and the air temperature is close to 0°C .

Using the parameterizations in eq 7 and neglecting q_k and q_i , we get an analytical expression for the intensity I :

$$I = k_a \left(\frac{v \rho_a}{D \mu} \right)^{1/2} L_f^{-1} - t_a + \frac{k L_e}{c_p p_a} (e_s - e_{as}) - \frac{r v^2}{2 c_p} - L_f^{-1} (E w c_w + \sigma a) t_a. \quad (17)$$

The values of k_a , ρ_a , μ , c_p and e_{as} in eq 17 depend on the air temperature and can be found from tables or expressed in analytical form in computer simulations. L_f , L_e , c_w , e_s , p_a , σ , a and r can be considered constants. With information on the droplet size spectrum and cylinder diameter, the collection efficiency E can be found, as described for rime. Equation 17 can be used to estimate the intensity of accretion in the wet-growth regime on the stagnation line of a cylinder of arbitrary diameter as a function of air temperature t_a , wind speed v , liquid water content w and droplet diameter d .

The conditions under which the ice accretion process changes from wet growth to dry growth or vice versa can be found by equating the intensities for dry and wet growth given by eqs 2 and 17. By doing so and by taking into account that at the boundary between dry and wet growth $q_r = 0$, we obtain the following expression for the critical liquid water content w_c :

$$w_c = \frac{k_a}{E} \left(\frac{\rho_a}{v D \mu} \right)^{1/2} \frac{-t_a + \frac{k L_e}{c_p p_a} (e_s - e_{as}) - \frac{r v^2}{2 c_p}}{L_f + c_w t_a} - \frac{\sigma a t_a}{E v (L_f + c_w t_a)}. \quad (18)$$

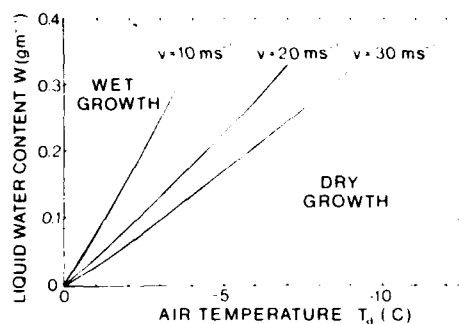


Figure 10. The lines separating the dry-growth and wet-growth processes on a 5-cm-diameter cylinder (stagnation line). The droplet diameter is 30 μm . (From Makkonen 1981b.)

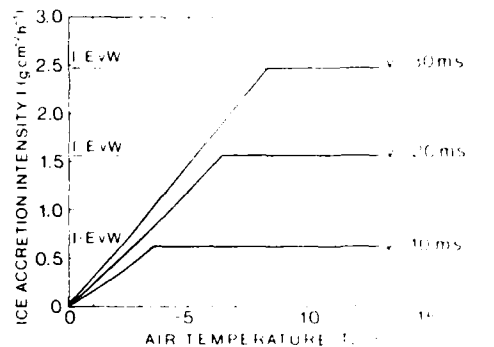


Figure 11. Ice accretion intensity in the stagnation region of a 5-cm-diameter cylinder as a function of the air temperature ($w = 0.3 \text{ g m}^{-3}$ and $d = 30 \mu\text{m}$). (After Makkonen 1981b.)

In a similar manner other critical parameters, such as critical air temperature and critical wind speed, can be solved (although not analytically) for given fixed values of other parameters. Figure 10 shows an example of the critical lines of t_a and w for different wind speed values.

Having established the formulas for estimating the icing intensity for dry growth (eq 2), wet growth (eq 17) and critical conditions (eq 18), we can estimate the icing intensity for the whole range of atmospheric conditions. This is done in Figure 11 by presenting the

icing intensity as a function of the air temperature for different wind speeds, using 0.3 g m^{-3} for the liquid water content of air. An example of the dependence of the accretion intensity on the wind speed, with fixed values for other parameters, is given in Figure 12. The icing efficiency E_i increases with increasing wind due to an increase in the collection efficiency E ($n = 1$ in dry growth) up to the wind speed where the change to the wet-growth process occurs (4 m s^{-1} in Fig. 12), and then decreases due to the decreasing freezing fraction.

Makkonen (1981b) showed that the effect of the runoff term q_r is small during atmospheric ice accretion in conditions near the ground or sea sur-

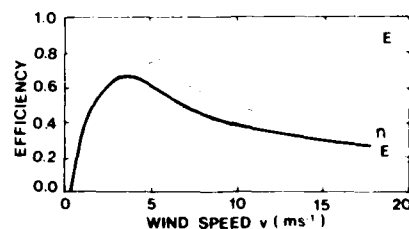


Figure 12. Icing efficiency E_i , freezing fraction n and collection efficiency E on the stagnation line of a 15-mm-diameter cylinder as a function of the wind speed ($t_a = -1^\circ\text{C}$, $w = 0.2 \text{ g m}^{-3}$ and $d = 30 \mu\text{m}$). (After Makkonen 1981b.)

face. For liquid water content values less than 0.5 g m^{-3} (Table 2), the error in icing intensity I caused by neglecting q_r is less than 10% with all combinations of the other parameters relevant to atmospheric icing at sea. This is of great practical importance since it allows the formulation of wet-growth accretion, which is independent of the liquid water content w and the collection efficiency E . Equation 17 then becomes

$$I = \frac{h \left[-t_a + \frac{k L_e}{c_p p_a} (e_s - e_{as}) - \frac{r v^2}{2c_p} \right] - \sigma a t_a}{L_f + c_w t_a} \quad (19)$$

The advantage of eq 19 is that fog properties, which are usually not known and are difficult to forecast, need not be considered, except that enough supercooled droplets must be present for wet-growth icing to occur. Because the maximum intensity of ice accretion at fixed values of v and t_a is reached in the wet-growth process, eq 19 can be used for estimating the maximum intensity of droplet icing at sea. Since w seldom exceeds 0.3 g m^{-3} during atmospheric icing at sea, the curves in Figure 11 can be used as a first approximation of maximum glaze intensity at the stagnation line of cylindrical objects with diameters of more than 5 cm for each combination of v and t_a .

There are two possible mechanisms affecting I that were not considered when deriving eqs 17 and 19. First, hailstone growth simulations show that the excess water, instead of being shed, may be incorporated into the ice structure, giving a spongy ice deposit (Macklin 1961, Roos and Pum 1974). Observations of unfrozen water in glaze deposits on stationary structures under natural conditions have not been reported, however, which is probably because the values of atmospheric parameters in near-ground conditions are quite different from those prevailing during hailstone growth. Lesins et al. (1980) showed that the liquid water fraction of ice on slowly rotating cylinders (0.5 Hz) depends strongly on liquid water content in air; with the smallest value of w in the tests ($w = 2 \text{ g m}^{-3}$) spongy ice was not formed when $-4^\circ\text{C} \geq t_a \geq -16^\circ\text{C}$ and $v = 19 \text{ m s}^{-1}$, which also indicates that spongy ice is not likely in the case of atmospheric icing at sea ($w \ll 2 \text{ g m}^{-3}$).

Second, ice crystals mixed with supercooled water droplets may affect I . Mixed conditions do not seem to lead to greatly enhanced icing rates, however (Ashworth and Knight 1978, Lozowski et al. 1979). Furthermore, the occurrence of ice crystals in liquid water clouds is unlikely in the air temperatures typical of glaze formation (Mason 1971).

In the case of freezing rain and drizzle there are some special aspects in the theoretical treatment of the icing intensity that should be considered. The air temperature is close to 0°C during freezing precipitation, so that it is not likely that dry-growth conditions would prevail except when the liquid water content w is very small. In this case w can be approximated according to eq 20 (Best 1950):

$$w = 0.072 P^{0.88} \quad (20)$$

where P is the precipitation rate in mm h^{-1} . Since the maximum value of P during freezing precipitation is about 4.8 mm h^{-1} according to Stallabrass (1983), w should not exceed about 0.3 g m^{-3} in freezing rain and drizzle. Hence, the use of eq 19 instead of eq 17 seems to be justified in the case of freezing precipitation, too. However, the droplets in freezing rain are large and may therefore not be in complete thermal balance with their environment, as assumed in eqs 17 and 19. This means that the terms q_w and q_r in eq 7 may not be estimated using w and t_a only. Large rain droplets may also bounce from the surface, and the temperature they have when leaving the surface is not known (List et al. 1976). Fortunately the contribution of the terms q_w and q_r to the total heat balance is large only when the icing intensity I is small, so that these problems are overcome when estimating maximum intensities. This is because $(q_w + q_r)/q_f = c_w E v w \Delta t / I L f = c_w \Delta t / n L f \approx 10^{-2} \Delta t / n$, where Δt is the difference in the droplet temperature after bouncing or shedding and before impact. Since Δt can hardly be above 5°C , $(q_w + q_r)/q_f$ is large only if n is small, but then the icing intensity I is also small (eq 6) and far from its maximum value.

As pointed out earlier the maximum intensity of ice accretion for fixed values of t_a and v is reached in the wet-growth process, and is therefore limited by t_a and v (Fig. 11). Hence, these parameters do not reach their extreme values during freezing precipitation. For freezing precipitation the mean value of t_a was -0.4°C (minimum -6.5°C) and the mean value for v was 5.9 m s^{-1} (maximum 14.9 m s^{-1}) in a 10-year period at Toronto Airport, according to Stallabrass (1983). Even at coastal regions v seldom reaches high values during freezing precipitation (Austin and Hensel 1956). According to Stallabrass (1983), 98.5% of the hourly wind readings during freezing precipitation are contained within the velocity-temperature envelope by the relation

$$v = 1.5 t_a + 18 \quad (21)$$

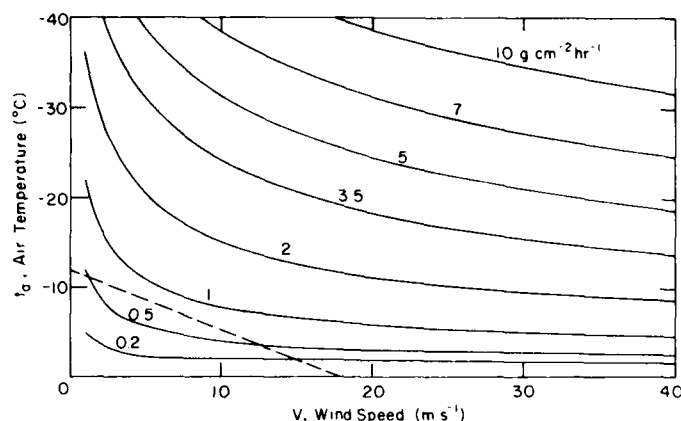


Figure 13. Theoretical icing intensity as a function of wind speed and air temperature. The calculation is made for a 5-cm-diameter cylinder supposing unlimited liquid water content (wet growth for all combinations of v and t_a) but neglecting the effect of runoff water on the heat balance. The dotted line represents eq 21.

where v is in m s^{-1} and t_a is in $^{\circ}\text{C}$. Equation 21 may be used with eq 19 in estimating the maximum icing intensity during freezing precipitation. This is demonstrated in Figure 13, where the line representing eq 21 is presented along with the icing intensity I as a function of t_a and v as calculated from eq 19.

The ice deposit diameter D is involved with the calculation of the icing intensity (eq 17), and the surface area for the heat exchange between the deposit and air to take place depends on D as well. Moreover, the shape of the ice accretion on fixed objects usually becomes noncylindrical, and this also alters the surface area and the local and overall heat exchange coefficients. Therefore, as with dry-growth simulation, time-dependent models have been developed for calculating ice loads after some time of accretion (e.g. Lozowski et al. 1979, MacArthur 1983). An example of the results from a time-dependent model by Makkonen (in press) that simulates icing on wires in both dry and wet growth is presented in Figure 14.

Finally, Borisenkov's (1969) formula for estimating the rate of ice accretion on sea structures should be mentioned. It has been widely cited and suggested for use (e.g., Panov and Schmidt 1971, Borisenkov and Pchelko 1972, McLeod 1977, Minsk 1977, Lundqvist and Udin 1978, Aksiutin 1979), although a sound theoretical description of ship icing intensity has been presented by

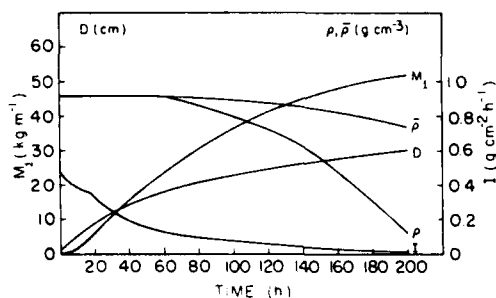


Figure 14. Numerical simulation of ice accretion on a 1-cm-diameter wire. The simulated quantities are ice load M_i , ice deposit diameter D , icing intensity I , density of accreting ice ρ and the total deposit density $\bar{\rho}$. The wind speed is 20 ms^{-1} , the air temperature is -1°C , the liquid water content is 0.3 g m^{-3} , and the median-volume droplet diameter d_m is $25 \text{ }\mu\text{m}$. (From Makkonen, in press.)

Kachurin and Gashin (1969) and in a more sophisticated form by Kachurin et al. (1974). The formula by Borisenkov (1969) for atmospheric icing ($t_{\text{drop}} = t_{\text{air}}$) reads

$$I = \frac{t_s - t_a + 2.6 L_e p_a^{-1} (e_{as} - e_s)}{L_f + c_i (t_a - t_s) + c_w (t_s - t_a)} \quad (22)$$

where c_i is the specific heat of ice.

According to eq 22, I increases with increasing e_{as} , which seems illogical since evaporation decreases with increasing e_{as} (eq 11). Also, the effect of the term q_w in eq 19 is reversed in eq 22. Finally, the term $c_i (t_a - t_s)$ in eq 22 represents the heat released in cooling of the ice after it has turned into ice, but this heat flux must be directed inwards, since the ice near the surface is warmer than the underlying ice and should therefore not be involved with the surface heat balance controlling icing intensity in wet growth. In dry growth, on the other hand, the heat balance does not restrict I at all. Because of these inconsistencies eq 22 is not recommended. It gives values for I more than an order of magnitude smaller than those from eq 19 and those obtained experimentally for atmospheric icing.

Wet snow. Wet snow accretes on a structure when snowflakes covered by a thin water film strike the structure's surface and adhere to it. Snow particles become wet while falling through a layer where the air temperature is above 0°C . This layer must not be too thick or the snowflakes would melt completely; therefore, t_a at the surface layer where the snow accretion on structures occurs is close to 0°C .

Snow accretion on structures is frequently observed in humid air and in air temperatures somewhat above the freezing point of water, which reveals that no external cooling of the snow deposit is required for the deposit to grow (Makkonen 1981a, Colbeck and Ackley 1983). In fact, Wakahama et al. (1977) demonstrated that the free-water content of the deposit increases dur-

ing accretion. Also, the observations that snow accretions on wires are often not attached to them but form a loose-fitting cylinder around the wire (Bauer 1973) indicate melting in the deposit. That the density and strength of the snow deposit increase and that it turns hard and often nearly transparent in spite of melting in the deposit can be explained by deformation in the deposit caused by the impact of the snow particles and by wind drag. These forces create a packing stress on the snow, which becomes denser and undergoes a deformation process in which large snow particles grow at the expense of smaller particles (Colbeck 1979, Colbeck and Ackley 1983). This process is comparable to what happens when squeezing a snowball.

Since freezing of the snow deposit is not necessary for the accretions to grow, it is apparent that heat exchange with the environment does not substantially control the growth rate I_s of wet snow deposits. Therefore, the theoretical approach used for rime (eq 2) is more appropriate in estimating I_s than heat balance considerations. The amount of snowflakes in air w_s can be used in eq 2 as w was for rime formation. The snow content w_s may be obtained from visibility data, for example (Wasserman and Monte 1972, Stallabrass 1983). According to Stallabrass (1978a), w_s and visibility λ (in meters) are related by

$$w_s = 2100 \lambda^{-1.29}. \quad (23)$$

Wakahama et al. (1977) showed that the collection efficiency E in eq 2 is close to one for wet snowflakes accreting on objects the size of power line conductors in moderate wind speeds, so that applying eq 2 to the snow problem would be easy in this respect, too.

Unfortunately there are some additional problems that arise when using eq 2 in calculating snow accretion. First, although the snow particles would strike the icing surface so that $E = 1$, they are not eventually collected since they tend to rebound from the surface. The "final collection efficiency" may be as low as 0.2 due to rebounding (Wakahama et al. 1977); the factors controlling the portion of rebounding particles are not known. Second, the excess free water in the wet snow deposit may be removed from the lee side of the deposit, reducing its weight. Consequently our ability to estimate the growth rate of wet snow deposits is limited, and more experimental data are needed. Laboratory experiments are being made to clarify the problem (Wakahama 1979, Wakahama et al. 1979).

One possibility for estimating the wet snow accretion rate is to relate it to the measured precipitation rate during icing conditions (Shoda 1953), but large errors are probable with this method because of unknown factors controlling snow deposit growth on structures and because of inaccurate precipitation measurements during snowfall, especially at high wind speeds.

When wet snow accretes on a wire such as an electrical conductor or a guy wire, twisting of the wire or sliding of the snow deposit along the wire surfaces seem to be necessary for heavy snow deposits to grow, since these processes allow a cylindrical deposit that envelopes the wire effectively (Wakahama 1979). If the object is fixed or if sliding to the lee side of the deposit is prevented, the deposit is more easily broken or blown away by the wind. Therefore, vertically situated objects and large objects are likely to experience less severe wet snow accretion than do horizontally elongated wires and small structures, for instance.

Hoarfrost. According to the eddy diffusion theory the mass growth rate I of hoarfrost formed by condensation is controlled by the water vapor pressure in air e_a , by the water vapor pressure at the icing surface e_i , and by the wind speed v according to the equation

$$I = k C_e \rho_a v (e_a - e_i) / p_a \quad (24)$$

where C_e is an empirical transfer coefficient for water vapor, which depends on the surface roughness and the thermal stability of the boundary layer (compare with eq 11). Although I is controlled by eq 24, the growth rate of frost thickness seems to be independent of the ambient conditions of mass transfer (Schneider 1978) because of a corresponding change in the frost density. It follows from eq 24 that frost growth is possible if the surface is sufficiently cold compared to air, but that it is also possible when the surface temperature and air temperature are the same if the relative humidity in air is close to 100%. This is seldom the case in the natural boundary layer, so surface cooling is usually required for hoarfrost to form in the natural environment. Cooling in the surface lowers e_i and therefore controls the intensity of frost formation I , according to eq 24. It follows, then, that we can estimate the maximum growth rate I_m by examining the heat balance of the icing surface, since this balance controls the surface temperature and hence the saturation water vapor pressure e_i at the ice surface. For practical purposes this is a simpler method for estimating I_m than eq 24 because of the difficulties in estimating e_i and the transfer coefficient C_e .

The heat balance (eq 7) in the absence of supercooled water droplets becomes

$$q_f - q_e = -q_v + q_c + q_s + q_i \quad (25)$$

where $q_f - q_e = q_{\text{cond}}$, the latent heat released in condensation. Also,

$$q_{\text{cond}} = I L_c \quad (26)$$

where L_c is the latent heat of condensation. Since we wish to estimate the maximum intensity I_m , we can neglect the terms q_c and q_v , which in the situation examined give heat to the surface and tend to reduce icing intensity. Furthermore, for objects which are not internally cooled, the surface temperature is lower than the temperature inside the ice or in the structure, so the conductive term q_i also tends to warm the surface and can be neglected. Without q_c , q_v and q_i , eq 25 becomes

$$q_{\text{cond}} = q_s \quad (27)$$

Combining this with eq 26, we get

$$I = q_s / L_c \quad (28)$$

which gives the theoretical maximum intensity of hoarfrost formation. According to eq 28, the rate of frost growth is controlled by radiation from the surface in such a way that the radiative heat loss is balanced by the latent heat released by condensing water vapor. Using the value $q_s = 100 \text{ W m}^{-2}$ for the maximum radiative loss on a horizontal surface (Gavrilova 1966), we obtain $I = 0.013 \text{ g cm}^{-2} \text{ h}^{-1}$ ($0.3 \text{ g cm}^{-2} \text{ d}^{-1}$). The highest observed condensation rates are on the order of $0.1 \text{ g cm}^{-2} \text{ d}^{-1}$ (Nyberg 1966). These estimates clearly show that the formation of hoarfrost is negligible compared to the typical growth rates of glaze, rime and wet snow.

Empirical verification

The dry-growth theory has been found to predict fairly accurately the icing intensity I and the ice surface temperature in laboratory experiments (Lozowski et al. 1979, Stallabrass and Hearty 1979). Also, the change from dry growth to wet growth found in laboratory experiments (Ludlam 1951, Macklin 1961) was predicted by the theory. Comparisons of the wet-growth theory with laboratory conditions have shown satisfactory agreement as well (Stallabrass and Lozowski 1978, Lozowski et al. 1979). There are, however, some

discrepancies in the results from different experiments, probably due to wind tunnel blockage, turbulence, and inaccuracy in determining liquid water content w and droplet diameter d . The theoretical predictions of I in wet-growth have generally slightly underestimated the growth rate, which may be due to underestimation of the heat exchange coefficient h for ice deposits with somewhat uneven shapes and rough surfaces. Unfortunately for those studying atmospheric icing on sea structures, practically all the laboratory experiments attempting to confirm the wet-growth theory have been made with much higher values of w and v than those typical for atmospheric icing. However, the agreement between theory and experiment seems to be better for low than for high values of w and v (Lozowski et al. 1979). Stallabrass and Hearty (1967) found in the laboratory experiments that the resulting ice thickness does not depend on the cylinder diameter D , in contradiction with eq 17. This suggests that the Nusselt number Nu at the stagnation line of a rough ice deposit would be proportional to Re rather than to $Re^{1/2}$ (eq 15). Another reason for this result may be that for the blockage ratio of more than 6%, the flow is distorted considerably (West and Apelt 1982); in the wind tunnel experiments by Stallabrass and Hearty (1967) this ratio varied from 3 to 26%, depending on D .

The decisive verification of the theoretical results should, of course, be made in the real outdoor environment. This is extremely difficult, however, mainly because of the difficulties in accurately determining the atmospheric conditions, especially the liquid water content w and the droplet size distribution. Moreover, the variability of conditions in nature is not easy to take into account in theoretical simulations. For these reasons there are not many experimental results from the outdoor environment that could be used to quantitatively verify the theory, but by fixing some parameters in theoretical calculations it is possible to achieve qualitative results for the effects of the other parameters that then can be compared to observations. For example, the dependence of ship icing severity on wind speed and air temperature in Figure 15 can be compared to Figure 13. Iwata (1973) and Kachurin et al. (1974) also verified the heat balance theory for estimating ship icing intensity, with satisfactory results. The dependence of icing efficiency E_i on wind speed according to the data of Glukhov (1971) in Figure 16 is comparable to the theoretical prediction of Figure 12. Figure 17 shows an attempt to compare quantitatively the theoretical icing intensity I with observations from nature; the near-linear dependence of I on

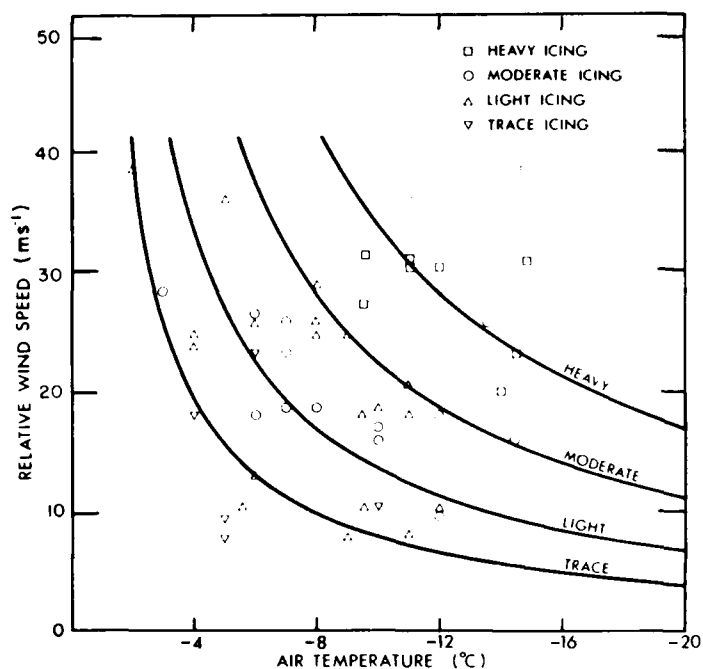


Figure 15. Effect of air temperature and relative wind speed on reported icing severity for fishing vessels steaming at low speeds (2 ms^{-1} and below) according to Stallabrass (1980).

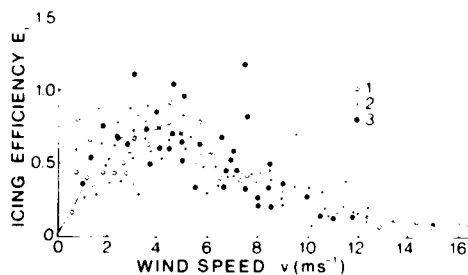


Figure 16. Dependence of the overall icing efficiency on the wind speed for various liquid water contents w according to Glykhov (1971), where 1) $w = 0.12-0.16 \text{ g m}^{-3}$, 2) $w = 0.17-0.21 \text{ g m}^{-3}$, 3) $w = 0.22-0.26 \text{ g m}^{-3}$. (From Makkonen 1981b.)

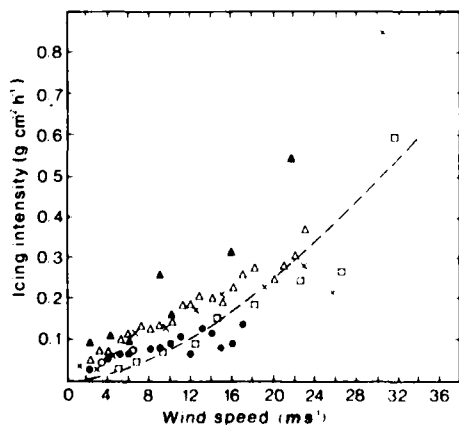


Figure 17. Dependence of cylinder icing intensity on wind speed according to observations in the natural outdoor environment and according to the theory with arbitrary constant parameters (dotted curve). x = Waibel (1956); \square = Rink (1938); \circ = Ahti and Makkonen (1982); \bullet = Baranowski and Liebersbach (1977), soft rime; Δ = Baranowski and Liebersbach, hard rime; \blacktriangle = Baranowski and Liebersbach, glaze. The points, except those by Baranowski and Liebersbach, represent a mean value for a wind speed interval. The theoretical curve is calculated for dry growth using the values $D = 5 \text{ cm}$, $d = 25 \text{ }\mu\text{m}$ and $w = 0.1 \text{ g m}^{-3}$.

v , on the average, is demonstrated. The scatter of the points in Figure 17 is considerable, although they represent mean values of the data for different wind speed intervals. The magnitude of the scatter of the individual observations can be seen in Figure 18, showing that v explains only a small portion of the variance of the intensity of icing. The linear correlation coefficient between I and v is about 0.5 for glaze and hard rime, but much lower for soft rime. The formula

$$I = 10^{-2} v \quad (29)$$

where I is in $\text{g cm}^{-2} \text{ h}^{-1}$ and v in m s^{-1} , roughly describes the mean behavior of I in Figures 17 and 18, but the relationship between I and v is somewhat different for each ice type, as seen in Figure 18. This is probably because the mean values of w and d are different for each ice type, as indicated by the theory. The theoretical result that I is independent of air temperature in dry growth agrees with Figure 19, which shows the intensity of icing scaled with the wind speed as a function of t_a . For glaze the dependence of E_{iw} on t_a is contrary to the theoretical prediction with constant w and d , indicating that w decreases with decreasing t_a , on the average. As can be seen in Figure 7, this may not be the case at sea, however. This demonstrates that the results from continental locations, such as those in Figures 17-19, must be used with great care when making predictions for the marine

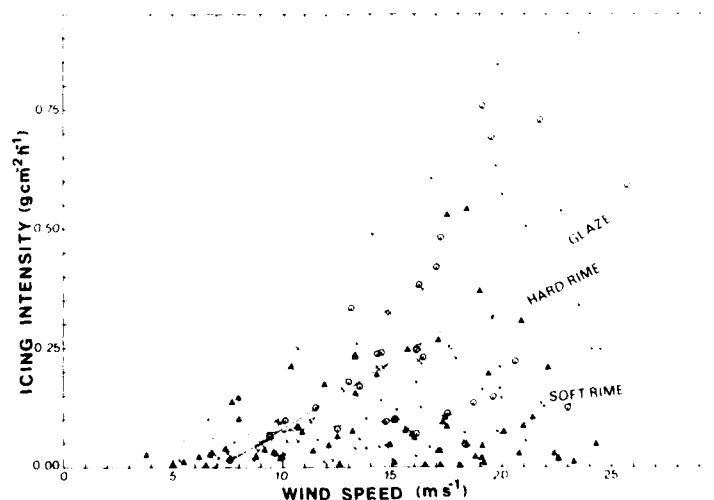


Figure 18. Icing intensity vs wind speed. The linear correlation coefficients are $r = 0.54$ for glaze and hard rime and $r = 0.20$ for soft rime. \circ = glaze; Δ = hard rime; \times = soft rime. (Data from Rink 1938.)

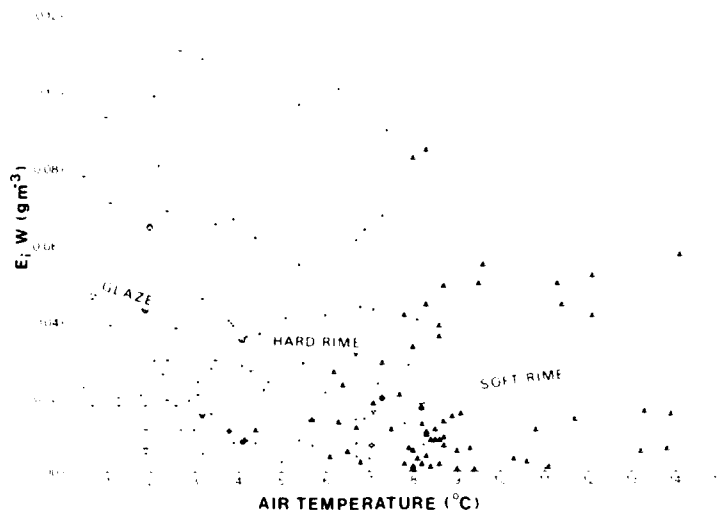


Figure 19. Icing intensity divided by wind speed vs air temperature. (Data from Rink 1938.)

environment. The statistical relationship between I and wind speed is not determined only by the mechanisms of icing and the mean values of the relevant parameters, but also by the correlations of these parameters. These correlations may be substantially different over the sea and in continental locations. If I at sea is estimated from data such as in Figures 17-19, the scatter of the values of I in relation to v , for example, is considerable, which is not encouraging. However, the maximum icing intensity seems to be more closely related to v in Figure

18. Also, Makkonen and Ahti (1983) showed that, at least in a continental region, ice loads can be estimated using the wind speed and duration of icing only (Fig. 20). If the liquid water content can be estimated (eq 20, Fig. 1 and 7, Table 6), then useful predictions of the ice loads on sea structures should be within reach.

METEOROLOGICAL CONDITIONS DURING ICING EVENTS

To be able to forecast icing and analyze statistical risks based on meteorological data it is important to know the atmospheric conditions in

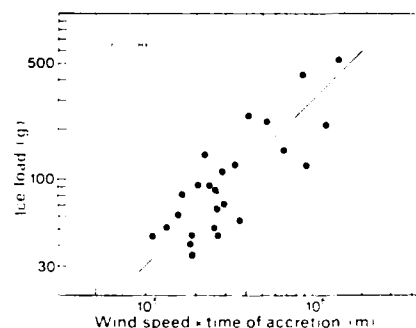


Figure 20. Ice load vs wind speed multiplied by the estimated time of in-cloud conditions according to Makkonen and Ahti (1983).

which atmospheric ice accretion is likely. The meteorological conditions that prevail during ship icing have been studied widely (Shektman 1968, Tabata 1968, Borisenkov and Pchelko 1972, Smirnov 1974, Lundqvist and Udin 1977, Stallabrass 1980). In the data of these studies atmospheric icing events are rare and have in most cases not been distinguished from spray icing events. Therefore, ship icing data are not very useful in calculating the conditions where atmospheric icing occurs, so theory and observations from continental locations must be used.

Boundary layer conditions

Air temperature and wind. In general, rime or glaze may form when there is liquid water in the air, the air temperature t_a is below 0°C , and there is air movement with respect to the object considered. However, there are some deviations from this generalization. For example, ice accretion is possible when $t_a > 0^{\circ}\text{C}$ if the icing surface is cooler than 0°C due to radiative cooling or evaporation. Icing does not occur in low air temperatures if the surface is warmer than 0°C due to internal heat transfer in the structure or due to solar radiation.

The practical upper limit for t_a during ice accretion by water droplets seems to be about 2°C for vertical surfaces (Sadowski 1965, Volobueva 1975) and about 3°C for horizontal surfaces (Lenhard 1955, McKay and Thompson 1969). The difference is obviously due to more intensive outgoing radiation in the vertical direction. The upper limit for wet snow accretion is about 1.5°C in nature (Shoda 1953, Sadowski 1965), but in laboratory simulations wet snow accretions have been grown at air temperatures as high as 2.0°C (Wakahama et al. 1977).

There seems to be no lower limit for t_a during droplet accretion in the range of t_a values probable over the sea. The lower limit for t_a observed in different studies varies according to local conditions, but icing is not rare at air temperatures below -20°C (Dranevic 1971, Volobueva 1975, Makkonen and Ahti 1983). [The lowest air temperature reported during wet snow accretion is -4°C (Sadowski 1965).] The theoretical lower limit for t_a is determined by the temperature at which the supercooled water droplets crystallize. According to Bashkirova and Krasikov (1958) this temperature is about -20°C over the sea. The limiting values of t_a for the different ice types are discussed in more detail later.

In addition to the maximum and minimum air temperatures during icing it is interesting to know the frequency of icing in different temperature intervals, since these data can be used in estimating icing probabilities. Data on the distribution of icing events with air temperature are available for many continental regions, but they are apparently not representative of the marine environment due to different statistical features of the boundary layers over the ground and over the sea. It seems reasonable, however, to assume that since atmospheric icing in continental areas mostly occurs close to 0°C (Fig. 21), this will be the case at sea as well. According to McLeod's (1981) data for the Gulf of Alaska t_a is in the range of -3° to 0°C for the reported icing events. However, evaporation fogs, which are a potential source of icing at sea, are formed at low air temperatures, so it is possible that the atmospheric icing probability distribution according to air temperature has two peaks. More data from actual offshore conditions are necessary to clarify this.

There are no data on the effect of wind speed on the frequency of occurrence of atmospheric icing over the sea. Based on continental data, Figure 22 shows the distribution of icing events according to wind speed in one location, and Figure 23 shows the frequency of icing with vertical wind shear in the atmospheric boundary layer.

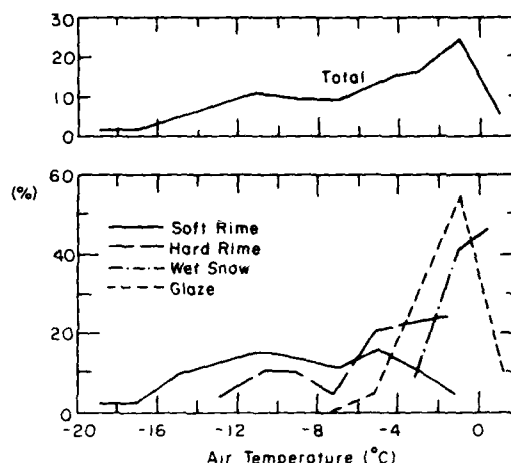


Figure 21. Frequency of atmospheric ice accretion related to the air temperature. (After Sadowski 1965.)

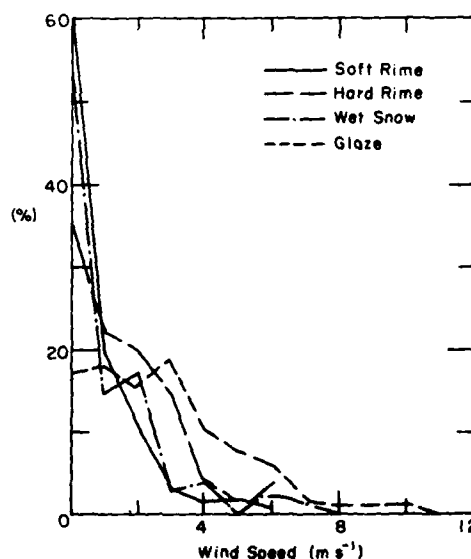


Figure 22. Frequency of atmospheric ice accretion related to the wind speed. (After Sadowski 1965.)

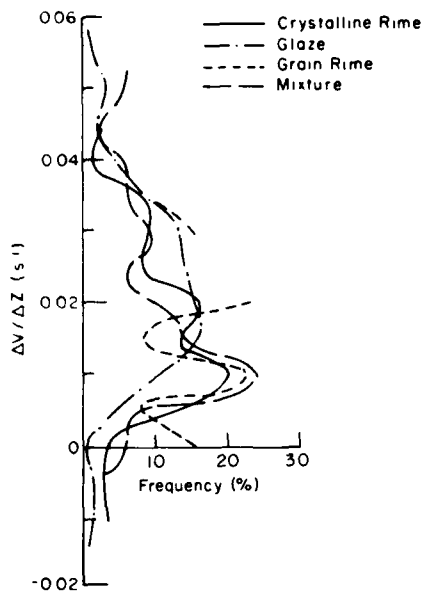


Figure 23. Frequency of atmospheric ice accretion related to the wind shear in the lowest 300 m of the boundary layer. (From Dranevic 1971.)

The distribution of icing cases according to wind direction is usually quite uneven in continental regions. This is probably true at sea as well. Generally winds from the north are more likely to be associated with icing on the open sea than winds from the other quarters (in the northern hemisphere). However, local differences are large, depending on the local synoptic conditions and the direction to the nearest coast.

Precipitation and humidity. It is well known that supercooled precipitation may cause serious damage in continental regions. However, the views regarding the contribution of precipitation events to the total ice loads, that is, its importance compared to icing due to fogs (in-cloud icing), are contradictory. Some authors have seen precipitation as a necessary condition for atmospheric icing (Lenhard 1955, McLeod 1981); others have used precipitation as the main parameter in models for forecasting icing (e.g. McKay and Thompson 1969, Chaine 1974). On the other hand, Waibel (1956) and Ahti and Makkonen (1982) showed that icing intensity has no correlation with measured precipitation amounts, and Rink (1938) and Sadowski (1965) showed that the majority of icing events are observed on days with no precipitation. These discrepancies can be partly explained by the fact that the frequency of precipitation during icing in continental regions clearly depends on locality, mostly because of orographic effects (Lomilina 1977).

The question of the importance of supercooled precipitation is even more troublesome over the sea, since experimental data are lacking. Ship reports

do not give much data for this problem because liquid precipitation has usually not been distinguished from fog or snow in these observations. Coastal and island data may not be representative either, since the temperature inversion necessary for the falling water droplets to supercool (see the solid curve in Fig. 24) mostly develops due to radiative or advective cooling of the air in the surface layer, and this cooling is much less pronounced over water due to mixing and the large heat capacity of water, which prevent the surface temperature from decreasing rapidly. Moreover, it is impossible for the surface layer in air above water to cool much below 0°C (to -2°C at the most), so the formation of a surface inversion at freezing temperatures is unlikely over the sea. For these reasons freezing precipitation at sea far from the coasts or sea ice boundaries is not to be expected. However, a secondary temperature inversion, as shown by the dotted curve in Figure 24, is possible near the coast during offshore winds. This kind of surface layer is unstable and does not extend very far from the coast.

The humidity conditions during atmospheric icing vary within a rather large interval. One might expect that during fog or precipitation the relative humidity R would be quite close to 100%, but Figure 25 shows that this

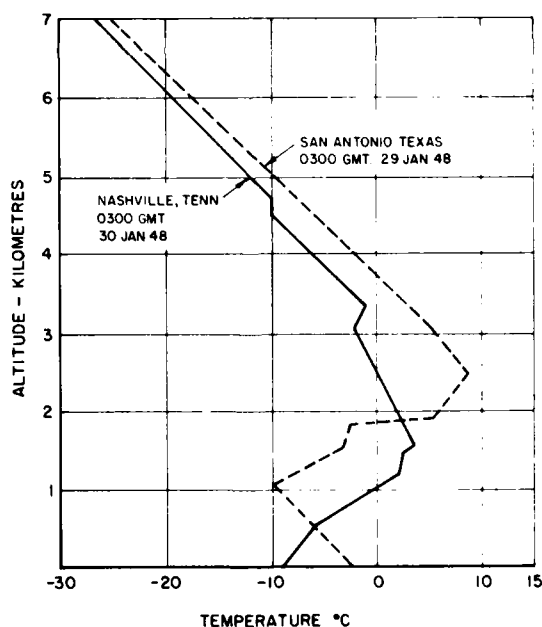


Figure 24. Typical temperature profiles during supercooled precipitation at the ground. (From Stalla-brass 1983.)

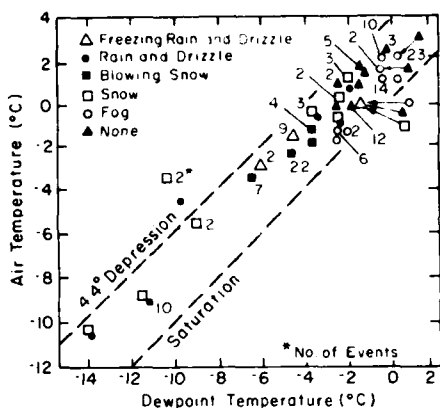


Figure 25. Icing events related to air temperature and dewpoint spread. (After McLeod 1977.)

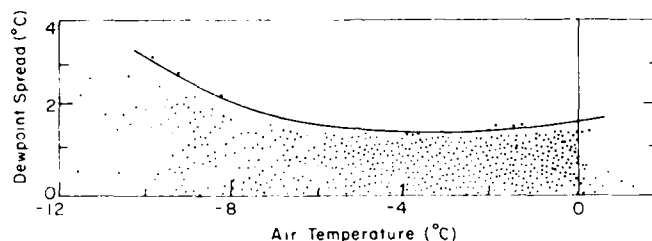


Figure 26. Glaze events related to air temperature and dewpoint spread. (From Dranevic 1971.)

is apparently not always the case. For icing in a fog, this is probably because of the heterogeneity of air humidity produced by turbulence and entrainment and because droplets can form from water vapor when R is slightly below 100% (Woodcock 1978). Also, supersaturation in air is reached with respect to ice before it is reached with respect to water as R increases. During freezing precipitation R may be as low as 70%. According to data from Toronto R was less than 90% during 20% of the time with freezing precipitation (Stallabrass 1983). Figure 26 gives continental data for the dewpoint spread during glaze formation at different air temperatures. According to Dranevic (1971) the dewpoint spread is slightly smaller during rime formation than during glaze formation at the same air temperature.

Matsuo et al. (1981) have derived equations for relative humidities favorable for wet snow occurrence at different air temperatures based on continental observations. Qualitatively the level of R at which wet snow occurs decreases with decreasing t_a . This is probably true at sea as well, but there are no quantitative data.

Fogs. For severe atmospheric ice accretion to occur it is necessary to have supercooled water droplets in the air. In most cases this means fog in the atmospheric boundary layer. Since other conditions necessary for severe ice accretion (freezing temperatures, strong winds) are quite common in arctic waters, the existence of fogs at air temperatures below 0°C is the key factor determining the frequency of atmospheric ice accretion at sea. For this reason the conditions favorable for the formation of supercooled fogs in the marine environment are discussed in more detail.

Fogs are often classified into three categories: radiation fogs, which develop when air cools as a result of radiative cooling of the underlying surface; advection fogs, which form when warm air is cooled when it moves over a cold surface; and evaporation fogs, which result when air moistened by evaporation from a water surface is mixed with colder air, resulting in condensation and droplet formation. Radiative fogs do not occur at sea because the sea surface cools too slowly.

Advection fogs, on the other hand, are quite common over the sea, the fogs in the English Channel and the Grand Banks of Newfoundland being the best-known examples. However, icing from supercooled advection fog is rare. Cooling of surface air to temperatures below 0°C is possible only if the surface temperature of the sea t_w is below 0°C . Therefore, supercooled advection fogs may occur only over oceans with saline water and with $t_w < 0^{\circ}\text{C}$. Supercooled advection fogs formed over land and brought over the sea can prevail only under the same conditions, the surface layer being otherwise unstable. The other limiting condition is that the air temperature is higher than the surface temperature; this is significant because the maximum icing intensity is limited by the air temperature, so extreme icing rates are not possible in advection fogs, whose temperature must be above -2°C . This is demonstrated in Figure 27, which shows the temperature conditions necessary for supercooled advection fog.

Evaporation fog (sea smoke) typically occurs at low air temperatures and is therefore a possible source of severe icing if its liquid water content is high and strong winds prevail (Lee 1958, Shannon and Everett 1978). Several conditions have been suggested as necessary for the occurrence of evaporation fog. Jacobs (1954) suggested that the sea-air temperature difference must be more than 9°C for the onset of evaporation fog. According to Church (1945) the vapor pressure difference between the water surface and the air must be more than 0.5 kPa for evaporation fog to develop. Vapor pressure in air e_a

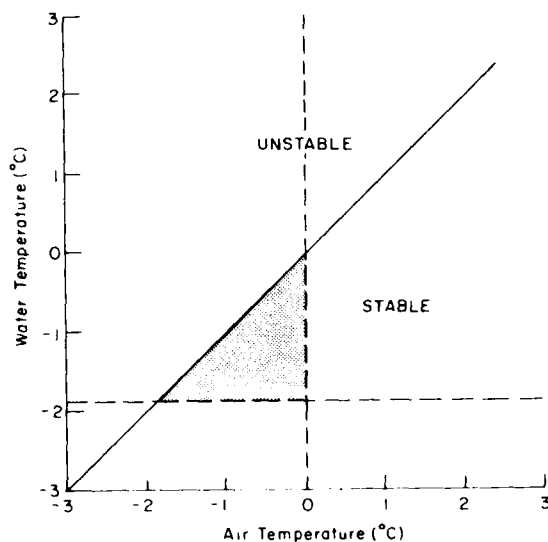
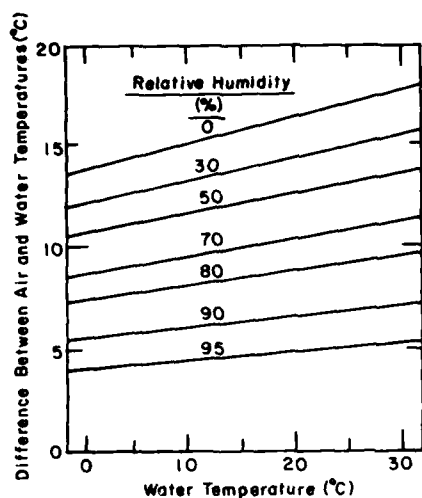


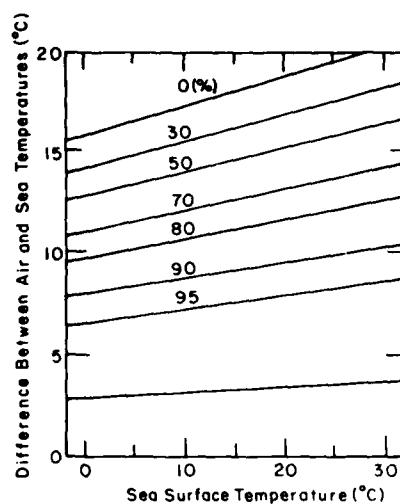
Figure 27. Regime of supercooled advection fog over the ocean (shaded area). The solid line represents thermally neutral conditions, the horizontal dotted line the limiting water temperature, and the vertical dotted line the limiting air temperature.

correlates strongly with air temperature t_a , and these determine the relative humidity R . On the other hand, water vapor at the water surface e_s is a function of the water temperature t_w . Therefore, the conditions suggested by Church (1945) can also be formulated by means of t_a , t_w and air humidity. This has been done by Currier et al. (1974), giving the index $i = (t_w - t_a) / (e_{as} - e_a)$, where e_{as} is the saturation water vapor pressure in air [$e_{as} = f(t_a)$]. In the data of Currier et al. (1974) the probability of the occurrence of evaporation fog varied from 0.04 for $i = 10$ to 1.00 for $i > 90$. Saunders (1964) derived theoretical conditions that also include t_a , t_w and R ; his results are presented in Figure 28. Utaaker (1979) has verified the theoretical conditions and found a satisfying agreement with actual observations. Wind speed has not been found to have any effect on whether evaporation fog forms (Hicks 1977).

The onset of supercooled fog is not always the threshold condition for icing on marine structures, because these fogs are often limited to only a few meters above the sea surface. The vertical extent z_f of evaporation fog is therefore important. The height z_f can be from 0 to at least 100 m, where it can reach (or form) a stratus cloud (Church 1945). Observations by Utaaker (1979) show that z_f clearly depends on the sea-air temperature difference, that is, on the difference between t_w and the threshold value of t_a based on Figure 28. These observations are shown in Figure 29, which shows that the scatter of z_f values at the same temperature difference is quite large, indicating that there are additional factors affecting z_f . One possible factor



a. Necessary properties of air for the steaming of freshwater.



b. Necessary properties of air for the steaming of saline water (salinity 35 ‰).

Figure 28. Conditions necessary for evaporation fog. The relative humidity is measured near the surface in the cold air. (From Saunders 1964.)

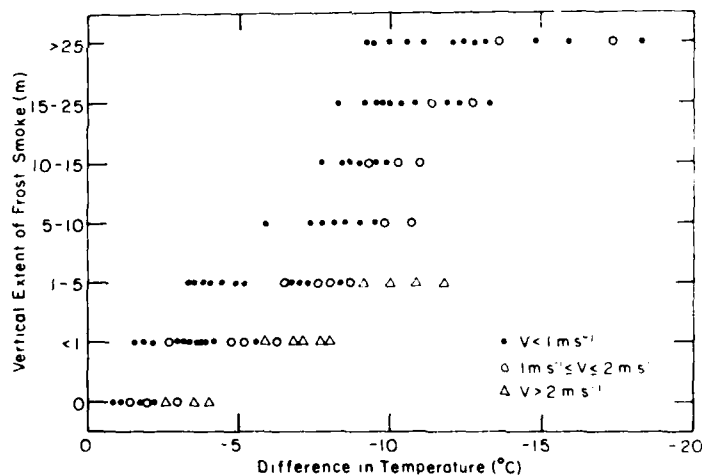


Figure 29. Vertical extent of evaporation fog vs the difference between the air temperature at 2 m and the critical temperature given by the theory of Saunders (1964). (From Utaaker 1979.)

is wind speed v ; Wessels (1979) suggested on theoretical grounds that z_f can be determined by

$$z_f = 0.003 P_f^{-3.05} (-L) \quad (30)$$

where P_f is the critical rate of mixing, which depends on temperature and humidity conditions only (Wessels 1979), and L is the Monin-Obukhov length characterizing the stability conditions in the atmospheric surface layer. According to Wessels, for moderate wind speeds and water surface about 15°C warmer than air, the definition for L can be simplified to

$$-L \approx 3.2 v^2 / (\theta_w - \theta_a) \quad (31)$$

where v is wind speed at a height of 10 m, and θ_w and θ_a are the potential temperatures of water and air at 10 m, respectively. If z_f is roughly proportional to $-L$, as indicated by eq 30, then it follows from eq 31 that z_f is strongly affected by the wind speed v (other conditions being fixed) such that z_f increases with increasing v . Also, the results of an evaporation fog model by Matveev and Soldatenko (1977) show an increase in z_f with increasing v . This increase is important because high wind speeds are associated with the most serious icing conditions. The models of Wessels (1979) and Matveev and Soldatenko (1977) are also capable of simulating the properties of evaporation fog (such as z_f and w) as a function of the downwind distance from the shore (Table 6). These aspects dealing with the horizontal extent of icing risk from the shore are discussed in more detail later.

Sea surface temperature and salinity. Sea surface temperature has, naturally, no direct effect on atmospheric icing (in contrast to spray icing), but it has an indirect influence. First, the modification of cold air flowing from the continent over the sea is controlled by the sea surface temperature t_w along the air trajectory. Air temperature (and to a lesser extent, wind speed and the characteristics of fog and precipitation) is affected by surface layer stability, which is partly determined by t_w . Second, the occurrence of advection fogs (Fig. 27) and evaporation fogs (Fig. 28) is controlled by t_w .

Figure 28 shows that the salinity of seawater affects the onset of evaporation fogs such that fogs develop at smaller water-air temperature differences and higher relative humidities over freshwater than over saline water. The air temperature range for the possible occurrence of supercooled advec-

tion fogs is more limited when water salinity is low (Fig. 27). Supercooled advection fogs obviously cannot extend over freshwater surfaces for long distances.

Synoptic weather conditions

Forecasts of meteorological variables in the boundary layer are generally based largely on synoptic weather maps and numerical analyses of synoptic-scale phenomena. Therefore, one possible way of forecasting icing at sea is to relate surface icing conditions directly to synoptic weather conditions. There are, however, many difficulties in doing this, especially in coastal regions where mesoscale phenomena are very important in determining the surface conditions due to changes in surface roughness and temperature over the coastline. For example, situations that look similar on a synoptic weather map may be associated with quite different surface conditions in different seasons due to differences in sea surface temperature and ice edge location. Also, the variety of synoptic weather conditions is so large that any classification of typical weather conditions where icing occurs must be very rough.

In spite of these difficulties synoptic weather conditions have been used as a preliminary indicator of local surface icing (e.g. Orlicz and Orliczowa 1954, Dranevic 1971, Bugaev and Peskov 1972), but no general rules that would be valid regardless of location have been found. This can be seen in Table 3, which shows the distribution of ship icing according to the position in relation to low pressure areas. Borisenkov and Pchelko (1972), among others, described the synoptic conditions during ship icing in various sea areas more exactly. Ship icing data are obviously useful in examining the synoptic conditions during atmospheric icing since spray icing and atmo-

Table 3. Synoptic conditions at the time of ship icing. (After Borisenkov and Pchelko 1972.)

| Sea | Rear of low-pressure area (%) | Forward part of low (%) | Other conditions (%) | No. of cases |
|--------------------------------|--|----------------------------------|----------------------------|-----------------|
| Bering Sea | 57 | 32 | 11 | 442 |
| Sea of Okhotsk | 70 | 23 | 7 | 312 |
| Sea of Japan, Tatarskii Strait | 93 | 3 | 4 | 140 |
| Western Pacific Ocean | 75 | 19 | 6 | 182 |
| Barents and Norwegian Seas | 40 | 50 | 10 | 596 |
| Baltic Sea | 4 | 66 | 30 | 44 |
| Black Sea and Sea of Azov | 79 | 16 | 5 | 18 |

spheric icing on ships often take place simultaneously (Table 1). Ship icing is most common in the rear of low-pressure areas with cold winds from the north or northwest (Vasilieva 1967, Sawada 1970) (Table 3). If the horizontal temperature gradient in air is large, icing may occur in the forward part of a low (Kaplina and Chukanin 1971). An air temperature below -18°C at the 85-kPa surface is an index of severe ship icing risk, according to Borisenkov and Pchelko (1972).

Supercooled fogs during the winter are mostly associated with occlusion fronts, although all types of fogs near a coast seem to be rare that time of year (Spinnangr 1949). Evaporation fogs are most probable when a cold air outbreak is from the direction of the coast. For supercooled advection fogs and freezing precipitation to form, a temperature inversion such as the one drawn by the solid line in Figure 24 is necessary; this can be expected near the coastline when a warm front is moving from the continent over the sea.

EFFECT OF METEOROLOGICAL CONDITIONS ON PROPERTIES OF THE ICE

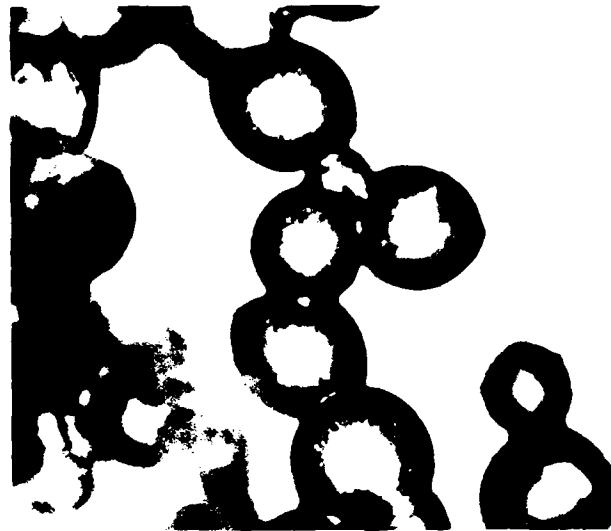
Density

The density ρ of ice is important in estimating the hazards due to icing for the following reasons:

- 1) Icing reports are often given in terms of ice thickness, so it is necessary to know ρ for determining the ice load.
- 2) Adhesive strength and mechanical properties of accreted ice are correlated with ρ .
- 3) Modeling the profiles of ice deposits requires an estimate of ρ (Bain and Gayet 1983).
- 4) The critical ice deposit diameter above which icing theoretically does not occur is reached at different ice loads depending on ice density, so time-dependent modeling of the growth of ice loads on structures requires an estimate of ρ (Makkonen, in press).

As pointed out earlier the structure and density of the accreted ice depend mainly on the heat balance at the icing surface and on the spreading of the impinging droplets (Fig. 30). Macklin (1962) presented the basic principles in estimating the density of ice formed by droplet accretion; he derived eq 32 based on laboratory experiments on cylinders

$$\rho = 0.11 \left(- \frac{d v_o}{2 t_s} \right)^{0.76} = 0.11 M^{0.76} \quad (32)$$



a. $t_a = -27^\circ\text{C}$, $t_s = -15^\circ\text{C}$. Magnification 200x.



b. $t_a = -27^\circ\text{C}$, $t_s = -10^\circ\text{C}$. Magnification 200x.

Figure 30. Accreted 100- μm -diameter droplets at different air temperatures t_a and deposit temperatures t_s . (From Macklin and Payne 1968.)



c. $t_a = -27^\circ\text{C}$, $t_s = -5^\circ\text{C}$. Magnification 200x.



d. $t_a = -27^\circ\text{C}$, $t_s = -1^\circ\text{C}$. Magnification 80x.

Figure 30 (cont'd). Accreted 100- μm -diameter droplets at different air temperatures t_a and deposit temperatures t_s . (From Macklin and Payne 1968.)

where ρ = ice density (g cm^{-3})

d = droplet diameter (μm)

v_0 = droplet impact speed at the stagnation line of the cylinder (m s^{-1})

t_s = mean temperature of the riming surface ($^{\circ}\text{C}$)

M = ice density parameter.

The impact speed v_0 can be calculated according to the theory described in the section on rime, and the surface temperature t_s can be calculated from the heat balance equation of the riming surface. Equation 32 has been verified by Buser and Aufdermaur (1972), Pflaum and Pruppacher (1979) and Bain and Gayet (1983) with good results, although small modifications have been made. Makkonen (in press) used these modifications to create eq 33 as part of his wire icing model;

$$\begin{aligned} \rho &= 0.1 && \text{for } M < 1 \\ \rho &= 0.11 a^{0.76} && \text{for } 1 \leq M < 10 \\ \rho &= a/(a + 5.61) && \text{for } 10 \leq M < 60 \\ \rho &= 0.92 && \text{for } M \geq 60. \end{aligned} \tag{33}$$

Equations 32 and 33 show that ice density ρ generally decreases with decreasing impact speed (and wind speed), decreasing droplet size, and decreasing air temperature t_a (t_s decreases when t_a decreases). Decreasing liquid water content results in a lower surface temperature t_s , so ρ decreases as well. Since v_0 depends not only on wind speed and droplet size, but also on the dimensions of the icing object, then in the same atmospheric condition ρ is higher on small structures than on large ones. Furthermore, ρ continuously decreases during ice accretion as the deposit size increases (Makkonen, in press). Also, ρ differs at different points on the icing object in dry-growth conditions (Bain and Gayet 1983). These factors make it difficult to simply relate the ice density measured after an icing storm to the conditions that prevailed. If this were not true, one could calculate the droplet size (which is difficult to measure) from eq 33 by means of density measurements.

The quantitative relationship between the density of wet snow accretions and the growth conditions is not known, but obviously wind speed has the most pronounced effect on ρ since wind stress is the primary cause of the deformation process that leads to dense, strongly adhering deposits. Wet snow accretions formed at low wind speeds typically have densities near 0.2 g cm^{-3} ; those formed in strong winds may have densities as high as 0.9 g cm^{-3} (Shoda 1953, Wakahama et al. 1977). The air temperature and the duration of strong

winds after the snowstorm may have an influence as well, but this has not been quantified.

In some cases it may be important to know the probable change of ice density with height. Glukhov's data (1972) from a continental location show an increase in ρ with height (Fig. 2); this is predicted by theoretical considerations, since wind speed in the surface layer usually increases with height, and the time that the higher part of a tall structure spends above the cloud base (where the liquid water content is high) is expected to be longer. Whether this is the situation at sea is uncertain and requires experimental evidence. It may even be reversed; because air temperature in icing conditions over the sea decreases rapidly with height and because evaporation fogs are usually limited to lower heights, the liquid water content may decrease with height.

Ice type

Different types of ice and the theoretical distinctions between wet-growth and dry-growth processes have been discussed earlier (Fig. 10). Here some empirical results are discussed.

As can be seen in Figures 10 and 31, when the wind speed is high, glaze (and in general more compact ice) is favored instead of porous rime. Also, when liquid water content is high and droplets are large, glaze is more likely; this is also true when the air temperature is close to 0°C . Ice type seems to be more critically affected by air temperature than by wind speed, as shown in Figures 10 and 31. The extreme air temperature limits are approximately from $+2^{\circ}$ to -9°C for glaze, from 0° to -15°C for hard rime, below -1°C for soft rime and from $+2^{\circ}$ to -4°C for wet snow (Gaponov 1939, Sadowski 1965, Volobueva 1975, Makkonen and Ahti 1983).

As with ice density, ice type depends on the dimensions of the icing object and may vary along the object surface and with time. Ice is often more glaze-like in the interior of the deposit and more porous in the surface layer.

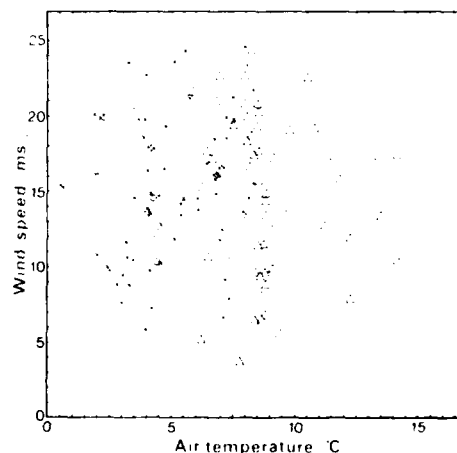


Figure 31. Atmospheric icing events in relation to air temperature and wind speed. o = glaze; x = hard rime; Δ = soft rime. (Data from Rink 1938.)

Examples of the distribution of different kinds of ice deposits according to air temperature and wind speed are shown in Figures 21 and 22. These figures are, however, merely indicative of marine conditions, since liquid water content and droplet size may be systematically different from the conditions in continental locations, from which the data originate.

The predominating ice type varies with height. According to Glukhov (1972) glaze is more common in the upper parts of high structures; there is also an increase in ice density with height (Fig. 2). Again, the situation in the marine environment may be considerably different. McLeod (1981) has suggested that the relationships of the different ice types by Glukhov (1972) in Figure 2 will hold true regardless of location. This is, however, somewhat questionable, since the boundary layer structure and the sources of icing are quite different on land and at sea.

Crystal structure

Close to the object surface (i.e. in the initial stage of the icing process) the crystal size is largely determined by the properties of the substrate (Golubev 1974, Mizuno 1981). At some distance (5-20 mm) from the substrate the effect of the substrate becomes very small, and beyond that point the crystal structure is determined only by the growth conditions. In practice this means that the mean crystal size increases with distance above the surface (Fig. 32). Figure 32 also shows that the crystal size decreases with decreasing air temperature t_a . This relationship is nearly exponential when the other conditions are fixed (Levi and Prodi 1978). Droplet size, impact speed, and liquid water content seem to have only a small effect on the crystal size (Rye and Macklin 1975, Laforte et al. 1983b). However, Prodi et al. (1982) observed that the average surface area of the grains is lower in wet-spongy accretions than in dry ones grown at the same air temperatures and at deposit temperatures just

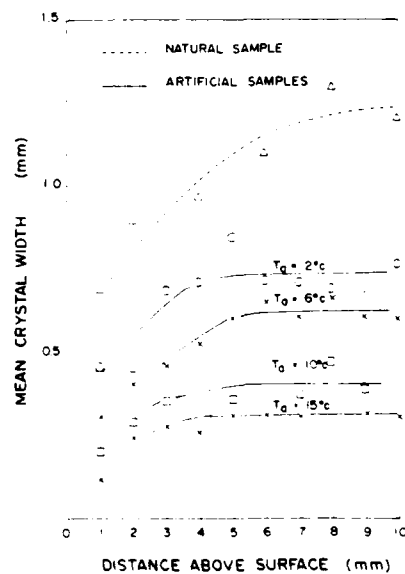


Figure 32. Variation of mean width of ice crystal with the ambient temperature and the radial distance above the conductor surface. (From Laforte et al. 1983a.)

below 0°C , which implies that liquid water content has some effect on crystal size, at least near the critical conditions. When analyzing the specimens from full-scale ship icing tests (using saline ice) Golubev (1972) found that larger crystals are formed on horizontal surfaces than on vertical surfaces. This has not been verified for glaze ice from atmospheric icing.

In the case of freezing rain the droplets will be solidified into single crystals (monocrystallization). Polycrystallization is also possible, but at lower air temperatures (Hallett 1964, Mizuno 1981), in which case the number of crystals nucleated from one droplet increases with decreasing air temperature.

Crystals in wet snow deposits are smaller than in glaze. This is probably related to the dimensions of the ice crystals of the original snowflakes.

The c-axis orientation of ice crystal is close to perpendicular to the growth direction in accretions grown in wet-growth conditions, and parallel to the growth direction if grown in dry-growth conditions (Levi and Aufdermaur 1970, Ackley and Itakagi 1974). At very low air temperatures c-axis orientation tends to shift toward 45° in dry growth.

Strength of adhesion

It might be expected that the adhesive strength would be closely related to ice density and that the methods used for finding density could therefore be used as an index of adhesive strength. This seems not be to the case, however, as can be seen in Figure 33. There is a trend towards low adhesive strength with decreasing ice density ρ , but the adhesive strength may vary considerably for ice deposits of the same density, especially for high-density ice. There are three apparent reasons for this. First, the detachment of glaze and hard rime is usually a pure adhesive failure, so the cohesive strength of the ice deposit is important only for soft rime. Second, since the failure of ice is mostly adhesive, only a very thin ice layer near the substrate is relevant to ice removal, and this initial ice layer is often formed closer to the wet

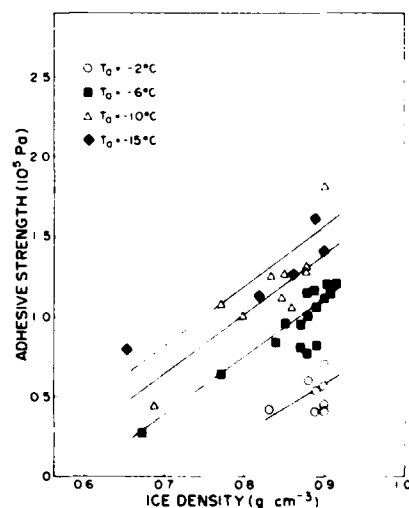


Figure 33. Adhesive strength of ice accretion vs density at various air temperatures. (From Laforte et al. 1983a.)

Table 4. Glaze and rime adhesion on different substances. (From Phan et al. 1978.)

| Substances | Wind speed 20 ms ⁻¹ | | Wind speed 10 ms ⁻¹ | |
|---------------------|---|---|---|---|
| | Glaze* Adhesion strength (kN m ⁻²) | Hard rime† Adhesion strength (kN m ⁻²) | Glaze* Adhesion strength (kN m ⁻²) | Hard rime† Adhesion strength (kN m ⁻²) |
| Aluminum cylinder | 15, 35 | 120, 75 | 75 | 75 |
| Teflon cylinder | 80 | 25, 80 | 40 | 55 |
| Plexiglass cylinder | 80 | 60 | 40 | 10, 30 |
| Rubber cylinder | 85 | 100, 85 | 40 | 50 |
| Bare conductor | 90 | 100 | 40, 90 | 100 |
| Polyethylene | 240 | 140 | 90 | 80 |
| Polyester resin | 260 | 240 | 140 | 130 |
| Epoxy resin | 170 | 190 | 130 | 150, 130 |
| Paraffin wax | 190 | 170 | 160 | 140 |
| Silicone rubber | 50, 25 | 10, 20 | 25 | 15 |
| Grease | 10, 15 | 10 | 10 | 0 |
| LPS 1 | 0, 40, 70 | 15 | 0 | 10 |

*Temperature = -12°C; Water content = 1.5 g m⁻³; Ice density = 0.9 g cm⁻³.
 †Temperature = -12°C; Water content = 1 g m⁻³; Ice density = 0.8 g cm⁻³.

growth limit than is the major part of the deposit. The differences in ρ in this thin layer may vary less than ρ in the bulk of the ice. Finally, the adhesive bonding for pure ice depends on the temperature conditions during the icing process. That the effect of ρ on adhesion is small is demonstrated by the fact that the adhesive strengths of hard rime and glaze are not noticeably different (Phan et al. 1978) (Table 4).

The adhesive strength of hard rime and glaze increases when air temperature decreases down to approximately -10° to -15°C and then slightly decreases (Fig. 34), similar to the adhesion of ice formed by spray icing (Kamenetskii et al. 1971).

An increase in wind speed (or impact velocity of the droplets) seems to increase the adhesive strength of ice formed by droplet accretion (Table 4), probably because the mechanical bonding is stronger when the droplets pene-

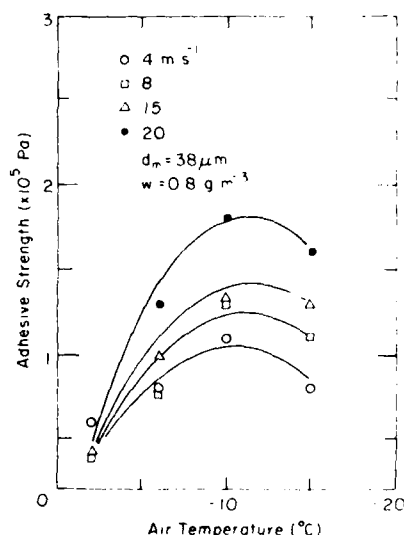


Figure 34. Adhesive strength of ice accretion grown at different ambient temperatures and air velocities. (From Laforte et al. 1983a.)

trate surface irregularities more effectively. The effect of wind speed is less pronounced at air temperatures close to 0°C (Fig. 34). Liquid water content has only a small effect on adhesion, according to Laforte et al. (1983a).

The results presented in this section apply mainly to high-density ice grown close to or at the wet-growth limit. If the combination of atmospheric parameters is such that rime formation is favored, then the relationship between adhesive strength and growth conditions may be changed. For example, when air temperature decreases below -10°C , soft rime is typically formed, and its porosity increases with decreasing t_a , in which case the force required for ice removal probably also decreases with t_a , in contrast to what is seen in Figure 34. The effect of the properties of the substrate on the adhesive strength will be discussed later.

Shape

The shape of the ice deposit formed by droplet accretion varies considerably depending on the atmospheric conditions. This is important in studying icing on sea structures because 1) the intensity of icing at a specified moment is related to the dimensions of the ice deposits at that moment, 2) the difficulties encountered in ice removal may depend on the ice profile, that is, on the surface area in contact with the substrate, and 3) the ice shape on a structure affects the sail area and consequently wind drag, which are often the critical factors influencing the possible failure of high structures in icing conditions.

The basic parameters affecting the shape of an ice accretion are the same as those determining the density of ice: air temperature t_a , wind speed v , liquid water content w and droplet size d . Qualitatively the role of these parameters in determining the ice profile has long been well known, based on both observations and theoretical considerations (e.g., Melcher 1951, Dickey 1952, Imai 1953, Ono 1967). Figure 35 shows some typical basic ice profiles observed in near-constant atmospheric conditions. With high wind speed, air temperature and liquid water content and with large droplets, the ice profile resembles A or B in Figure 35, the growth conditions being wet and some runoff taking place. When v , t_a , w and d decrease, the icing process progressively changes to dry growth and the ice profile resembles C, D or E in Figure 35. With very small droplets and low values of w , only rime feathers are formed, as in profile F.

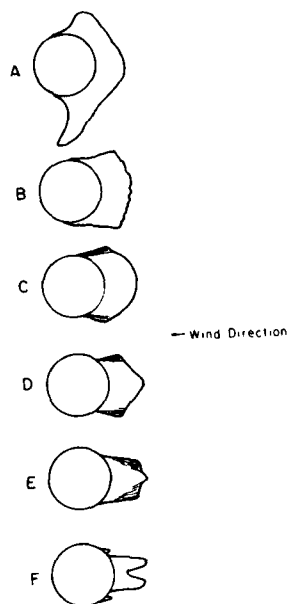


Figure 35. Typical ice profiles on cylinders. (From Imai 1953.)

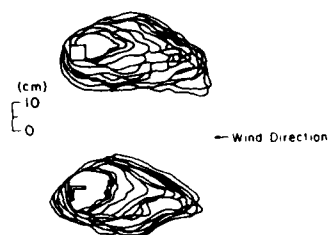


Figure 36. Horizontal (above) and vertical (below) cross sections of an ice deposit formed by droplet accretion. (From Kolbig 1973.)

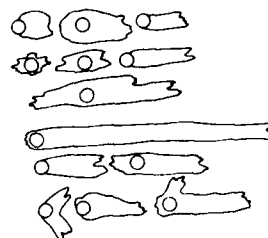


Figure 37. Observed ice profiles. (From Klinov and Boikov 1974.)

There is generally not much difference in ice profiles on vertical and horizontal objects, except in very wet conditions (case A), where runoff water may produce icicles. Also, on structures with the same vertical and horizontal extent the ice profile appears to be quite similar, both vertically and horizontally, under atmospheric icing conditions (Fig. 36).

Dickey (1953) argued that there are three basic ice deposit shapes that are stable; that is, all other shapes would gradually change into one of these shapes in constant atmospheric conditions. This would mean that the shape of the collecting object does not affect the ultimate shape of the ice deposit. There is, however, no direct proof of this. This problem might be examined using the recent finite element models of McComber and Touzot (1981) and MacArthur (1983), which are able to predict local collection efficiencies on irregular surfaces.

Much attention has been paid to theoretical modeling of ice shapes on cylindrical and airfoil surfaces because of the importance of icing effects on fixed or rotary wings. On helicopter rotor blades, for example, ice accretion may considerably affect the aerodynamic lift. The recent models can predict the shape of ice fairly well, especially at the low speeds corresponding to atmospheric icing on stationary structures (Stallabrass and Lozowski 1978, Lozowski et al. 1979). Application of the results from these models is not easy, however; the observed ice shapes in Figure 37 demonstrate

that the ice shape is affected by air turbulence and variation in the atmospheric conditions (especially in wind direction) during icing, resulting in ice shapes far from the idealized model predictions.

GEOGRAPHICAL AND SEASONAL DISTRIBUTION OF ICING PROBABILITIES

Icing observations at sea are distributed unevenly, both geographically and seasonally. This is because the majority of all the icing reports are from ships using more or less fixed routes or working in certain fishing areas only, and navigating only during part of the year. Moreover, the cause of icing (spray or atmospheric) is seldom clearly distinguished in the reports. Hence, it is very difficult to form a clear picture of the distribution of atmospheric icing cases in different sea areas. Table 5 shows the periods of probable icing for the sea areas where Soviet ship icing reports have been available. These observations include mostly spray icing. Regions where icing on ships was observed in the Soviet data are plotted on a map in Figure 38. More data on spray icing probabilities can be found in various charts published for this purpose (e.g., U.S. Navy Hydrographic Office 1958, DeAngelis 1974, Kolosova 1974, Stallabrass 1975, Korniushev and Tiurin 1979), but data on atmospheric ice accretion are rare. Some indications of atmospheric icing frequencies may be found from aircraft icing observations (Heath and Cantrell 1972), but these data may be misleading regarding icing on sea structures because the parameters involved with icing change rapidly with height over the sea.

Table 5. Period of ship icing according to Borisenkov and Panov (1974).

| Seas and Oceans | No. of cases | Period of possible icing |
|--|--------------|--------------------------|
| Western seas | 584 | 1 Jan - 31 Mar |
| Eastern seas | 931 | 15 Dec - 15 Mar |
| Northwest Atlantic | 85 | 15 Dec - 15 Mar |
| Norway & Greenland seas | 109 | 15 Dec - 31 Mar |
| North Atlantic | 63 | 15 Dec - 15 Apr |
| Barents Sea | 390 | 1 Jan - 15 Mar |
| Baltic Sea | 21 | 15 Dec - 28 Feb |
| Baffin Bay & Hudson Bay | 7 | 1 Dec - 31 Mar |
| Newfoundland region | 15 | 1 Jan - 15 Mar |
| Bering Sea | 185 | 1 Dec - 31 Mar |
| Okhotsk Sea | 337 | 1 Dec - 31 Mar |
| Sea of Japan | 226 | 1 Dec - 28 Feb |
| Northwest Pacific | 183 | 15 Dec - 31 Mar |
| Arctic Sea (Kara, Laptev, Eastern Siberia & Chukotsk) | 71 | 15 Jun - 15 Nov |

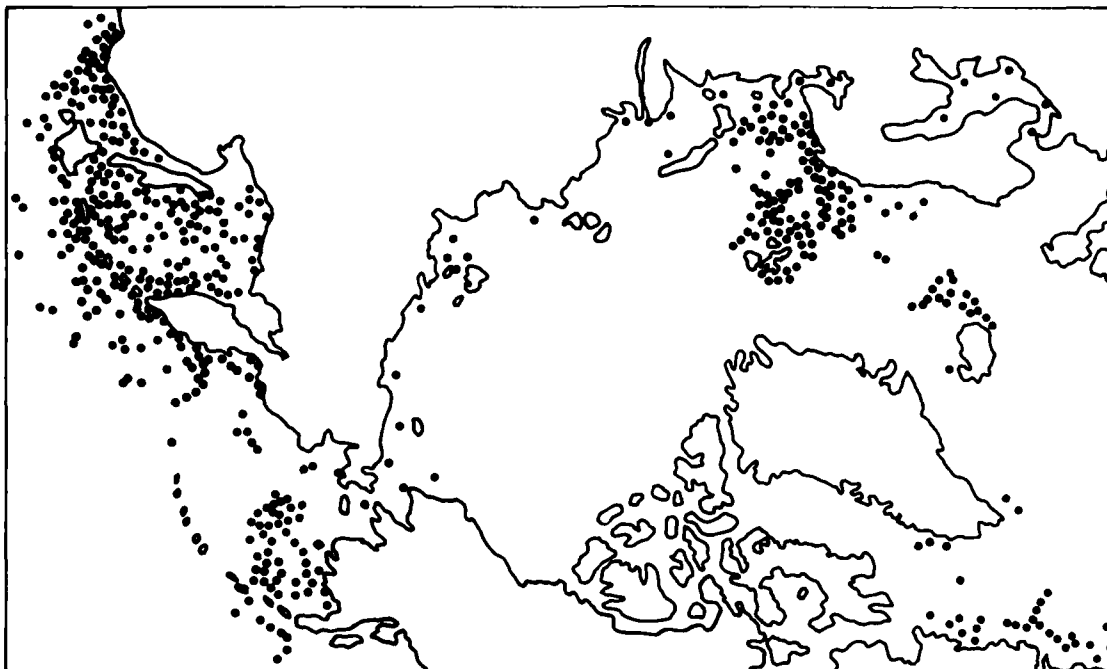
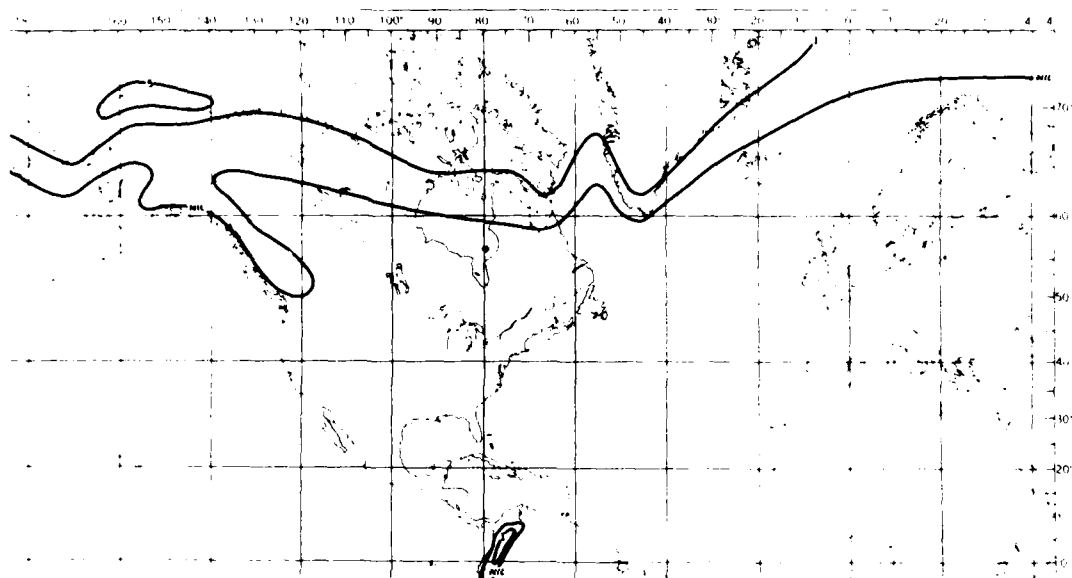


Figure 38. Regions where ship icing was observed by Soviet observers according to Panov (1978).

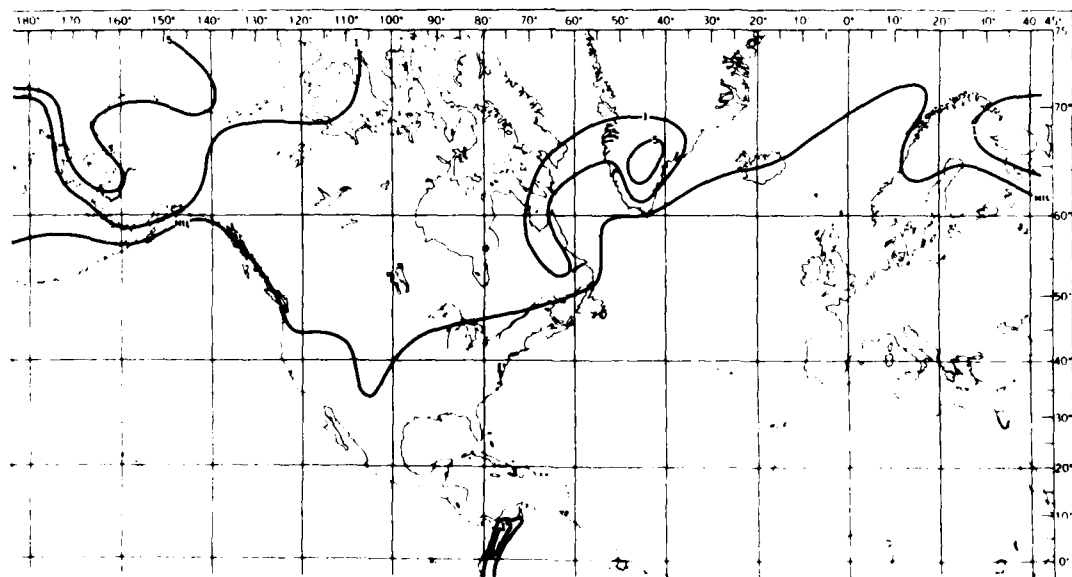
Because of the lack of representative atmospheric icing observations at sea, studies of the probabilities of atmospheric icing must be partly based on the frequencies of combinations of generally measured atmospheric parameters that are expected to cause icing on structures. But the amount of this kind of data from the open sea is small also, so observations from islands and coastal stations must be used. For this reason, the results of these studies should be interpreted with care; observations made over land may not represent real offshore conditions, since icing phenomena are affected by latitude, sea surface temperature patterns, proximity of land, and orography.

The combinations of atmospheric parameters used as indicators of atmospheric icing are slightly different in different studies. In the Soviet classification the combination chosen to represent atmospheric icing conditions on ships is $t_a \leq 0^\circ\text{C}$, $v \leq 7 \text{ m s}^{-1}$ and the occurrence of precipitation and fog (e.g., Kolosova 1974). This criterion is perhaps not well justified, since there seems to be no reason why atmospheric icing should not occur during high wind speeds. Another possible criterion is therefore simply $t_a \leq 0^\circ\text{C}$, which has been used by Dunbar (1964) in constructing charts for the areas where superstructure icing is probable in different seasons.

The occurrence of supercooled fogs is an obvious atmospheric icing condition. Guttman (1971) studied the worldwide occurrence of supercooled fogs; his charts for part of the Northern Hemisphere are shown in Figure 39. The apparent conclusion from Figure 39 is that supercooled fogs are seldom met at sea, except in ice-covered areas and close to coasts or the ice edge. The same conclusion was reached earlier.

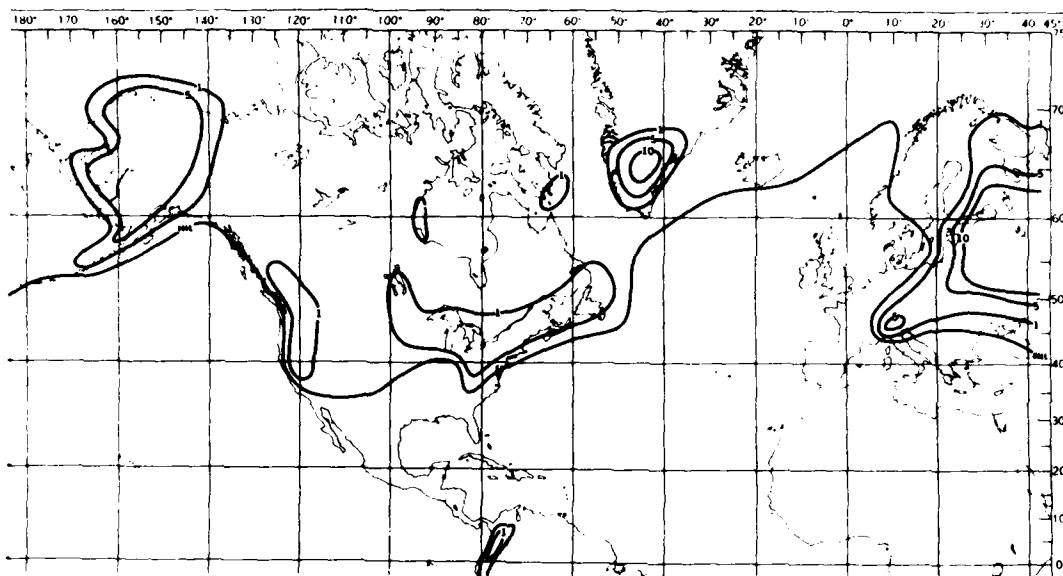


a. September.

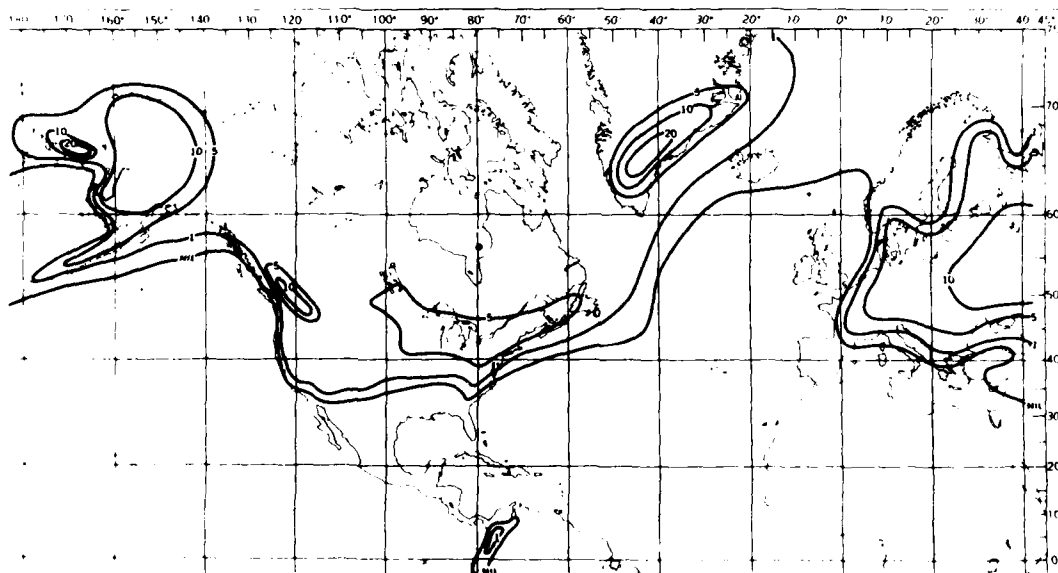


b. October.

Figure 39. Probability of supercooled fog by month according to Guttman. (From Minsk 1977.)

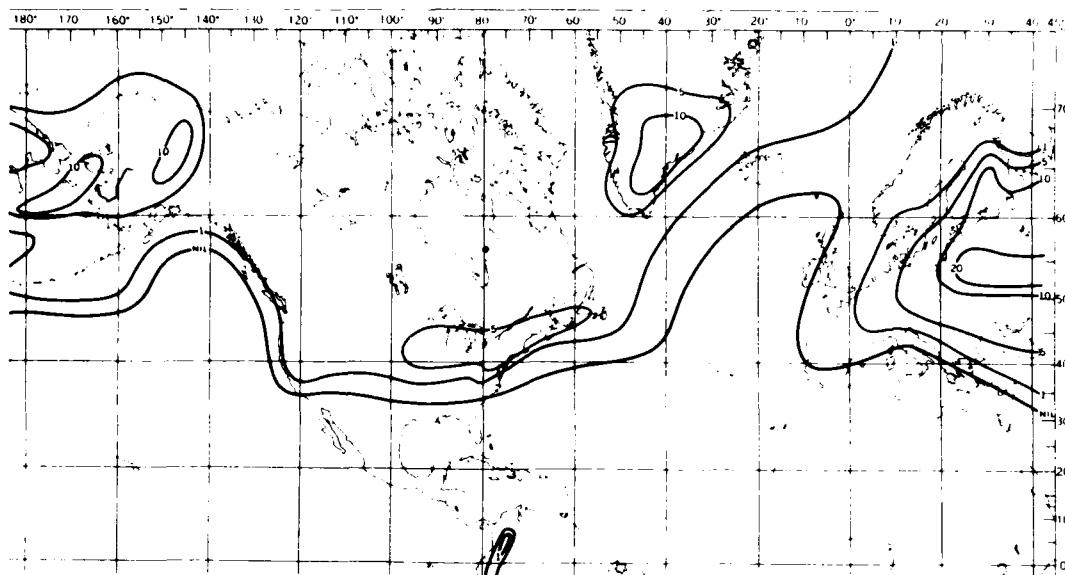


c. November.

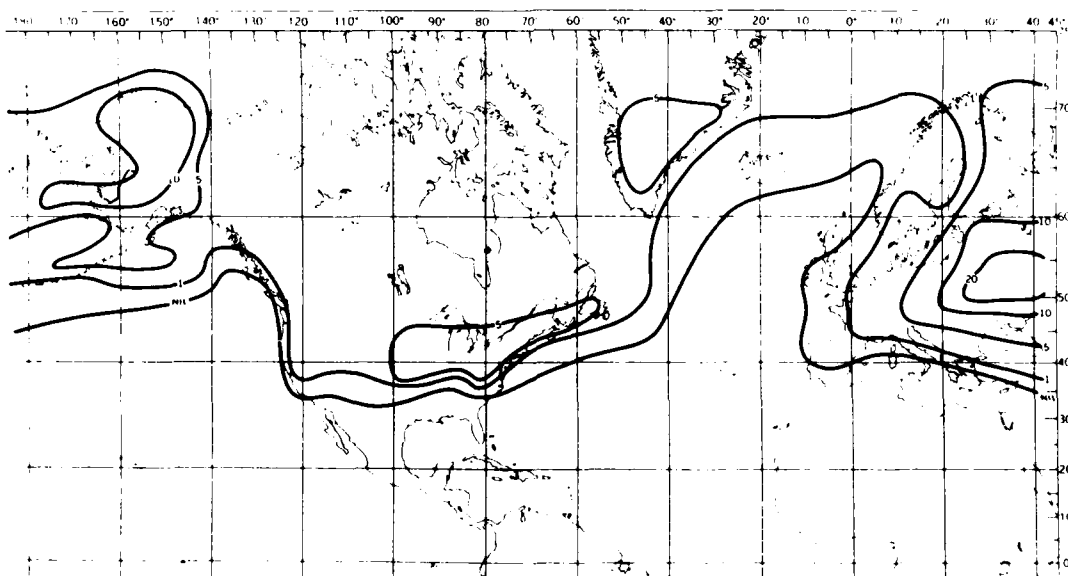


d. December.

Figure 39 (cont'd).

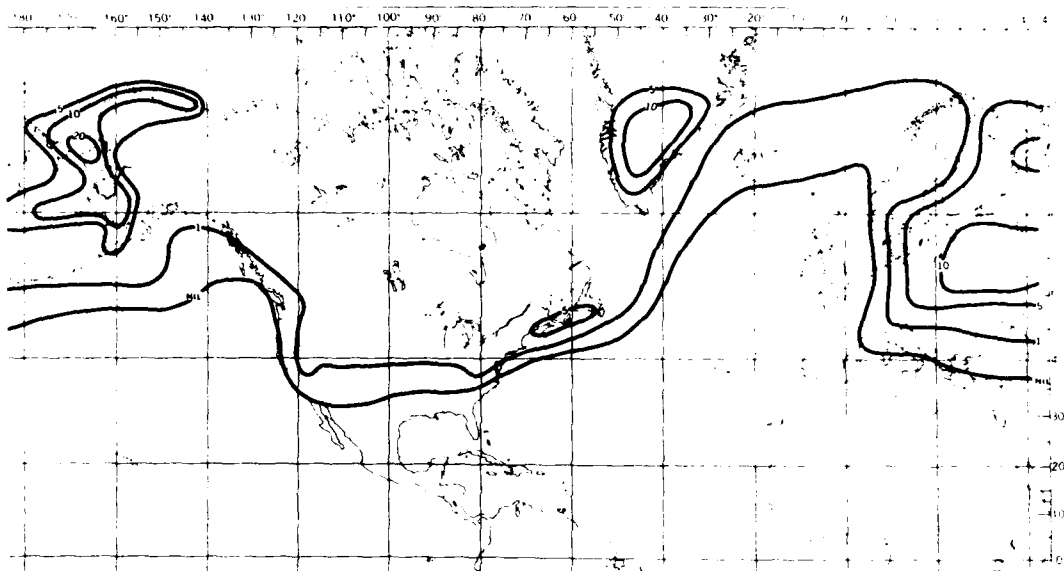


e. January.

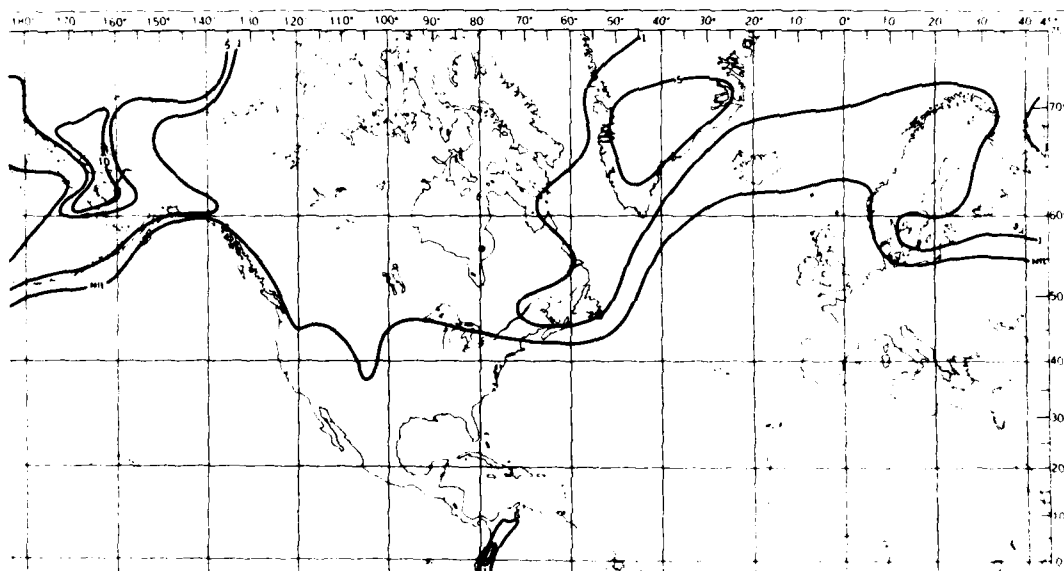


f. February.

Figure 39 (cont'd). Probability of supercooled fog by month according to Guttman. (From Minsk 1977.)



g. March.



h. April.

Figure 39 (cont'd).

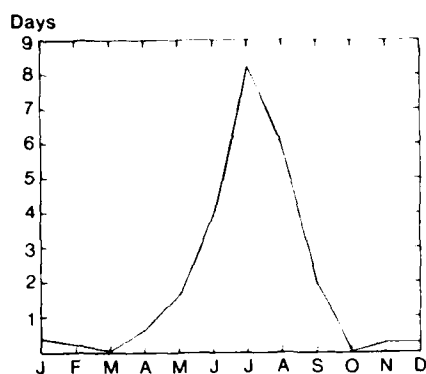
At least once, however, evaporation fog has been observed 300 km from the coast (Hay 1953), although it lasted for less than an hour and was not reported to have caused any icing. Lee (1958) reported a rather severe case of icing due to evaporation fog approximately 35 km from the ice edge.

The extent of evaporation fogs downwind from the shore has been studied using a theoretical model by Wessels (1979); he also concluded that evaporation fogs are restricted to coastal waters. The precise downwind extent and the liquid water content of the fog depend, however, on the properties of the initial continental boundary layer (e.g., temperature profile, humidity and wind speed). The model results for one situation are shown in Table 6. Unfortunately the theoretical model results are quite sensitive to the assumed rate of entrainment with dry air, showing, for example, that after sufficient development of an internal boundary layer over the sea, fog thickness z_f may either increase or decrease with distance from the shore, depending on the assumed rate of entrainment (Matveev and Soldatenko 1977). Therefore, more theoretical and experimental work is needed to confirm the limited range of supercooled fogs from the shore.

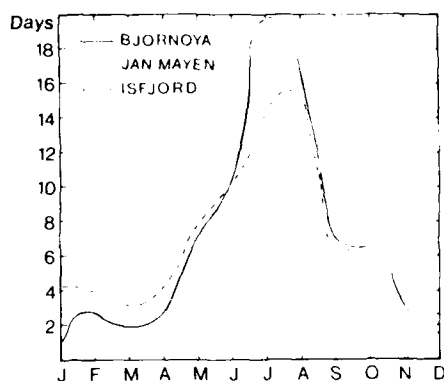
Supercooled fogs are not only restricted to coastal waters, but their frequency in these areas is small (Fig. 40, 41). According to Figure 40 the frequency of fogs at the coastal stations of northern Norway is practically zero when the average air temperature is below 0°C (December-March, according to U.S. Weather Bureau 1959). According to Brower et al. (1977) the frequency of fogs in winter is 0-10% in the Gulf of Alaska, 10-20% in the Bering Sea

Table 6. Example of the properties of the adiabatic mixed layer as functions of the downwind distance from the shore, with a lifted inversion ($h_0 = 250$ m), according to the model by Wessels (1979).

| Distance from shore (km) | Height (m) | | Maximum liquid water content (g m^{-3}) | |
|--------------------------------|------------|-------------|--|--------|
| | Fog | Mixed layer | Fog | Cloud |
| 0 | 6 | 250 | 0.29 | - |
| 1 | 6 | 252 | 0.28 | - |
| 2 | 6 | 254 | 0.27 | < 0.01 |
| 3 | 6 | 256 | 0.26 | 0.01 |
| 5 | 6 | 260 | 0.25 | 0.03 |
| 10 | 4 | 270 | 0.23 | 0.05 |
| 20 | 3 | 292 | 0.18 | 0.09 |
| 30 | 1 | 316 | 0.13 | 0.12 |
| 50 | - | 358 | 0.08 | 0.15 |
| 100 | - | 459 | - | 0.17 |

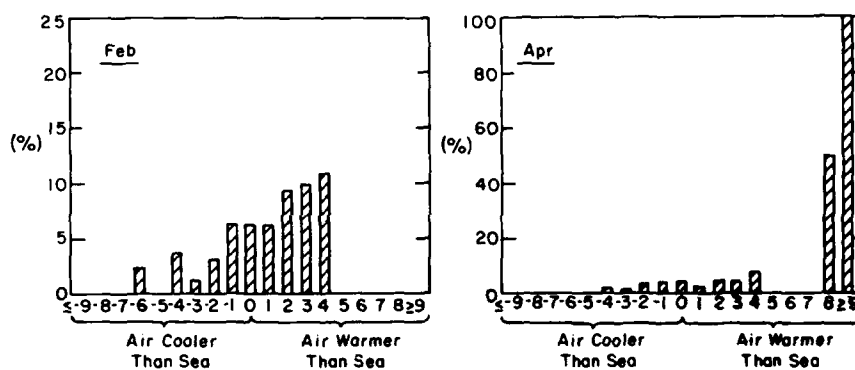


a. On the coast, Nordkapp-Vardo.

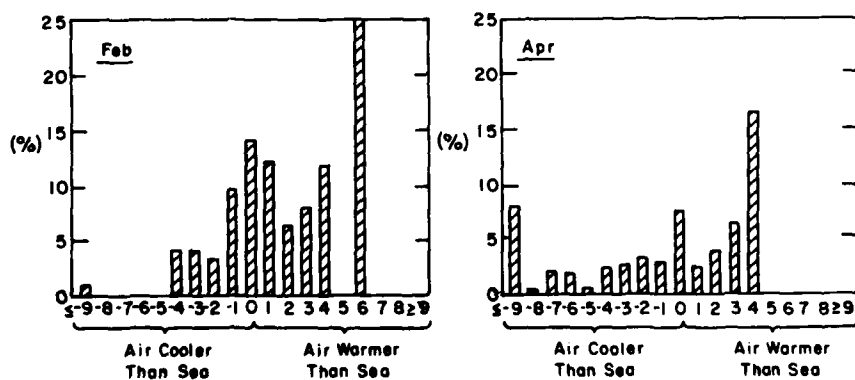


b. At three Norwegian arctic stations.

Figure 40. Average number of days with fog at coastal stations in northern Norway. (From Spinnangr 1949.)



a. Middleton Island, Gulf of Alaska.



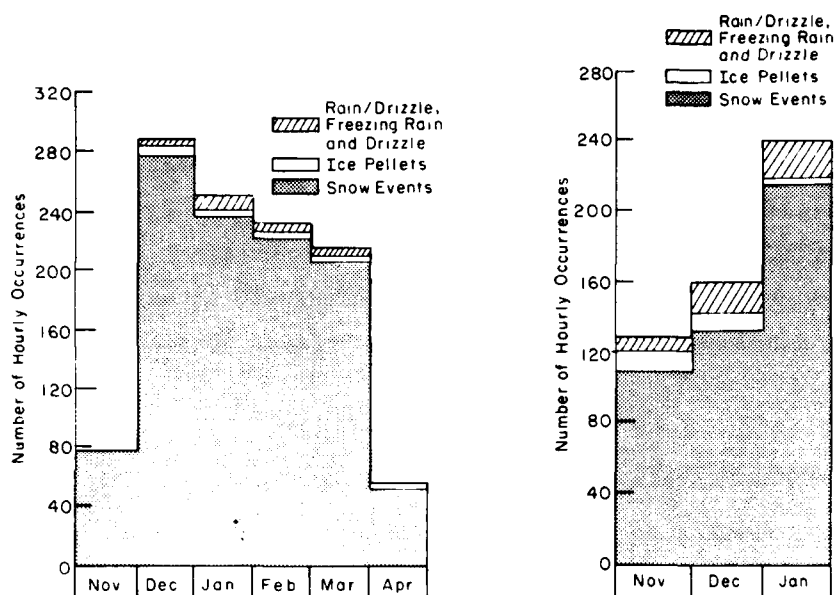
b. St. Paul Island, Bering Sea.

Figure 41. Distribution of fog events in relation to air-sea temperature difference (in $^{\circ}\text{C}$) at two arctic marine weather stations according to Brower et al. (1977).

and 10-15% in the Chukchi and Beaufort seas. However, only a small portion of these fogs occurs at air temperatures below 0°C. Figure 41 shows the distribution of winter fogs at some arctic locations according to air-sea temperature differences. The mean winter sea surface temperatures in these areas, combined with the data in this figure, show that supercooled fogs are very infrequent, occurring 1-2 times a month at most. The onset of evaporation fogs, when the air is much colder than the sea surface, can be seen as a concentration of fog frequency in Figure 41 for the Bering Sea when $t_a - t_w \leq -9^\circ\text{C}$.

In addition to the frequency of icing, it is interesting to consider the duration of icing conditions when they do occur. There are not many data on duration, but some conclusions can be reached from storm and visibility statistics. According to Smirnov (1974) storms at freezing temperatures lasting for more than three days occur on the average three times a year near Iceland. Poor visibility (< 3.7 km) occurs in arctic areas in 4-10% of all observations, and its duration is less than 12 hours in 90% of the cases and more than 24 hours in 1-3% of the cases (U.S. Navy Hydrographic Office 1963). The number of hourly occurrences of freezing precipitation for two arctic stations is given in Figure 42. This figure gives some indications of the icing potential, although nonprecipitating supercooled fogs are not included in the data. Charts giving the percentage of hourly weather observations with liquid precipitation and wet snow in different parts of the world have been presented by Bennett (1959) (Fig. 43). These charts include parts of coastal areas, but it is not known what part of the data has been associated with structural icing.

McLeod (1981) suggested that the data such as those in Figure 2 are representative of the entire sea area (Bering Sea). Also, Brower et al. (1977) claimed that the data in Figure 41 represent the sea area approximately 500 km from the coast. However, it is questionable whether observations from the coast or from islands are representative of offshore areas. As explained earlier the formation and maintenance mechanisms of freezing fog and precipitation are different over the land and over the sea surface. This is the case even if the land area is small, such as an island, and if the observation point is very close to the coastline. When an offshore wind is blowing, observations in general represent the atmospheric surface layer over the continent, not over the sea. This is almost always the case when atmospheric icing at sea takes place. For example, for many, if not most, of the cases



a. Middleton Island, Gulf of Alaska.

b. St. Paul Island, Bering Sea.

Figure 42. Ten-year summaries (1948-1958) of the number of precipitation events occurring during freezing air temperatures at two arctic marine weather stations. (From McLeod 1981.)

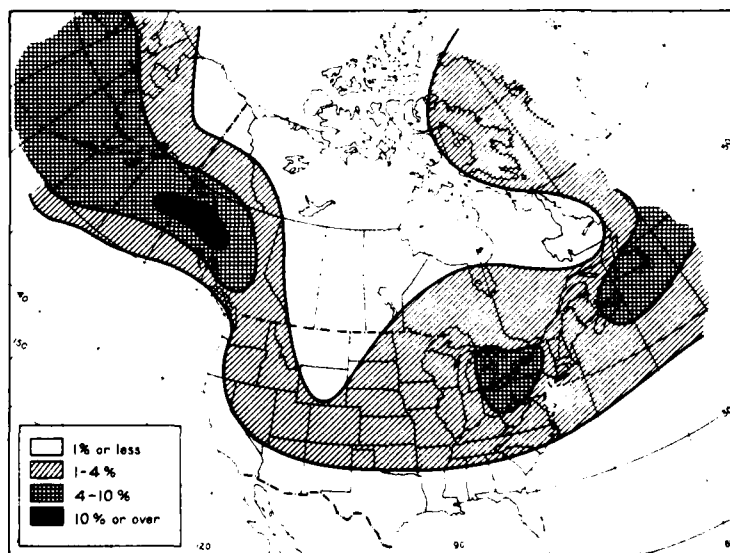


Figure 43. Mean annual percentage of hourly weather observations with freezing rain, North America. This is based on a map prepared in 1943 by the Weather Information Service of the U.S. Army Air Forces (Bennett 1959). (From Minsk 1980.)

in which freezing air temperatures are reported at a coastal station or an island, the air temperatures over the sea surface at some distance from the observation point are not below 0°C, due to the warming effect of the sea. Hence, to use the available icing data from coastal locations in estimating icing probabilities at offshore locations, we need a more complete understanding of how the properties of the atmospheric surface layer that affect icing potential change over the coastline. This could be achieved, for example, by making simultaneous measurements at a coastal location and at an offshore platform.

METHODS FOR MEASURING ICING SEVERITY

Most of the results on ice loads in the marine environment have been obtained by simple manual ice thickness measurements, by weighing the removed ice, or by visual estimates. On ships the change in the freeboard has generally been used as an ice-load indicator. These methods are rather inaccurate and are only suitable for rough estimates in severe icing conditions. The instruments that are used in continental measurements must be used at sea if high accuracy is required. These instruments are mostly cylindrical objects such as steel cylinders and wires; metal plates have also been used. The most commonly used devices are the combination of horizontal wires used widely in the USSR (e.g., Nikiforov 1983) and the so-called Grunow net, which is quite commonly used in Central Europe (Grunow and Tollner 1969, Baranowski and Liebersbach 1977). The Grunow net is a tube of wire netting and is often installed on top of a precipitation gauge. Tabata et al. (1976) used a device similar to the Grunow net in measuring ship icing (Fig. 44). To determine the icing rate with this kind of simple instrument, the ice is usually melted and weighed manually.

Manual icing rate measurements can be made easily and rapidly (within a few minutes) by the rotating cylinder method (Fraser et al. 1953). This method, generally used in laboratory experiments and cloud microstructure studies, is similar to the other methods except that the cylindrical icing object is rotating and is very small (diameter ≈ 1 mm). The amount of ice is determined by weighing the instrument before and after it is exposed to icing. Relating the re-

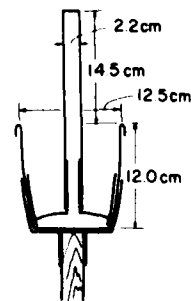


Figure 44. Icing gauge of Tabata et al. (1967).

sults from the rotating cylinder method to the icing of larger structures is not straightforward, but must be determined theoretically using the value for the liquid water content in eq 2; this value can be determined using the rotating cylinder if the growth conditions on the instrument are dry (see Rush and Wardlaw 1957, Stallabrass 1978).

Manual icing measurements are difficult and often dangerous to make in the marine environment. Also, there is a need for icing data at unmanned marine installations. Therefore, instruments that can measure and record icing rates automatically are needed. One possibility is simply to install an icing cylinder or rod on a weighing machine

with electronic data recording. This method, used in remote mountain areas (e.g., Rothig 1973), has been applied to ship icing measurements by Tabata et al. (1963) (Fig. 45). Weighing instruments have proved useful, but there are some problems that restrict their reliability. First, ice makes the weighing mechanism inoperative unless it is protected by heating (Fig. 45). Heating, on the other hand, may affect the instrument's icing rate. Second, heavy wind drag, which is often associated with icing, is felt by the weighing machine and may be mistakenly interpreted as an increased ice load. Finally, the whole instrumentation may become encapsulated by ice.

To avoid these problems Rosemount, Inc., developed a more sophisticated device, whose working principle is entirely different from the previous detectors. This instrument is available in several versions, though it was originally designed to be used in turboengine intakes. However, it has been used successfully in near-ground icing conditions (Ackley et al. 1973, 1977, Tattelman 1982) and in the marine environment (McLeod 1981). The small, cylindrical sensing probe of the Rosemount detector (Fig. 46) is forced to vibrate parallel to its axis by a magnetostrictive oscillator. This vibration is at its resonant frequency when the probe is free of ice, but ice accretion causes a shift in resonance corresponding to the increase in mass adhering to the probe. After a thin layer of ice (about 0.5 mm) has accumulated, an alarm circuit is triggered and the sensor is deiced by an internal heater. The heating cycles are then recorded, and from their frequency the ice accretion rate can be evaluated fairly accurately, although changes in

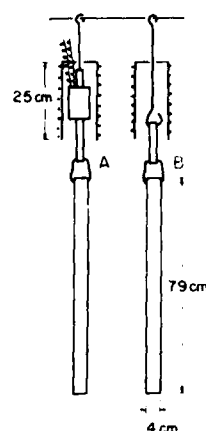


Figure 45. Icing rod of Tabata et al. (1967).

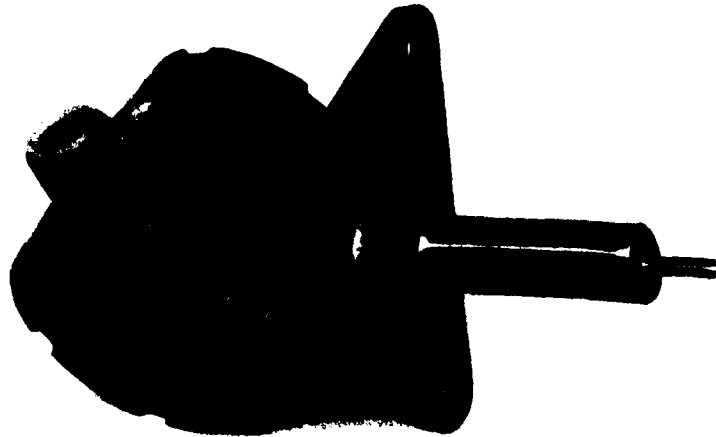


Figure 46. Rosemount Model 872DC Ice Detector. The sensing probe sits atop the 25.4-cm strut. During de-icing, the sensor and the top 7.6 cm of the strut are heated. (Photograph courtesy of Rosemount, Inc.)

ice density and calibration problems cause some scatter (Tattelman 1982). Rosemount detectors still require more testing in the marine environment, but they are the most promising practical method to measure icing rate at sea. Their ability to operate through long icing periods with little human involvement makes them superior to all other ice detectors.

ANTI-ICING METHODS

Methods for alleviating the hazards and inconveniences of icing can be divided into anti-icing measures, which try to prevent or reduce ice accretion, and deicing measures, which try to remove the accreted ice. Some of the methods may be classified in either of these categories, depending on the application.

Structural design

Perhaps the most important and generally used anti-icing method is to minimize small structures and replace them with fewer, large objects. The design of superstructures of fishing trawlers, for example, is based on this principle. Small structures have larger icing efficiencies than large ob-

jects; in the dry-growth regime the collection efficiency E decreases rapidly with increasing size, and in the wet-growth regime the heat transfer coefficient decreases with increasing size. These effects should not, however, be overestimated since the collecting surface area and the heat exchange area also increase as a function of object size. Makkonen (in press), in fact, showed theoretically that the initial size of a cylindrical object has only a very small effect on the ultimate ice load after long-term icing, with cylinder diameters in the range of 1-5 cm and ice deposits that remain cylindrical. This indicates, for example, that the number of separate objects on a ship superstructure may be more important than their size in determining how ice loads form. On the other hand, if the structures are large enough, icing may not occur at all.

The theoretical result that E decreases towards zero for large objects has been applied to the protection of high masts and towers with promising results (Jaakkola et al. 1983). Ice formation has been considerably reduced by covering the masts with cylindrical plastic covers several meters in diameter. There are, however, some disadvantages that have restricted the use of this method; the large surface area generates heavy wind drag, which may lead to vibrations of the mast structure. Therefore, the method requires more testing, but it already appears to be a promising, practical anti-icing measure for towers and masts that have sufficient steadiness against wind forces caused by the increased sail area of the sheltering cylinder.

Heating

The most obvious method for preventing icing is heating. However, it is far from being the most practical because of the large amount of latent heat required to melt ice or to prevent its formation. For example, the power required for anti-icing, when the calculated icing rate on a nonheated surface is $3 \text{ g cm}^{-2} \text{ h}^{-1}$, is about 2 kW m^{-2} . For a medium-size trawler this corresponds to about 2-3 MW for the whole vessel.

Large energy requirements of thermal methods have restricted their use mostly to small objects. In these cases internal heating is usually used, since external heating, such as protecting meteorological instruments with infrared heaters, is quite ineffective (Gerger 1974, Ahti 1978). For example, anti-icing a cup anemometer requires 300-700 W (Ahti 1978).

One way of heating sea structures is to use a thermosyphon, the principle of which is demonstrated in Figure 47. The working fluid can be, among others, ammonia or Freon 21. This method can be applied to structures such as masts and handrails, the structures themselves acting as heat pipes. It is also possible to cover flat surfaces with loops of heat pipes. Both of these techniques were applied when constructing the first practical thermal deicing system on a Japanese ship (Okiyara et al. 1980, Zosen 1981). This thermostatically controlled heating system, which can use different heat sources, is shown schematically in Figure 48. The heat consumption of the system has been found to be about 1 kW m^{-2} in field tests under typical icing conditions (Okiyara et al. 1980). It is in principle possible to use the waste heat from the vessel's engines as the energy source of the system. A heat pipe method has also been used in deicing navigation buoys (Larkin and Dubuc 1976).

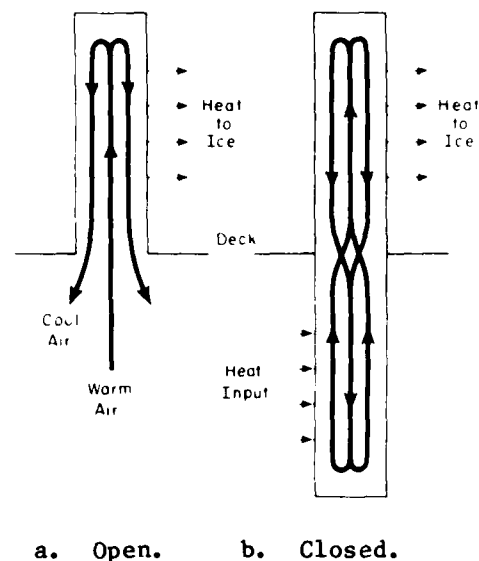


Figure 47. Working principle of a thermosyphon. (After Lock 1972.)

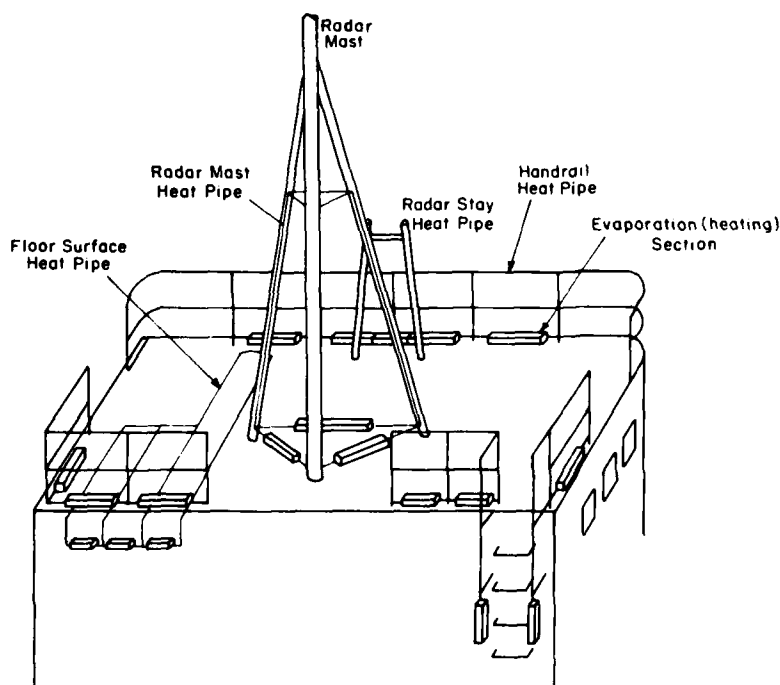


Figure 48. Heat pipe deicing system installed on a ship. (After Zosen 1981.)

Current-conducting coatings may be used for heating small surface areas, such as bridge windows (King 1973). This method may work for larger surfaces too, if combined with coatings that reduce ice adhesion. This may reduce the power consumption to a level realistic for practical applications (Paniushkin et al. 1974e).

Chemical methods

The application of chemicals on an icing surface to reduce ice adhesion has been tested, mostly with poor success. The anti-icing effect of silicone oil, vaseline and Kilfrost has been found to be small (Alexeiev 1974). Moreover, these chemicals deteriorate easily by weathering and by the accreting ice (Ackley et al. 1973). Fixed coatings, which are more effective in reducing the adhesion strength, will be discussed later.

Another kind of chemical measure for preventing icing is to apply freezing point depressants on surfaces. The major problems of this method are optimizing the amount of the chemicals and distributing them uniformly on the surface. If these problems could be overcome, it would be possible to reduce icing considerably by using ethylene glycol (Gerger 1974, Stallabrass 1970) or Santomelt 990-CR organic anti-icing fluid (Bates 1973). Salts such as calcium nitrate (Semenova 1974) have also been tested; these chemicals can reduce, but not prevent, ice load formation (Ackley et al. 1973).

Chemical methods can be appropriate for protecting small objects (bridge windows, automatic meteorological instruments, etc.) and objects that require ice removal for only a short time (helicopters before take-off, for example). Chemicals are difficult to apply on large structures for long-term ice prevention since their rapid deterioration makes the method uncertain and expensive. Other disadvantages include making horizontal surfaces slippery and contaminating the catch of trawlers.

Other methods

Ice has been prevented from forming on meteorological instrument housings by installing a shelter net around them (Gerger 1974). The same method could be used on a larger scale for preventing icing on ships or stationary sea structures. If a large number of wires were formed into a net in the bow of a ship or around a stationary structure, icing could be reduced on the protected superstructure. Icing of the wire net could be prevented by heating, the anti-iced surface area in this case being smaller than the protected object. Another possibility is to use two nets, so one can be lowered into

the water for melting while the other is used for protection (Lock 1972). The water temperature must, of course, be above 0°C when using this method; for spray icing it must be $\approx 0^{\circ}\text{C}$, because the accreted ice is less saline than the water where it originates, so that its melting temperature is higher than the freezing temperature of seawater. To confirm the usefulness of this method more exact estimates should be made of the rate of melting of ice in seawater and the rate of ice accretion.

Minsk (1977) suggested deflecting the supercooled water droplets from their original trajectories by use of an air curtain, preventing them from striking the protected object. This method seems to be particularly suitable in preventing atmospheric icing since the droplet size, and hence the droplet inertia, is small compared to spray icing. The method has not been tested. Energy requirements may be a problem.

Ice accretion due to evaporation fog is usually found only in a narrow zone (some tens of meters) from the downwind edge of the water body (Mook 1965, Utaaker 1979). Therefore, it might be possible to reduce icing on sea structures by preventing evaporation in the vicinity of the structures. Surface films of liquids such as oil are not usable because of pollution problems, but floats constructed of sheets of closed-cell buoyant plastic might be used. One possibility is simply to surround the object to be protected with a platform of sufficiently large horizontal dimensions. These floats would be useful for reducing spray icing as well, because of their role in damping waves.

Another way of avoiding the existence of supercooled fog is artificial fog dissipation by liquid propane seeding (Hicks 1966). This has been shown to be effective in cold room conditions at air temperatures below -0.5°C (Kumai 1982).

Melcher (1951) showed that the density of ice decreases if it grows in an electric field. Phan and Laforte (1981) confirmed this and showed that the adhesion strength of the accreted ice on wires depends on the applied electric field (Fig. 49). In some applications this phenomenon might be of benefit in anti-icing, but no practical tests have been made.

The formation of ice deposits on wire, especially from wet snow, is promoted if the wire rotates or if the deposit slides to the lee side, so that a cylindrical deposit enveloping the wire is formed. In this case an anti-icing effect is achieved by anti-torsion weights, which prevent the wires

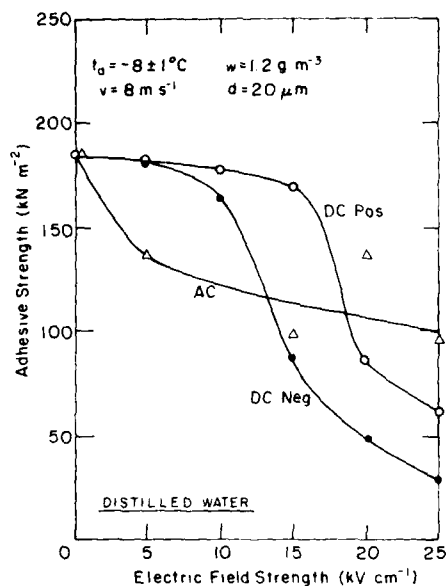


Figure 49. Adhesive strength of ice vs electric field strength. (After Phan and Lafort 1981.)

from twisting, and by small rings or a pair of plastic fins attached to the wire, which prevent the ice from sliding (Wakahama et al. 1977).

DEICING METHODS

Mechanical methods

Manual deicing has been the only method generally used in combating ice at sea so far. The ice is removed by crew members using mallets, axes, hammers, baseball bats, etc. This method is not satisfactory because of its low efficiency; many ships have been lost in spite of manual deicing attempts. Moreover, conditions on deck during severe icing are hazardous, and movement is almost impossible when deicing is needed most. The use of motorized cutters for removing ice (Churakov et al. 1976) is usually possible only after the icing storm. It is seldom possible at any time to manually remove ice from the upper parts of the structures most critical to ship stability and the endurance of stationary structures.

To avoid manual ice removal automatic and semiautomatic deicing methods have been developed. The most effective of these devices is a pneumatic deicer, a series of tubes standing alone or built into a rubber mat (Fig. 50). When the tubes are inflated with air, they expand and break the ice adhering to the surface. The same principle has long been used for protecting aircraft wings from icing. Pneumatic deicers have proven to be effective on small cylindrical objects and large flat surfaces (Stallabrass 1970, Ackley

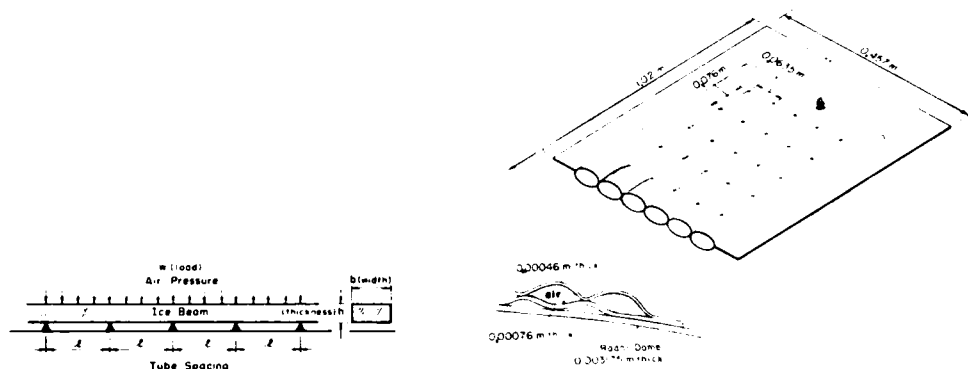


Figure 50. Pneumatic deicer. (From Ackley et al. 1977.)

et al. 1973, 1977). Disadvantages of this method are the cost and the likelihood of damage to the deicers if used in working areas. Otherwise, this method seems to be very suitable, especially in deicing the upper parts of sea structures. Combined with automatic icing control devices, pneumatic deicers might be a solution for protecting unmanned ocean installations.

Economical mechanical deicing can be achieved by using a flexible coating that moves due to wind drag. Hartranft (1972) tested this kind of coating in sheltering radar antennas, but the results were not completely satisfactory, probably because accreting ice makes the coating partly inflexible. Alexeiev (1974) covered small-scale models of meteorological masts with flexible coatings, fixing the coatings with the aid of guy ropes. Vibration of the mast and the guy ropes is supposed to move the coating sufficiently for ice removal. Also, a large number of small, conical plastic shelters that move in the wind have been tested with some success in small-scale tests. Results from full-scale tests of these methods have not been reported. A mechanical deicer based on metal plates and wires moving by means of electromagnetic induction, activated by discharge from a condenser through a solenoid situated near the surface of the plates, has also been used in protecting meteorological instruments (Alexeiev 1974).

Jaakkola et al. (1983) successfully used a vibrator for deicing the guy wires of tall masts. A frequency of 20-30 Hz loosens thick ice from the wires after 2-3 minutes. Vibration of the object does not, however, prevent icing, as shown by anemometers that often are covered by ice. Klinov's (1970) test instruments vibrating at a frequency of 50 Hz collected the same amount of ice as the stationary ones.

Thermal methods

Heating is not an economical deicing method, especially compared to mechanical measures. Melting of ice at 0°C requires the energy W_t ;

$$W_t = L_f \rho V \quad (34)$$

where ρ is the ice density and V is the volume of the melted ice. If the removal of ice with a density of 0.9 g cm^{-3} from a vertical surface requires that a 1-mm-thick ice layer be melted (Ackley et al. 1973), then the heat W_t needed for deicing a 1-cm^2 surface would be $W_t \approx 30 \text{ J}$ (from eq 34). Mechanical removal of the same amount of ice would require energy W_m ;

$$W_m = F A \delta \quad (35)$$

where F = adhesive strength

A = surface area

δ = distance moved before the ice is displaced.

If δ is less than 1 cm and taking a typical value 4.7 kg cm^{-2} (0.48 N cm^{-2}) for F (Table 8), $W_m < 0.5 \text{ J}$ for a 1-cm^2 surface. Hence, the ratio $W_t/W_m > 60$, which demonstrates the inefficiency of heating compared to mechanical ice removal.

Hot water is rather effective in short-term ice prevention and is sometimes used as a deicing method on ships [in 4% of the cases when combating icing (Panov 1978)]. A disadvantage of this method, in addition to high heat consumption, is that water for protecting the upper parts of the structures falls and flows along the surfaces and may increase icing at lower levels. Unheated seawater may also be used in anti-icing by producing a water film on structure surfaces. However, this method is not effective if icing is severe (at low air temperatures, for example) and may lead to increased icing if improperly controlled. Thermal and mechanical methods are combined in the so-called seawater lance, which consists of a high-pressure jet of seawater capable of removing ice by melting and dynamic pressure.

Surface materials and coatings

Surface material does not have much influence on the intensity of ice accretion, so coatings, for example, are not an effective anti-icing method. This has been demonstrated in experiments where ice accretion on surfaces of different materials has been compared (e.g., Rink 1938, Kreutz 1941, Popolansky and Kruzik 1976). Only in the very initial stage of icing has some anti-

icing effect been observed on coatings such as organosilicone epoxy (Paniushkin et al. 1974e). This effect is probably due to high hydrophobicity of the surface, which allows the impinging droplets to run off rapidly before they turn to ice at air temperatures close to 0°C. Theoretically the heat conductivity of the surface material affects the icing intensity in the wet-growth regime, but this effect is small and is also restricted to the initial stage of the icing process. Black paint can be used to promote the absorption of solar radiation, but this is of little use in arctic areas in winter. The effect of black paint is weak during the icing process since the sun is obscured by fog or clouds; it is also weak when a thick ice layer has already developed.

The use of low-adhesion surface coatings is a deicing measure, but it is not very effective if used alone. This is because none of the presently available surface materials has an adhesive strength low enough to promote a spontaneous release of ice, that is, a release due to the weight of the ice alone. However, combined with mechanical and thermal methods, coatings and paints can be very effective in making deicing easier. For example, the time needed for deicing a surface by heating is reduced considerably when the surface is coated with a suitable material (Hanamoto et al. 1980). Also, the ease of manual and automatic mechanical ice removal is very sensitive to the strength of adhesion of the ice to the material (eq 35). Polymer coatings have proved to be especially useful in routine service when deicing meteorological instruments (Gerger 1974, Strangeways and Curran 1977) and navigation lock walls (Frankenstein et al. 1976).

There are several theories explaining the adhesion phenomenon, among them electrostatic, diffusion, mechanical, chemical and mechanical-deformation theories (for references, see Phan et al. 1978). None seems to give a completely satisfactory description of the nature of ice adhesion, although some progress in the theoretical approach has been made recently (Oksanen 1982). Therefore, investigations of the adhesion of ice to different substances have been mostly empirical using laboratory instrumentation (e.g., Paniushkin et al. 1974c, Phan et al. 1978, Jellinek and Chodak 1983). The lack of a satisfactory theory of ice adhesion has resulted in considerably different views in the literature on the usefulness of deicing coatings. Generally the Soviet views (e.g., Borisenkov and Panov 1974, Paniushkin et al. 1974a,b) are more optimistic than those found in the western literature (e.g., Porte and Napier 1963, Lock 1972, Minsk 1977). These views are some-

what contradictory, probably because the experimental results are confusing as well. There are considerable difficulties in making reliable and comparable adhesive strength measurements; repeatable results are difficult to obtain, even in laboratory conditions (Phan et al. 1978). Moreover, the environmental conditions during and after ice accretion, as well as at the time of contact, affect the results.

When developing synthetic coatings having low adhesion to ice, researchers have looked for relationships between adhesive strength and other properties that are easy to measure. Quantitative indicators of adhesive strength have not been found, but it has been observed qualitatively that low adhesion to ice is generally connected with low permeability and absorption capacity and high hydrophobicity. Substances that meet these requirements, such as synthetic polymer surfaces, have proved to be effective in reducing ice adhesion. An example of the effect of a Soviet product, organosilicone epoxy "G," can be seen in Table 7. Tables 4 and 7 show that polymer coatings have a decisive effect on the adhesive strength. The adhesive strength with polymer coatings is more than an order of magnitude less than on uncoated surfaces. In full-scale tests on a ship the best coatings were Teflon-4, organosilicone epoxy "G," and a vinyl polymer sheet with perfluorinated film (Paniushkin et al. 1974b,c). Laboratory tests with ice accreted in a wind tunnel (Phan et al. 1978) showed that the durability and effectiveness of silicone rubber made it the most promising surface coating for wires such as electrical conductors and guy wires of masts (Table 4). Reports of the effect of a poly-bisphenol-A-polycarbonate block copolymer have also been encouraging (Jellinek et al. 1978, Jellinek and Chodak 1983).

Tables 4 and 7 should be interpreted with care, since there are many sources of scatter in the data. As mentioned, differences in ambient condi-

Table 7. Ice adhesion on different coatings.
(After Paniushkin et al. 1974.)

| Type of coating | Adhesion of ice (kg cm ⁻²) |
|--------------------------------------|--|
| Type "G" coating | 0.1 |
| Perfluorinated | 0.1 |
| Standard coating (oil-base) | 4.67 |
| Standard with perfluorinated surface | 0.84 |
| Standard with organosilicon surface | 0.98 |

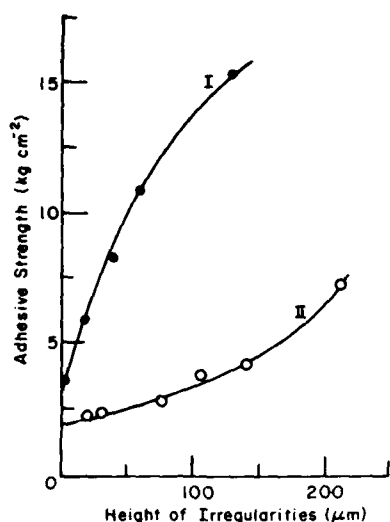


Figure 51. Dependence of adhesion of ice on the height of irregularities: I = clean steel; II = steel with sorbed toluene film. (From Paniushkin et al. 1974d.)

tions and technical difficulties in making the experiments may weaken the results. Also, Paniushkin et al. (1974d) showed that adhesive strength of ice depends markedly on the roughness of the icing surface (Fig. 51). Impurities in the water from which the ice is formed are not meaningless either; for example, salt in the water leads to weaker bonding (Paniushkin et al. 1974d, Oksanen 1982). Moreover, bulk-formed ice may be different from ice formed by droplet accretion. This is of great interest in studying problems caused by atmospheric ice accretion, and more adhesion measurements with real glaze and rime deposits should therefore be made. The importance of this aspect is demonstrated by the fact that Stallabrass (1963) and Phan et al. (1978) (Table 4) found Teflon to be quite ineffective in reducing adhesion of ice produced by droplet accretion, while the adhesive strength of bulk-formed ice on Teflon has been shown to be very low in many other studies (Aksiutin 1979). These differences are probably due to the fact that the impinging droplets in droplet accretion are more effective at penetrating the relatively porous surface of Teflon and creating a strong mechanical bond. It therefore seems that the sizes of the surface roughness elements and the impinging droplets may have an important effect on the adhesive strength of ice formed by droplet accretion. Indications that the impact speed of the droplets have this kind of effect have already been found experimentally (Table 4).

Flexible surface-coating materials whose deicing effect is not based on low adhesive strength but on the ease of ice removal on impact have also been tested on ships (e.g., Tabata 1968, Stallabrass 1970, Sewell 1971). The sur-

faces tested were plastic foam mats, either alone or covered with a sheet of neoprene rubber. This type of coating is not very successful, although it makes the ice somewhat easier to remove manually. However, ice has spontaneously detached from a rubber mat on the outer side of a ship's bulwark. High costs, relatively poor durability and problems in attaching the rubber mats firmly are the main reasons for the limited use of the flexible coatings.

SUMMARY AND CONCLUSIONS

Atmospheric icing alone rarely causes severe ship icing, but when it occurs simultaneously with spray icing it may form a risk to ship stability. It can accumulate on upper parts of the ship that are not reached by spray droplets. On stationary structures spray icing is usually limited to the bottom 10 m, so atmospheric icing is the major risk to high structures at sea.

Estimating the intensity and probability of atmospheric icing on sea structures is difficult because a large number of environmental factors are involved and representative data are lacking. The approach to the problem in this paper was by theoretical considerations, by statistical relationships between icing and meteorological conditions, and by data from continental locations. These results should be interpreted with care because of uncertainties in the theory and in the representativeness of the data.

The theoretical treatment of icing intensity was based on the droplet trajectory calculations in the case of rime and on the heat balance of the icing surface in the case of glaze. It qualitatively explains the basic features of the icing phenomenon and allows estimates of the icing rate, which agree reasonably well with laboratory experiments. In nature, however, determining the relevant atmospheric parameters is difficult, hampering the applicability of the theoretical methods. Therefore, progress in estimating the severity of atmospheric ice accretion at sea is closely related to progress in determining and forecasting the properties of the atmospheric boundary layer over the sea. Estimating the maximum intensities of glaze and rime formation is easier since maximum intensities are less sensitive to the liquid water content and droplet size, which are the most uncertain parameters involved with icing intensity calculations. The maximum intensities of icing due to supercooled fog and precipitation over the sea are about $3 \text{ g cm}^{-2} \text{ h}^{-1}$. A satisfactory theory for the rate of wet snow accumulation still

needs to be developed. It seems, however, that wet snow does not form heavy loads on structures other than wires, which may be encapsulated by snow, and large horizontal surfaces. The rate of formation of hoarfrost is negligible compared to the typical growth rate of glaze and rime.

The meteorological conditions under which icing occurs are rather well known in continental conditions, but not over the sea. The most common mechanism of atmospheric icing at sea is the formation of evaporation fog. Advection fogs and freezing precipitation occur only very close to the coasts. Evaporation fog is also very unlikely more than 50 km from the nearest coast or sea-ice boundary, and atmospheric icing should not cause any serious problems. Icing events are usually associated with winds blowing from the coast or sea-ice boundary.

Air temperature, wind speed, liquid water content and droplet size all affect the properties of the accreting ice. High values of these parameters favor the growth of compact ice with high adhesive strength, particularly glaze instead of rime.

Geographical distribution of atmospheric icing probabilities is uncertain because data are lacking. Data from coastal regions and islands are not representative. Therefore, information in this respect is mainly limited to the frequencies of freezing air temperatures, which may be used as a first approximation. The new self-deicing automatic icing detectors provide means of quite reliably measuring icing intensity, except possibly during very severe icing.

Anti-icing and deicing involve many serious problems that restrict their general use; thermal heating is not economical on large surfaces, and chemical methods and many of the anti-adhesive coatings are impractical because of weathering. Preventing evaporation fog from forming by covering the sea surface around the structures, and dissipating fog by liquid propane seeding are examples of possibilities that require more testing. Pneumatic deicers combined with automatic icing detection may be a solution for protecting unmanned ocean installations. Flexible coatings and coatings with low adhesive strength are effective in making the mechanical removal of ice easier, but they don't produce spontaneous breakup of ice from stationary structures. More effective mechanical devices for ice removal and coatings with lower adhesion and higher durability will probably be available in the near future, but a complete solution to ice prevention is not within sight. Only dramatic progress in solving the energy requirement problems involved

with thermal anti-icing and deicing methods would substantially improve our chances in combating icing on sea structures economically.

LITERATURE CITED

- Achenbach, E. (1977) The effect of surface roughness on the heat transfer from a circular cylinder to the cross flow of air. International Journal of Heat and Mass Transfer, 20: 359-369.
- Ackley, S.F. and K. Itagaki (1974) The crystal structure of a natural freezing rain accretion. Weather, 29: 189-192.
- Ackley, S.F. and M.K. Templeton (1979) Computer modeling of atmospheric ice accretion. U.S.A. Cold Regions Research and Engineering Laboratory, CRREL Report 79-4. ADA-068 582.
- Ackley, S.F., K. Itagaki and M. Frank (1973) An evaluation of passive deicing, mechanical deicing and ice detection. U.S.A. Cold Regions Research and Engineering Laboratory, Internal Report 351. AD-777947.
- Ackley, S.F., K. Itagaki and M. Frank (1977) Deicing of radomes and lock walls using pneumatic devices. Journal of Glaciology, 19: 467-478.
- Ahti, K. (1978) On factors affecting rime formation in Finland. M.S. thesis, Department of Meteorology, University of Helsinki (in Finnish).
- Ahti, K. and L. Makkonen (1982) Observations on rime formation in relation to routinely measured meteorological parameters. Geophysica, 19(1): 75-85.
- Aksiutin, L.R. (1979) Ship icing. Leningrad: Sudostroenie (in Russian).
- Alexeev, Ju.K. (1974) Protecting sensors and masts of automatic meteorological stations against icing. World Meteorological Organization Technical Note, 135: 7-16.
- Austin, J.M. and S.L. Hensel (1956) Analysis of freezing precipitation along the eastern North American coastline. Massachusetts Institute of Technology, Technical Report 112.
- Ashworth, T. and C.A. Knight (1978) Cylindrical ice accretions as simulations of hail growth: I. Effects of rotation and mixed clouds. Journal of the Atmospheric Sciences, 35: 1987-1996.
- Bain, M. and J.F. Gayet (1982) Aircraft measurements of icing in supercooled and water droplet/ice crystals clouds. Journal of Applied Meteorology, 21: 631-641.
- Bain, M. and J.F. Gayet (1983) Contribution to the modeling of the ice accretion process: Ice density variation with the impacted surface angle. Proceedings of First International Workshop on Atmospheric Icing of Structures (L.D. Minsk, Ed.). U.S.A. Cold Regions Research and Engineering Laboratory, Special Report 83-17, pp. 13-20.

- Baranowski, S. and J. Liebersbach (1977) The intensity of different kinds of rime on the upper tree line in the Sudety Mountains. Journal of Glaciology, 19: 489-497.
- Bashkirova, G.M. and P.N. Krasikov (1958) Certain microphysical characteristics of winter fogs over the Angara River near the city of Irkutsk. Glavnaia Geograficheskaiia Observatoriia, Trudy 73: 37-49. Leningrad: Gidrometeoizdat [in Russian, cited in Saunders (1964)].
- Bates, C.C. (1973) Navigation of ice covered waters. International Congress of Navigation, Brussels, Report 23.
- Bauer, D. (1973) Snow accretion on power lines. Atmosphere, 11: 88-96.
- Beard, K.V. and H.R. Pruppacher (1969) A determination of the terminal velocity and drag of small water drops by means of a wind tunnel. Journal of the Atmospheric Sciences, 26: 1066-1072.
- Bennett, I. (1959) Glaze, its meteorology and climatology, geographical distribution and economic effects. Quartermaster Research and Engineering Center, Technical Report EP-105.
- Best, A.C. (1950) The size distribution of raindrops. Quarterly Journal of the Royal Meteorological Society, 76: 16-36.
- Borisenkov, E.P. (1969) Physical justification of combinations of hydrometeorological conditions that produce ship icing. Arkticheskii i Antarkticheskii Nauchno-Issledovatel'skii Institut. Leningrad: Gidrometeoizdat (in Russian).
- Borisenkov, E.P. and V.V. Panov (1974) Basic results and prospects of research on hydrometeorological conditions on shipboard. In Investigation of the Physical Nature of Ship Icing. U.S.A. Cold Regions Research and Engineering Laboratory, Draft Translation 411, pp. 1-30. ADA003215.
- Borisenkov, E.P. and I.G. Pchelko (1975) Indicators for forecasting ship icing. U.S.A. Cold Regions Research and Engineering Laboratory, Draft Translation 481. ADA30113.
- Brower, W.A., Jr., H.V. Searby, J.L. Wise, H.F. Diaz and A.S. Prechtel (1977) (1977) Climatic atlas of the outer continental shelf waters and coastal regions of Alaska. Vols. I-III. Arctic Environmental Information and Data Center, University of Alaska, Anchorage.
- Brownscombe, J. and J. Hallett (1967) Experimental and field studies of precipitation particles formed by the freezing of supercooled water. Quarterly Journal of the Royal Meteorological Society, 93: 455-474.
- Bugaev, V.A. and B.E. Peskov (1972) The state and perspectives of operative forecasting of especially dangerous hydrometeorological phenomena. Meteorologiya i Gidrologiya, 6: 106-115 (in Russian).
- Buser, O. and A.N. Aufdermaur (1972) The density of rime on cylinders. Quarterly Journal of the Royal Meteorological Society, 98: 388-391.

- Cansdale, J.T. and I.I. McNaughtan (1977) Calculation of surface temperature and ice accretion rate in mixed water droplet/ice crystal cloud. Royal Aircraft Establishment, Technical Report 77090.
- Chaine, P.M. (1974) Industrial meteorology. Study V, In-cloud icing. Environment Canada, Toronto.
- Churakov, L.Ia., V.K. Savinykh and R.N. Bobrov (1976) Snow and ice removal methods used for steamships in Siberia. Institut inzhenerov vodnogo transporta, Novosibirsk. Trudy, 94: 3-8 (in Russian).
- Church, P.E. (1945) Steam-fog over Lake Michigan in winter. Transactions of the American Geophysical Union, 26: 353-357.
- Colbeck, S.C. (1979) Grain clusters in wet snow. Journal of Colloid and Interface Science, 72: 371-384.
- Colbeck, S.C. and S.F. Ackley (1983) Mechanisms for ice bonding in wet snow accretions on power lines. Proceedings of First International Workshop on Atmospheric Icing of Structures (L.D. Minsk, Ed.). U.S.A. Cold Regions Research and Engineering Laboratory, Special Report 83-17, pp. 25-30.
- Currier, E.L., J.B. Knox and T.V. Crawford (1974) Cooling pond steam fog. Journal of the Air Pollution Control Association, 24: 860-864.
- DeAngelis, R.M. (1974) Superstructure icing. Mariner's Weather Log, 18: 1-7.
- Dickey, T.A. (1952) Analysis of the effects of certain variables in determining the form of an ice accretion. Aeronautical Engineering Laboratory. Naval Air Experimental Station, Philadelphia, Report AEL-1206.
- Diem, M. (1956) Ice loads on high voltage conductors in the mountains. Archiv fur Meteorologie, Geophysik und Bioklimatologie, Ser. B, 7: 84-85 (in German).
- Dranevic, E.P. (1971) Glaze and Rime. Leningrad: Gidrometeoizdat (in Russian).
- Dunbar, M. (1964) Geographical distribution of superstructure icing in the Northern Hemisphere. Defence Research Board, Canada, Miscellaneous Report G-15.
- Fitzgerald, J.W. (1978) A numerical model of the formation of droplet spectra in advection fogs off Nova Scotia. Journal of the Atmospheric Sciences, 35: 1522-1535.
- Frankenstein, G., J. Wuebben, H.H.G. Jellinek and R. Yokota (1976) Ice removal from the walls of navigation locks. Proceedings of Symposium on In-land Waters for Navigation, Flood Control and Water Division, Colorado, pp. 10-12.
- Fraser, D., C.K. Rush and D. Baxter (1953) Thermodynamic limitations of ice accretion instruments. Bulletin of the American Meteorological Society, 34: 146-154.

- Gaponov, B.S. (1939) Temperature limits for glaze and rime formation from supercooled fog. Izvestiia Akademii Nauk SSSR, Seriya Geograficheskaya i Geofizicheskaya, 2: 205-216 (in Russian).
- Gavrilova, M.K. (1966) Radiation Climate of the Arctic. Jerusalem: Israeli Program for Scientific Translation.
- Gerger, H. (1974) Methods used to minimize, prevent and remove ice accretion on meteorological surface instruments. World Meteorological Organization Technical Note, 135: 1-6.
- Glukhov, V.G. (1971) Evaluation of ice loads on high structures from upper-air observations. Soviet Hydrology, Selected Papers, 3: 223-228.
- Glukhov, V.G. (1974) Distribution of glaze-rime deposits in the lower 300-meter layer of the atmosphere. U.S. Army Foreign Science and Technology Center, Translation AD785965.
- Godier, R. (1966) Improvements in the measurements made by automatic weather stations under icing conditions. World Meteorological Organization Technical Note, 82: 63-66 (in French).
- Golubev, V.N. (1974) On the structure of ice formed during icing of ships. In Investigation of the Physical Nature of Ship Icing. U.S.A. Cold Regions Research and Engineering Laboratory, Draft Translation 411, pp. 108-116. AD003215.
- Goodman, J. (1977) The microstructure of California coastal fog and stratus. Journal of Applied Meteorology, 16: 1056-1067.
- Grunow, J. and H. Tollner (1969) Fog deposition in high mountains. Archiv fur Meteorologie, Geophysik und Bioklimatologie, Ser. B, 17: 201-218 (in German).
- Guttman, N.B. (1971) Study of worldwide occurrence of fog, thunderstorms, supercooled low clouds and freezing temperatures. Naval Weather Service Command, NAVAIR 50-1c-60.
- Hallett, J. (1964) Experimental studies of the crystallization of supercooled water. Journal of the Atmospheric Sciences, 21: 671-682.
- Hanamoto, H.G., J.J. Gagnon and B. Pratt (1980) Deicing a satellite communication antenna. U.S.A. Cold Regions Research and Engineering Laboratory, Special Report 80-18.
- Hartranft, G.J. (1972) Evaluation of polyurethane shroud designed to prevent TACAN weather outages. Federal Aviation Administration, Report FAA-RD-72-78.
- Hay, R.F.M. (1953) Frost smoke and unusually low air temperature at Ocean Weather Station India. Marine Observer, 23: 218-225.
- Heath, E.D. and M.L. Cantrell (1972) Aircraft icing climatology for the Northern Hemisphere. U.S. Air Force Air Weather Service, Technical Report 220.

- Herman, G.F. (1980) Thermal radiation in arctic stratus clouds. Quarterly Journal of the Royal Meteorological Society, 106: 771-780.
- Hicks, B.B. (1977) The prediction of fog over cooling ponds. Journal of the Air Pollution Control Association, 27: 140-142.
- Hicks, J.R. (1966) Improving visibility during periods of supercooled fog. U.S.A. Cold Regions Research and Engineering Laboratory, Technical Report 181.
- Horjen, J. (1981) Ice accretions on ships and marine structures. Marine Structures and Ships in Ice. Norwegian Hydrodynamic Laboratories, Report No. 81-02.
- Houghton, H.G. and W.H. Radford (1938) On the measurement of drop size and liquid water content in fogs and clouds. Massachusetts Institute of Technology Papers on Physical Oceanography and Meteorology (cited in Minsk 1977).
- Imai, I. (1953) Studies of ice accretion. Research on Snow and Ice, 1: 35-44 (in Japanese).
- Itagaki, K. (1977) Icing on ships and stationary structures under maritime conditions. U.S.A. Cold Regions Research and Engineering Laboratory, Special Report 77-27.
- Iwata, S. (1973) Ice accumulation of ships. Journal of the Society of Naval Architects of Japan, Selected Papers, 11: 60-86.
- Jaakkola, Y., J. Laiho and M. Vuorenvirta (1983) Ice accumulation on tall radio and TV towers in Finland. Proceedings of First International Workshop on Atmospheric Icing of Structures (L.D. Minsk, Ed.). U.S.A. Cold Regions Research and Engineering Laboratory, Special Report 83-17, pp. 249-260.
- Jacobs, L. (1954) Frost smoke. Marine Observer, 24: 113-114.
- Jellinek, H.H.G. and I. Chodak (1982) Adhesion of ice from helicopter rotor blades: Preliminary work. Proceedings of First International Workshop on Atmospheric Icing of Structures (L.D. Minsk, Ed.). U.S.A. Cold Regions Research and Engineering Laboratory, Special Report 83-17, pp. 97-107.
- Jellinek, H.H.G., H. Kachi, S. Kittaka, M. Lee and R. Yokota (1978) Ice releasing block-copolymer coatings. Colloid and Polymer Science, 256: 544-551.
- Johnson, D.A. and J. Hallett (1968) Freezing and shattering of supercooled water drops. Quarterly Journal of the Royal Meteorological Society, 94: 468-482.
- Kamenetskii, I.I., Z.I. Shvaishtein and A.A. Sergeeva (1971) Ice adhesion to anti-icing deck coatings. In Theoretical and Experimental Studies of Ship Icing (E.P. Borisenkov, Ed.). Arkticheskii i Antarkticheskii

- Neuchno-Issledovatel'skii Institut. Leningrad: Gidrometeoizdat (in Russian).
- Kaplina, T.G. and K.I. Chukanin (1971) Results of studies of synoptic conditions of ship icing. In Theoretical and Experimental Studies of Ship Icing (E.P. Borisenkov, Ed.). Arkticheskii i Antarkticheskii Neuchno-Issledovatel'skii Institut. Leningrad: Gidrometeoizdat (in Russian).
- Kachurin, L.G. and L.I. Gashin (1969) Calculation of icing of structures in a flow of supercooled aerosol in application to ship icing. Usloviia Obladeniia Sudov, pp. 21-30, Leningrad: Gidrometeoizdat (in Russian).
- Kachurin, L.G., L.I. Gashin and I.A. Smirnov (1974) Icing rate of small-capacity fishing vessels under various hydrometeorological conditions. Meteorologiya i Gidrologiya, 3: 50-60 (in Russian).
- King, R.D. (1973) Hyviz - A new high light transmission and electrically conducting film for heating ships' bridge windows. Marine Engineering Research, 1973: 37-38.
- Klinov, F.Ya. (1970) Rime and Glaze in the Lower 300-Meter Layer of the Atmosphere. Leningrad: Gidrometeoizdat (in Russian).
- Klinov, F. Ya. and V.P. Boikov (1974) Glaze/rime deposition in the lower 500-meter layer of the atmosphere as determined from interruptions in the operation of tv-towers. Glavnaiia Geograficheskaiia Observatoriia, Trudy 333: 22-29. Leningrad: Gidrometeoizdat (in Russian).
- Kolbig, J. (1973) Ice accretions on objects. Abhandlungen Meteorologie Dienst, DDR, 107: 36-40 (in German).
- Kolosova, N.V. (1974) Regions of possible ship icing in Chukotsk Sea during summer-autumn period. In Investigation of the Physical Nature of Ship Icing. U.S.A. Cold Regions Research and Engineering Laboratory, Draft Translation 411, pp. 161-171. ADA003215.
- Korniushin, O.G. and A.P. Tiurin (1979) Providing the fishing fleet with data on hazardous and very hazardous hydrometeorological phenomena. Meteorologiya i Gidrologiya, 2: 114-117 (in Russian).
- Kowalski, G.J. and J.W. Mitchell (1976) Heat transfer from spheres in the naturally turbulent, outdoor environment. Journal of Heat Transfer, 98: 649-653.
- Kreutz, W. (1941) A contribution to ice accretion studies. Das Wetter, 58: 137-150 (in German).
- Kumai, M. (1973) Arctic fog droplet size distribution and its effect on light attenuation. Journal of the Atmospheric Sciences, 30(4): 635-643.
- Kumai, M. (1982) Formation of ice crystals and dissipation of supercooled fog by artificial nucleation and variations of crystal habit at early growth stages. Journal of Applied Meteorology, 21: 579-587.

- Kolosova, N.V. (1974) Regions of possible ship icing in Chukotsk Sea during summer-autumn period. In Investigation of the Physical Nature of Ship Icing. U.S.A. Cold Regions Research and Engineering Laboratory, Draft Translation 411, pp. 161-171. ADA003215.
- Korniushin, O.G. and A.P. Tiurin (1979) Providing the fishing fleet with data on hazardous and very hazardous hydrometeorological phenomena. Meteorologiya i Gidrologiya, 2: 114-117 (in Russian).
- Kowalski, G.J. and J.W. Mitchell (1976) Heat transfer from spheres in the naturally turbulent, outdoor environment. Journal of Heat Transfer, 98: 649-653.
- Kreutz, W. (1941) A contribution to ice accretion studies. Das Wetter, 58: 137-150 (in German).
- Kumai, M. (1973) Arctic fog droplet size distribution and its effect on light attenuation. Journal of the Atmospheric Sciences, 30(4): 635-643.
- Kumai, M. (1982) Formation of ice crystals and dissipation of supercooled fog by artificial nucleation and variations of crystal habit at early growth stages. Journal of Applied Meteorology, 21: 579-587.
- Kumai, M. and K.E. Francis (1962) Size distribution and liquid water content of fog, Northwestern Greenland. U.S.A. Cold Regions Research and Engineering Laboratory, Research Report 100.
- Kuroiwa, D. (1965) Icing and snow accretion of electric wires. U.S.A. Cold Regions Research and Engineering Laboratory, Research Report 123.
- Laforte, J-L., C.L. Phan, B. Felin and R. Martin (1983a) Adhesion of ice on aluminum conductor and crystal size in the surface layer. Proceedings of First International Workshop on Atmospheric Icing of Structures (L.D. Minsk, Ed.). U.S.A. Cold Regions Research and Engineering Laboratory, Special Report 83-17, pp. 83-92.
- Laforte, J-L., C.L. Phan, D.D. Nguyen and B. Felin (1983b) Determining atmospheric parameters during ice accretion from the microstructure on natural ice samples. Proceedings of First International Workshop on Atmospheric Icing on Structures (L.D. Minsk, Ed.). U.S.A. Cold Regions Research and Engineering Laboratory, Special Report 83-17, pp. 175-184.
- Langmuir, I. and K.B. Blodgett (1946) A mathematical investigation of water droplet trajectories. U.S. Army Air Forces, Technical Report 5418.
- Larkin, B.S. and S. Dubuc (1976) Self-deicing navigation buoys using heat pipes. European Space Agency, ESA SP112, 1, pp. 529-535.
- Lee, A. (1958) Ice accumulation on trawlers in the Barents Sea. Marine Observer, 28: 138-142.
- Lenhard, R.W. (1955) An indirect method for estimating the weight of glaze on wires. Bulletin of the American Meteorological Society, 36(1): 1-5.

- Lesins, G.B., R. List and P.I. Joe (1980) Ice accretions. Part I: Testing of new atmospheric icing concepts. Journal of Atmospheric Research, 14: 347-356.
- Levi, L. and F. Prodi (1978) Crystal size in ice grown by droplet accretion. Journal of the Atmospheric Sciences, 35: 2181-2189.
- Lewis, W. and R.J. Brun (1956) Impingement of water droplets on a rectangular half body in a two-dimensional incompressible flow field. National Advisory Committee for Aeronautics, Technical Note 3658.
- List, R. (1977) Ice accretions on structures. Journal of Glaciology, 19(81): 451-465.
- List, R., P.I. Joe, G. Lesins, P.R. Kry, M.R. deQuervain, J.D. McTaggart-Cowan, P.W. Stagg, E.P. Lozowski, E. Freire, R.E. Stewart, C.G. List, M.C. Steiner and J. Von Niederhausern (1976) On the variation of the collection efficiencies of icing cylinders. Proceedings, International Conference of Cloud Physics, Colorado, pp. 233-239.
- Lock, G.S.H. (1972) Some aspects of ice formation with special reference to the marine environment. Transactions, North-east Coast Institute of Engineers and Shipbuilders, 88: 175-186.
- Lomilina, L.E. (1977) The effect of relief on glaze-ice and rime deposition. Meteorologiya i Gidrologiya, 2: 49-55. Also Soviet Meteorology and Hydrology, 2: 39-43.
- Lozowski, E.P. and M.M. Oleskiw (1983) Computer modeling of time-dependent rime icing in the atmosphere. U.S.A. Cold Regions Research and Engineering Laboratory, CRREL Report 83-2.
- Lozowski, E.P., J.R. Stallabrass and P.F. Hearty (1979) The icing of an unheated non-rotating cylinder in liquid water droplet-ice crystal clouds. National Research Council of Canada, Report LTR-LT-96.
- Ludlam, F.H. (1951) The heat economy of a rimed cylinder. Quarterly Journal of the Royal Meteorological Society, 77: 663-666.
- Lundqvist, J.-E. and I. Udin (1977) Ice accretion on ships with special emphasis on Baltic conditions. Winter Navigation Research Board, Norrkoping, Sweden, Research Report 23.
- MacArthur, C.D. (1983) Numerical simulation of airfoil ice accretion. Paper prepared for the 21st Aerospace Sciences Meeting, Reno, Nevada, AIAA-83-0112.
- McComber, P. and G. Touzot (1981) Calculation of the impingement of cloud droplets in a cylinder by the finite-element method. Journal of the Atmospheric Sciences, 38: 1027-1036.
- McKay, G.A. and H.A. Thompson (1969) Estimating the hazard of ice accretion in Canada from climatological data. Journal of Applied Meteorology, 8: 927-935.

- Macklin, W.C. (1961) Accretion in mixed clouds. Quarterly Journal of the Royal Meteorological Society, 87: 413-424.
- Macklin, W.C. (1962) The density and structure of ice formed by accretion. Quarterly Journal of the Royal Meteorological Society, 88: 30-50.
- Macklin, W.C. and G.S. Payne (1967) A theoretical investigation of the ice accretion process. Quarterly Journal of the Royal Meteorological Society, 93: 195-214.
- Macklin, W.C. and G.S. Payne (1968) Some aspects of the accretion process. Quarterly Journal of the Royal Meteorological Society, 94: 167-175.
- McLeod, W.R. (1977) Atmospheric superstructure ice accumulation measurements. Proceedings of Offshore Technology Conference, OTC 2950, pp. 555-564.
- McLeod, W.R. (1981) Atmospheric superstructure ice accumulation measurements. Proceedings of Sixth Conference on Port and Ocean Engineering under Arctic Conditions, pp. 1067-1093.
- Makkonen, L. (1979) Ice accretion on structures at sea. M.S. thesis, Department of Meteorology, University of Helsinki (in Finnish).
- Makkonen, L. (1981a) The heat balance of wet snow. Meteorological Magazine, 110: 82.
- Makkonen, L. (1981b) Estimating intensity of atmospheric ice accretion on stationary structures. Journal of Applied Meteorology, 20: 595-600.
- Makkonen, L. (in press) Modeling of ice accretion on wires. Submitted to Journal of Climate and Applied Meteorology.
- Makkonen, L. and K. Ahti (1983) The effect of meteorological parameters on rime formation in Finland. Proceedings of First International Workshop on Atmospheric Icing of Structures (L.D. Minsk, Ed.). U.S.A. Cold Regions Research and Engineering Laboratory, Special Report 83-17, pp. 167-174.
- Mason, B.J. (1971) The Physics of Clouds. Oxford: Clarendon Press.
- Matsuo, T., Y. Sasyo and Y. Sato (1981) Relationship between types of precipitation on the ground and surface meteorological elements. Journal of the Meteorological Society of Japan, 59:462-476.
- Matveev, L.T. (1967) Physics of the Atmosphere. Jerusalem: Israel Program for Science Transfer.
- Matveev, L.T. and S.A. Soldatenko (1977) On a theory of the formation and prediction of evaporation fogs. Meteorologiya i Gidrologiya, 2:24-31 (in Russian). Also Soviet Meteorology and Hydrology, 2: 18-24.
- Melcher, D. (1951) Experimental investigation of icing phenomenon. Zeitschrift fur Angewandte Mathematik und Physik, 2: 421-443 (in German).

- Miliutin, E.R. and Yu.I. Yaremenko (1981) An experimental study of the correlation between meteorological visibility range and the height of the lower cloud boundary. Meteorologiya i Gidrologiya, 3: 32-38 (in Russian).
- Minsk, L.D. (1977) Ice accumulation on ocean structures. U.S.A. Cold Regions Research and Engineering Laboratory, CRREL Report 77-17.
- Minsk, L.D. (1980) Icing on structures. U.S.A. Cold Regions Research and Engineering Laboratory, CRREL Report 80-31.
- Mizuno, Y. (1981) Structure and orientation of frozen droplets on ice surfaces. Low Temperature Science, Ser. A, 40: 11-23 (in Japanese).
- Mook, R.H.G. (1965) Steam fog on rivers. Archiv fur Meteorologie, Geophysik und Bioklimatologie, Ser. A, 14: 343-350.
- Murray, W.A. and R. List (1972) Freezing of water drops. Journal of Glaciology, 11: 415-429.
- Nature (1881) A singular case of shipwreck. 24: 106.
- Nikiforov, Eu.P. (1983) Icing related problems, effect of line design and ice load mapping. Proceedings of First International Workshop on Atmospheric Icing of Structures (L.D. Minsk, Ed.). U.S.A. Cold Regions Research and Engineering Laboratory, Special Report 83-17, pp. 239-245.
- Nyberg, A. (1966) Evaporation at a snow surface. Archiv fur Geophysik, 4: 577-590.
- Okihara, T., M. Kanamori, A. Kamimura, N. Hamada, S. Matsuda, J. Buturlia and G. Miskolczy (1980) Design, testing, and shipboard evaluation of a heat pipe deicing system. American Institute of Aeronautics and Astronautics 15th Thermophysics Conference, Colorado.
- Oksanen, P. (1982) Adhesion strength of ice. Technical Research Center of Finland, Research Report 123.
- Oleskiw, M.M. (1982) A computer simulation of time-dependent rime icing on airfoils. Ph.D. thesis, Division of Meteorology, University of Alberta.
- Ono, N. (1967) Studies of ice accumulation on ships. Part II, Conditions of icing and accreted ice weights. Defence Research Board, Canada, Translation T 94 J.
- Orlicz, M. and J. Orliczowa (1954) Rime in the Tatra Mountains. Przeglad Meteorologiczny i Hydrologiczny, 7: 107-140 (in Polish).
- Panov, V.V. (1976) Ship icing. Arkticheskii i Antarkticheskii Nauchno-Issledovatel'skii Institut, Trudy 334. Leningrad: Gidrometeoizdat (in Russian).
- Panov, V.V. (1978) Icing of ships. Polar Geography, 2(3): 166-186.

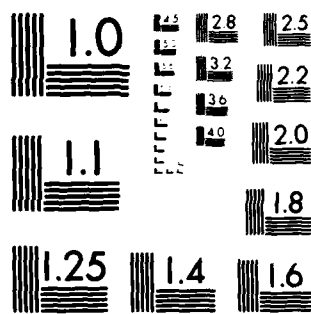
ATMOSPHERIC ICING ON SEA STRUCTURES(U) COLD REGIONS
RESEARCH AND ENGINEERING LAB HANOVER NH L MAKKONEN
APR 84 CRREL-MONO-84-2

22

F/G 8/12

NL

END
DATE
FILMED
9-84
DTIC



MICROCOPY RESOLUTION TEST CHART
NATIONAL BUREAU OF STANDARDS-1963-A

- Panov, V.V. and M.V. Schmidt (1971) Gradations of hydrometeorological complexes of icing considering their danger to ships. Problems of the Arctic and Antarctic, 38: 150-156.
- Paniushkin, V.B., V.B. Rozentsveig, Yu.B. Petrov, L.Ye. Gurvich and N.A. Sergacheva (1974a) Full-scale tests of coatings that reduce ice adhesion. In Investigation of the Physical Nature of Ship Icing. U.S.A. Cold Regions Research and Engineering Laboratory, Draft Translation 411, pp. 83-91. ADA003215.
- Paniushkin, V.B., Z.I. Shvaishtein and N.A. Sergacheva (1974b) On certain thermodynamic criteria for the choice of materials for coatings that reduce ice adhesion to construction materials. In Investigation of the Physical Nature of Ship Icing. U.S.A. Cold Regions Research and Engineering Laboratory, Draft Translation 411, pp. 49-57. ADA003215.
- Paniushkin, V.B., Z.I. Shvaishtein and N.A. Sergacheva (1974c) Method of determining adhesion of ice to construction materials and protective coatings by means of laboratory adhesiometer. In Investigation of the Physical Nature of Ship Icing. U.S.A. Cold Regions Research and Engineering Laboratory, Draft Translation 411, pp. 58-69. ADA003215.
- Paniushkin, V.B., Z.I. Shvaishtein, N.A. Sergacheva and V.S. Podokshik (1974d) Experimental investigations of ice adhesion to construction materials. In Investigation of the Physical Nature of Ship Icing. U.S.A. Cold Regions Research and Engineering Laboratory, Draft Translation 411, pp. 71-77. ADA003215.
- Paniushkin, V.B., Z.I. Shvaishtein, N.A. Sergacheva, V.B. Rozentsveig, A.P. Petrov and Yu.B. Petrov (1974e) Test results of certain means of combating ice under natural conditions. In Investigation of the Physical Nature of Ship Icing. U.S.A. Cold Regions Research and Engineering Laboratory, Draft Translation 411, pp. 92-97. ADA003215.
- Pflaum, J.C. and H.R. Pruppacher (1979) A wind tunnel investigation of the growth of graupel initiated from frozen drops. Journal of the Atmospheric Sciences, 36: 680-689.
- Phan, C.L. and J-L. Laforte (1981) The influence of electro-freezing on ice accumulation on high-voltage dc transmission lines. Cold Regions Science and Technology, 4: 15-25.
- Phan, C.L., P. McComber and A. Mansiaux (1978) Adhesion of rime and glaze on conductors protected by various materials. Transactions of the Canadian Society of Mechanical Engineers, 44: 204-208.
- Pillie, R.J. and W.C. Kocmond (1967) Project fog drops. Cornell Aeronautical Laboratory, Washington, D.C., NASA CR-675.
- Pinnick, R.G., D.L. Hoijhelle, G. Fernandez, E.B. Stenmark, J.D. Lindberg, G.B. Hoidale and S.G. Jennings (1978) Vertical structure in atmospheric fog and haze and its effects on visible and infrared extinction. Journal of the Atmospheric Sciences, 35: 2020-2032.

- Popolansky, F. and J. Kruzik (1976) Rime formation on various materials with different surface finish. Zeitschrift fur Meteorologie, 26: 310-313 (in German).
- Porte, H.A. and T.E. Napier (1963) Coating material for prevention of ice and snow accumulations. A literature survey. U.S. Naval Civil Engineering Laboratory, TN-541.
- Preobrazhenskii, L.Yu. (1973) Estimate of the content of spray drops in the near-water layer of the atmosphere. Fluid Mechanics: Soviet Research, 2: 95-100.
- Prodi, F. and L. Levi (1980) Hyperfine bubble structures in ice grown by droplet accretion. Journal of Atmospheric Research, 14: 373-384.
- Prodi, F., L. Levi, A. Frantini and C. Scarani (1982) Crystal size and orientation in ice grown by droplet accretion in wet and spongy regimes. Journal of the Atmospheric Sciences, 39:2301-2312.
- Pruppacher, H.R. and J.D. Klett (1978) Microphysics of Clouds and Precipitation. Dordrecht: D. Reidel Publishing.
- Reiquam, H. and M. Diamond (1959) Investigation of fog white-out. U.S.A. Cold Regions Research and Engineering Laboratory, Research Report 52.
- Rink, J. (1938) The melt water equivalents of rime deposits. Reichsamt fur Wetterdienst Wissenschaftliche Abhandlung, 5 (in German).
- Roos, D.S. and H.-D.R. Pum (1974) Sponginess of ice grown by accretion. Quarterly Journal of the Royal Meteorological Society, 100: 640-657.
- Rothig, H. (1973) A device for continuous measuring and recording of ice accretion. Abhandlungen Meteorologische Dienst DDR, 107: 26-30 (in German).
- Rush, C.K. and R.L. Wardlaw (1957) Icing measurements with a single rotating cylinder. National Aeronautical Establishment, Ottawa, Canada, Laboratory Report LR-206.
- Rye, P.J. and W.C. Macklin (1975) Crystal size in accreted ice. Quarterly Journal of the Royal Meteorological Society, 101: 207-215.
- Sadowski, M. (1965) Ice accretion on electric wires in Poland. Prace Panstowowego Inst. Hydrol.-Meteor., 87: 65-79 (in Polish).
- Sanderson, J.I. (1973) Occurrence of ice in the form of glaze, rime and hoarfrost with respect to the operation and storage of V/STOL aircraft. U.S. Army Engineer Topographic Laboratories, Ft. Belvoir, Virginia, Report ETL-SR-73-1. AD A001460.
- Saunders, P.M. (1964) Sea smoke and steam fog. Quarterly Journal of the Royal Meteorological Society, 90: 156-165.
- Sawada, T. (1970) Ice accretion on ships in the northern part of the Sea of Japan. Bulletin of the Hakodate Marine Observatory, 15: 29-35.

- Schlichting, H. (1979) Boundary-layer Theory. New York: McGraw-Hill.
- Schneider, H.W. (1978) Equation of the growth rate of frost forming on cooled surfaces. International Journal of Heat and Mass Transfer, 21: 1019-1024.
- Seban, R.A. (1960) The influence of free stream turbulence on the local heat transfer from cylinders. Journal of Heat Transfer, 82: 101-107.
- Semenova, Ye.P. (1974) Laboratory tests of chemical anti-icing agent in ANII cold chamber. In Investigation of the Physical Nature of Ship Icing. U.S.A. Cold Regions Research and Engineering Laboratory, Draft Translation 411, pp. 98-107. ADA003215.
- Sewell, J.H. (1971) Electro-impulse deicing system. Tech Air, 27: 6-9.
- Shannon, J.D. and R.G. Everett (1978) Effect of severe winter upon a cooling pond study. Bulletin of the American Meteorological Society, 59: 60-61.
- Shekhtman, A.N. (1968) The probability and intensity of the icing of ocean-going vessels. Nauchno-issledovatel'skii Institut Aeroklimat, Trudy 50: 50-65 (in Russian).
- Shellard, H.C. (1974) The meteorological aspects of ice accretion on ships. World Meteorological Organization, Marine Science Affairs, Report 10 (WMO 397).
- Shoda, M. (1953) Studies on snow accretion. Research on Snow and Ice, 1: 50-72 (in Japanese).
- Smith, M.E., R.V. Arimilli and E.G. Keshock (1983) Measurement of local heat transfer coefficient of four ice accretion shapes. Department of Mechanical and Aerospace Engineering, University of Tennessee, Final Technical Report, Part I.
- Smirnov, V.I. (1974) Conditions of ship icing and means of combating it. In Investigation of the Physical Nature of Ship Icing. U.S.A. Cold Regions Research and Engineering Laboratory, Draft Translation 411, pp. 178-182. ADA003215.
- Spinnangr, G. (1949) Fog and fog forecasting in northern Norway. Meteorologiske Annaler, 3: 75-136.
- Stallabrass, J.R. (1963) On the adhesion of ice to various materials. Canadian Aeronautics and Space Journal, 9: 199-204.
- Stallabrass, J.R. (1970) Methods for the alleviation of ship icing. National Research Council, Ottawa, Canada, Mechanical Engineering Report MD-51.
- Stallabrass, J.R. (1975) Icing of fishing vessels in Canadian waters. National Research Council, Ottawa, Canada. Department of Mechanical Engineering/National Aircraft Establishment Quarterly Bulletin, 1: 25-43.

- Stallabrass, J.R. (1978a) Airborne snow concentration and visibility. Proceedings of Second International Symposium on Snow Removal and Ice Control Research, U.S.A. Cold Regions Research and Engineering Laboratory, pp. 192-199.
- Stallabrass, J.R. (1978b) An appraisal of the single rotating cylinder method of liquid water content measurement. National Research Council, Ottawa, Canada, Laboratory Technical Report LTR-LT-92.
- Stallabrass, J.R. (1980) Trawler icing, a compilation of work done at National Research Council (NRC). National Research Council, Ottawa, Canada, Mechanical Engineering Report MD-56.
- Stallabrass, J.R. (1983) Aspects of freezing rain simulation and testing. Proceedings of First International Workshop on Atmospheric Icing of Structures (L.D. Minsk, Ed.). U.S.A. Cold Regions Research and Engineering Laboratory, Special Report 83-17, pp. 67-74.
- Stallabrass, J.R. and P.F. Hearty (1967) The icing of cylinders in conditions of simulated freezing sea spray. National Research Council, Ottawa, Canada, Mechanical Engineering Report MD-50.
- Stallabrass, J.R. and P.F. Hearty (1979) Further icing experiments on an unheated non-rotating cylinder. National Research Council, Ottawa, Canada, Laboratory Technical Report LTR-LT-105.
- Stallabrass, J.R. and E.P. Lozowski (1978) Ice shapes on cylinders and rotor blades. NATO Panel X Symposium on Helicopter Icing, London.
- Stanev, Sv. (1976) On ice accretion on mountains. Zeitschrift fur Meteorologie, 26:314-316 (in German).
- Strangeways, I.C. and J.C. Curran (1977) Meteorological measurements under conditions of icing: Some new attempts to solve the problem. World Meteorological Organization Technical Conference (TECIMO), Hamburg, pp. 7-12.
- Sunden, B. (1979) A theoretical investigation of the effect of freestream turbulence on skin friction and heat transfer for a bluff body. International Journal of Heat and Mass Transfer, 22: 1125-1135.
- Tabata, T. (1968) Research on prevention of ship icing. Defence Research Board, Ottawa, Canada, Translation T 95 J.
- Tabata, T., S. Iwata and N. Ono (1967) Studies of ice accumulation on ships. Part I. Defence Research Board, Ottawa, Canada, Translation T 93 J.
- Tattelman, P. (1982) An objective method for measuring surface ice accretion Journal of Applied Meteorology, 21: 599-612.
- Temkin, S. and H.K. Mehta (1982) Droplet drag in an accelerating and decelerating flow. Journal of Fluid Mechanics, 116: 297-313.
- Terziev, F.S. (1973) Experience of the hydrometeorological service of the USSR in providing services to mariners and fisheries in northern waters

- and the Atlantic Ocean. World Meteorological Organization, Marine Science Affairs, Report 8 (WMO 352), pp. 28-42.
- U.S. Navy Hydrographic Office (1958) Oceanographic atlas of polar seas, Part II. Hydrographic Office Publication No. 705.
- U.S. Navy Hydrographic Office (1963) Marine climatic atlas of the world. Vol. VI. Arctic Ocean.
- U.S. Weather Bureau (1959) Climatological and oceanographic atlas for mariners. Vol. I.
- Utaaker, K. (1979) Frost smoke downstream of hydroelectric power plants. Universitat Munchen, Wissenschaftliche Mitteilungen, 35: 206-210.
- Vasilieva, G.V. (1967) Hydrometeorological conditions causing ice accretion on ships. Defence Research Board, Ottawa, Canada, Translation T 486 R.
- Volobueva, G.V. (1975) Classification of glaze-rime deposits according to their weight. Glavnaia Geograficheskaiia Observatoriia, Trudy 303: 34-40. Leningrad: Gidrometeoizdat (in Russian).
- Waibel, K. (1955) Meteorological conditions of rime deposition on high voltage electrical lines in the mountains. Archiv fur Meteorologie, Geophysik und Bioklimatologie, Ser. B, 7: 74-83 (in German).
- Wakahama, G. (1979) Experimental studies of snow accretion on electrical lines developed in a strong wind. Journal of Natural Disaster Science, 1: 21-23.
- Wakahama, G., D. Kuroiwa and K. Goto (1977) Snow accretion on electric wires and its prevention. Journal of Glaciology, 19(81): 479-487.
- Wakahama, G., S. Kobayashi and K. Tusima (1979) In situ wind tunnel for snow accretion experiments using natural snowflakes. Low Temperature Science, Ser. A, 38: 183-187 (in Japanese).
- Wang, C.S. and R.L. Street (1978) Measurement of spray at an air-water interface. Dynamics of Atmospheres and Oceans, 2: 141-152.
- Wasserman, S.E. and D.J. Monte (1972) A relationship between snow accumulation and snow-intensity as determined from visibility. Journal of Applied Meteorology, 11:385-388.
- Wessels, H.R.A. (1979) Growth and disappearance of evaporation fog during the transformation of cold air mass. Quarterly Journal of the Royal Meteorology Society, 105: 963-977.
- West, G.D. and C.J. Apelt (1982) The effects of tunnel blockage ratio on the mean flow past a circular cylinder with Reynolds numbers between 10^4 and 10^5 . Journal of Fluid Mechanics, 114: 361-377.
- Woodcock, A.H. (1978) Marine fog droplets and salt nuclei. Part I. Journal of the Atmospheric Sciences, 35: 657-664.

World Meteorological Organization (1962) Precipitation measurements at sea.
World Meteorological Organization, Technical Note 47.

Wu, J. (1979) Spray in the atmospheric surface layer: Review and analysis of
laboratory and oceanic results. Journal of Geophysical Research, 84
(C4): 1693-1704.

Zosen (1981) First ship with practical deicing system. 26(7): 26.

A facsimile catalog card in Library of Congress MARC format is reproduced below.

Makkonen, Lasse

Atmospheric icing on sea structures/ by Lasse Makkonen. Hanover, N.H.: Cold Regions Research and Engineering Laboratory; Springfield, Va.: available from National Technical Information Service, 1984.

vii, 102 p., illus.; 28 cm. (CRREL Monograph 84-2.)

Bibliography: p. 77.

1. Atmospheric icing. 2. Ice. 3. Ice accretion. 4. Ice prevention. 5. Offshore environment. 6. Sea structures. I. United States. Army. Corps of Engineers. II. Cold Regions Research and Engineering Laboratory, Hanover, N.H. III. Series: CRREL Monograph 84-2.

